

**DEVELOPMENT OF A POLYMER FOR GREEN  
ENHANCED OIL RECOVERY**

BY

**Mohammad Said El-Shahat Mohammad**

A Thesis Presented to the  
DEANSHIP OF GRADUATE STUDIES

**KING FAHD UNIVERSITY OF PETROLEUM & MINERALS**

DHAHRAN, SAUDI ARABIA

In Partial Fulfillment of the  
Requirements for the Degree of

**MASTER OF SCIENCE**

In

**PETROLEUM ENGINEERING**

**APRIL 2019**

KING FAHD UNIVERSITY OF PETROLEUM & MINERALS  
DHAHRAN - 31261, SAUDI ARABIA  
DEANSHIP OF GRADUATE STUDIES

This thesis, written by **Mohammad Said El-Shahat Mohammad** under the direction of his thesis advisor and approved by his thesis committee, has been presented and accepted by the Dean of Graduate Studies, in partial fulfillment of the requirements for the degree of **MASTER OF SCIENCE IN PETROLEUM ENGINEERING.**



Dr. Dhafer A. Al Shehri  
Department Chairman



Dr. Salam A. Zummo  
Dean of Graduate Studies

23/7/2019  
Date



Dr. Bashirul Haq  
(Advisor)



Dr. Dhafer A. Al Shehri  
(Co-Advisor)



Dr. Mohamed Mahmoud  
(Member)



Dr. Salaheldin Elkatatny  
(Member)



Dr. Rahul N. Gajbhiye  
(Member)

© Mohammad Said El-Shahat Mohammad

2019

To my parents, Saeed and Ebtisam, may Allah give you health and joy.

To my beautiful family, sisters, and brothers,

To my loyal friends,

To all those who helped me with their support and prayers, thanks to Allah for enabling me to complete this work.

## ACKNOWLEDGMENTS

All praise be to Allah, first and foremost, for every success I have found and the knowledge I developed through this work.

I am grateful to the graduate department at KFUPM for giving me the opportunity to pursue my master's degree under their guidance. I am also thankful for my advisors, Drs. MD Haq and Dhafer Al Shehri, who gave me immense support and from whom I have learned so much in the domain of this research.

I am grateful for Dr. Mizan's kind support and brilliant ideas related to chemical reactions, without which I would not have been able to achieve my objectives.

I would also like to thank my thesis committee members, Drs. Mohammad Mahmoud, Salaheldin Elkatatny, and Rahul N. Gajbhiye, for their valuable guidance and support throughout this thesis work.

Special thanks to all of the members of the College of Petroleum and Geosciences who helped me to complete my thesis. Their support made this possible. Special thanks to Mr. Assad Barri for his knowledge of core flooding and Mr. Lionel Talley for his assistance with rheology analysis.

I could never fail to thank my family for their endless support and prayers. I am very grateful for all of them.

Last but not the least, I would very much like to thank my friends at KFUPM for their support and the enjoyable time we spent together.

# TABLE OF CONTENTS

<b>ACKNOWLEDGMENTS</b> .....	<b>V</b>
<b>LIST OF TABLES</b> .....	<b>VIII</b>
<b>LIST OF FIGURES</b> .....	<b>IX</b>
<b>LIST OF ABBREVIATIONS</b> .....	<b>XI</b>
<b>ABSTRACT</b> .....	<b>XIII</b>
ملخص الرسالة .....	<b>XV</b>
<b>CHAPTER 1 INTRODUCTION</b> .....	<b>1</b>
<b>1.1 Background</b> .....	<b>1</b>
1.1.1 Green Polymer-Based EOR.....	2
1.1.2 Using Polymers for EOR .....	2
<b>1.2 Thesis Objectives</b> .....	<b>4</b>
<b>1.3 Overview of Experimental Work</b> .....	<b>5</b>
1.3.1 Chemical and Physical Modifications .....	5
1.3.2 Rheology Measurements .....	5
1.3.3 Core Flood Experiments .....	5
<b>1.4 Chapters Descriptions</b> .....	<b>6</b>
<b>CHAPTER 2 LITERATURE REVIEW</b> .....	<b>7</b>
<b>2.1 Previous Work</b> .....	<b>7</b>
<b>2.2 Summary of Literature Review and Knowledge Gap</b> .....	<b>25</b>
2.2.1 Literature Review Summary.....	25
2.2.2 Knowledge Gap .....	29
<b>CHAPTER 3 METHODOLOGY</b> .....	<b>30</b>

<b>3.1 Materials .....</b>	<b>30</b>
3.1.1 Brine .....	30
3.1.2 Crude Oil .....	30
3.1.3 Xanthan Gum .....	30
3.1.4 Acrylic Acid .....	31
3.1.5 Dimethylaminopropyl .....	32
<b>3.2 Experimental Procedure .....</b>	<b>32</b>
3.2.1 Solution Preparation .....	32
3.2.2 Rheological Properties Measurements .....	35
3.2.3 Core flooding .....	35
3.3.1 Core flood experiment .....	37
 <b>CHAPTER 4 RESULTS AND DISCUSSIONS .....</b>	 <b>41</b>
<b>4.1 FT-IR and NMR Analysis .....</b>	<b>41</b>
4.1.1 FT-IR Analysis .....	41
4.1.2 NMR Analysis .....	45
<b>4.2 Rheological Properties Results .....</b>	<b>47</b>
4.2.1 Effect of Temperature .....	47
4.2.2 Effect of Salinity .....	49
4.2.3 Effect of Polyvinyl Alcohol .....	51
4.2.4 Effects of Temperature, Salinity, and PVA on Xanthan Viscosity .....	53
4.2.3 Blending Xanthan with Gluconic and Acrylic Acids and the Effect on Viscosity .....	54
4.2.4 Chemically Modified Xanthan Gum .....	59
<b>4.3 Core Flooding Results .....</b>	<b>67</b>
4.3.1 Porosity and Permeability Calculations .....	67
4.3.2 EOR Potential of the Modified Xanthan Gum .....	67
 <b>CHAPTER 5 CONCLUSIONS AND RECOMMENDATIONS .....</b>	 <b>74</b>
5.1 Conclusions .....	74
5.2 Recommendations .....	75
 <b>REFERENCES .....</b>	 <b>76</b>
 <b>APPENDIX: POROSITY AND PERMEABILITY CALCULATIONS .....</b>	 <b>83</b>
 <b>VITAE .....</b>	 <b>88</b>

## LIST OF TABLES

Table 1: Oil Recovery Results .....	19
Table 2: Comparison of Xanthan and HPAM Recoveries (Jang et al., 2015).....	20
Table 3 Literature Review Summary .....	25
Table 4: Core Properties .....	39
Table 5: Core #1 properties.....	69
Table 6: Recovery Results using Xanthan gum.....	69
Table 7: Core #2 properties.....	70
Table 8: Recovery Results using NP .....	70
Table 9: Oil recoveries results using Xanthan gum and NP .....	72
Table 10: Flow rate and pressure data of core #1 .....	84
Table 11: Flow rate and pressure data of core #2 .....	86

## LIST OF FIGURES

Figure 1: Chemical structure of xanthan gum (Jang et al., 2015).....	3
Figure 2: Advantages of xanthan gum (JIANLONG1).....	4
Figure 3: Xanthan/Cr (III) ionic bonding (Avery 1986).....	8
Figure 4: Xanthan/Cr (III) viscosity vs. shear rate (Avery 1986).....	8
Figure 5: Xanthan/Cr (III) viscosity vs. shear rate, 3,000 ppm (Chang 1988). ....	9
Figure 6: XG/Cr (III) viscosity vs. shear rate, 2,000 ppm (Chang 1988).....	10
Figure 7: Change in xanthan gum concentration vs. shear rate (Chang 1988). ....	10
Figure 8: FT-IR spectra of XGM and XG (Su 2003).....	12
Figure 9: X-ray diffraction spectra of XGM and XG (Su 2003). ....	12
Figure 10: Viscosity vs. polymer concentration composition (Reddy 2012). ....	13
Figure 11: Xanthan and xanthan with surfactant viscosities vs. shear rate (Wei 2014). ..	14
Figure 12: RF vs. pore volume (Wei 2014). ....	15
Figure 13: RRF vs. pore volume (Wei 2014). ....	15
Figure 14: Comparison of shear stabilities of different polymers (Bernd 2015).....	16
Figure 15: Polymer viscosities at different temperatures (Gao 2015). ....	16
Figure 16: Viscosity vs. Shear rates (Necla 2015).....	17
Figure 17: Oil recoveries from three polymer floods (Wei et al., 2015). ....	19
Figure 18: FT-IR spectra of XG, Px sample, and PMAO (Wang 2016). ....	21
Figure 19: TGA plots for xanthan, PX, and PMAO (Wang 2016). ....	21
Figure 20: Viscosity vs. shear rate, 2,000 ppm at 25 <sup>0</sup> C (Wang 2016).....	22
Figure 21: Effect of slug size on recovery (Esraa 2016). ....	23
Figure 22: Viscosity of XG nanopolymer vs. shear rate (Corredor 2018).....	24
Figure 23: Chemical structure of xanthan gum (Sworn, 2009). ....	31
Figure 24: Chemical structure of acrylic acid (Sigmaaldrich).....	32
Figure 25: Magnetic stirrer. ....	33
Figure 26: Rheology meter measuring up to 80 <sup>0</sup> C.....	35
Figure 27: Vacuum saturation setup, vacuum pump, and injection pump.....	37
Figure 28: Core Flooding System.....	38
Figure 29: FT-IR spectrum of acrylic acid. ....	42
Figure 30: FT-IR spectrum of xanthan gum. ....	43
Figure 31: FT-IR spectrum of modified xanthan gum.....	44
Figure 32: FT-IR spectra of two polymers. ....	45
Figure 33: 1H NMR spectrum of xanthan gum. ....	46
Figure 34: 1H NMR spectrum of modified xanthan gum.....	46
Figure 35: 0.5% xanthan viscosity vs. shear rate at different temperatures. ....	48
Figure 36: 0.5% xanthan gum viscosity vs. shear rate at 25 <sup>0</sup> C.....	49
Figure 37: Effect of adding NaCl to 0.5% xanthan viscosity vs. shear rate at 50 <sup>0</sup> C. ....	50

Figure 38: 0.5 % xanthan (2 wt% NaCl) vs. shear rate at different temperatures. ....	50
Figure 39: Effect of adding NaCl to 0.5% xanthan viscosity vs. shear rate at 80 <sup>0</sup> C. ....	51
Figure 40: Effect of adding PVA to 0.5% xanthan viscosity vs. shear rate at 50 <sup>0</sup> C.....	52
Figure 41: 0.5% Xan viscosity vs. Shear rate + 0.5% PVA at different temperatures. ....	52
Figure 42: Effect of adding PVA to 0.5% Xan viscosity vs. Shear rate at 80 <sup>0</sup> C.....	53
Figure 43: 1,500 ppm Xan and Xan + gluconic acid viscosities vs. shear rate at 25 <sup>0</sup> C. ..	55
Figure 44: 1,500 ppm Xan and Xan + acrylic acid viscosities vs. shear rate at 25 <sup>0</sup> C. ....	56
Figure 45: 1,500 ppm Xan and Xan + acrylic acid viscosities vs. shear rate at 50 <sup>0</sup> C .....	56
Figure 46: 1,500 ppm Xan & acrylic acid (blending) viscosities vs Shear rate at 25 <sup>0</sup> C...	57
Figure 47: 1,500 ppm Xan & acrylic acid (blending) viscosities vs Shear rate at 50 <sup>0</sup> C...	57
Figure 48: 0.5 % Xan and acrylic acid (blending) viscosities vs. shear rate at 50 <sup>0</sup> C. ....	58
Figure 49: NP and xanthan viscosities vs. shear rate at 25 <sup>0</sup> C.....	60
Figure 50: NP and xanthan viscosities vs. shear rate at 50 <sup>0</sup> C.....	60
Figure 51: Xanthan viscosity vs. shear rate at 25 <sup>0</sup> C and 50 <sup>0</sup> C.....	61
Figure 52: NP viscosity vs. shear rate at 25 <sup>0</sup> C and 50 <sup>0</sup> C.....	62
Figure 53: FT-IR spectrum of modified xanthan gum (sample No. 2).....	63
Figure 54: Comparison between Xanthan gum and Sample 2 FT-IR spectrum.....	64
Figure 55: <sup>1</sup> H NMR spectrum of modified Xanthan gum (sample number 2) .....	64
Figure 56: Salinity effect on Xanthan viscosity.....	65
Figure 57: Sample 2 viscosity vs. shear rate at 25, 60 and 70 <sup>0</sup> C .....	66
Figure 58: Xanthan recovery vs. No. of Inj PV.....	68
Figure 59: NP recovery vs. No. of Inj PV.....	70
Figure 60: Recovery comparison of xanthan and NP vs. No. of Inj PV.....	71
Figure 61: Pressure drop profile No. of Inj PV.....	73
Figure 62: The q vs. dp values for Core #1.....	84
Figure 63: The q vs. dp values for Core #2.....	86

## LIST OF ABBREVIATIONS

<b>EOR</b>	:	Enhanced oil recovery
<b>XG</b>	:	Xanthan gum
<b>PPM</b>	:	Parts per million
<b>FT-IR</b>	:	Fourier transform infrared
<b>NMR</b>	:	Nuclear magnetic resonance
<b>EC</b>	:	Ethylene carbonate
<b>DEC</b>	:	Glycerin carbonate
<b><math>K_{rw}</math></b>	:	Water relative permeability
<b><math>\mu_w</math></b>	:	Oil viscosity
<b><math>\lambda_w</math></b>	:	Water mobility
<b><math>\lambda_o</math></b>	:	Oil mobility
<b><math>K_{ro}</math></b>	:	Oil relative permeability
<b><math>\mu_o</math></b>	:	Oil viscosity
<b><math>N_{ca}</math></b>	:	Capillary number
<b>IOIP</b>	:	Initial oil in place
<b>RF</b>	:	Resistance factor
<b>RFF</b>	:	Residual resistance factor

<b>HPAM</b>	:	Hydrolyzed polyacrylamide
<b>PAMO</b>	:	Poly-maleic anhydride/1-octadecene
<b>ROS</b>	:	Residual oil saturation
<b>HPH</b>	:	High-pressure homogenization
<b>LBG</b>	:	Locust bean gum
<b>NP</b>	:	New polymer
<b>PVA</b>	:	Polyvinyl alcohol
<b>PV</b>	:	Pore volume
<b>API</b>	:	American Petroleum Institute

## ABSTRACT

Full Name : Mohammad Saeed El-Shahat Mohammad  
Thesis Title : DEVELOPMENT OF A POLYMER FOR GREEN ENHANCED OIL RECOVERY]  
Major Field : Petroleum Engineering  
Date of Degree : April 2019

Oil recovery from natural depletion is limited. This is true even with secondary recovery, during which water is mainly injected. Therefore, tertiary recovery (EOR) has been introduced to improve oil recovery rates. One EOR technique being used in the industry to improve the injected water's viscosity is the addition of polymers. Chemical polymers such as hydrolyzed polyacrylamide (HPAM) have been used in EOR for decades. However, because of environmental concerns, biopolymers have been introduced as an alternative. Xanthan gum, a biopolymer, has been used in EOR for many years. Yet due to certain limitations, it cannot be employed in harsh reservoir conditions such as when temperature and water salinity levels are high. In this research, xanthan gum was physically and chemically modified to increase its viscosity. Our results show that physically mixing or blending xanthan gum with PVA, gluconic acid, or acrylic acid did not improve viscosity. Conversely, by chemically modifying xanthan with acrylic acid, FT-IR and NMR analyses showed that the chemical structure of the xanthan gum was changed. Viscosity improved considerably at the same shear rate. For example, a 1,500 ppm xanthan solution had a viscosity of 578 mPa.S at a  $0.1 \text{ s}^{-1}$  shear rate, while the chemically modified xanthan gum had a viscosity of around 2,200 mPa.S at the same concentration and in similar test conditions.

Consequently, this increase in viscosity of the xanthan solution was reflected in the results produced via core flooding recovery. In a number of EOR experiments, a 12-inch Berea sandstone core 1.5 inches in diameter was divided into two 6 inch cores in order to make the results comparable. The brine that was used in the core saturation and secondary flooding recovery had a concentration of 3% NaCl (30,000 ppm). Arabian light oil with a viscosity of 19.8 cp at 25<sup>0</sup>C was used in the core flooding experiments. The results show that the secondary recoveries from Cores #1 and #2 were 44% and 43%, respectively. For EOR flooding, xanthan gum was used in Core #1; modified xanthan gum was used in Core #2. The xanthan gum obtained an additional recovery of about 14% of the initial oil in place. Meanwhile, the modified xanthan gum showed a 19% tertiary recovery, which was around 5% more than the xanthan gum.

## ملخص الرسالة

الاسم الكامل: محمد سعيد الشحات محمد

عنوان الرسالة: تطوير بوليمرات صديقة للبيئة لتحسين كفاءة إنتاج النفط

التخصص: هندسة البترول

تاريخ الدرجة العلمية: مارس 2019

إن كمية إنتاج النفط التي يمكن استخلاصها تحت الضغط الطبيعي للمكامن النفطية تكون محدودة, حتى مع المرحلة الثانية للإنتاج والتي يتم فيها عادة حقن المياه لاستخراج النفط. ولذا يتم تعزيز إستخلاص النفط عبر تقنيات المرحلة الثالثة لزيادة إنتاج النفط من الخزانات. وتعتبر إضافة البوليمرات لزيادة لزوجة الماء المحقون أحد أنواع المرحلة الثالثة لزيادة إنتاجية الخزانات. لقد تم استخدام البوليمرات الكيميائية لعدة عقود, ومن أهمها هو بولي أكرلاميد الذي يعتبر البولمر الأكثر استخدامًا في عمليات تحسين الإنتاجية. ولأن البوليمرات الكيميائية لها مضار بالبيئة وتحتاج إلى جهد إضافي لفصلها عن النفط المنتج, تم استحداث البوليمرات صديقة البيئة كحل بديل للبوليمرات الكيميائية. ومن أشهرها صمغ الزانتان الذي يعتبر أشهر بولمر كيميويحيوي ومن أقلها كلفة, إلا أنه يتكسر بسرعة مع وجود الظروف الصعبة من الضغط والحرارة ونسبة الملوحة العالية في المكامن النفطية.

وفي هذا البحث تم تعديل خواص واستخدام صمغ الزانتان بالطريقتين الكيميائية والفيزيائية من أجل تحسين كفاءة لزوجته. المواد التي استخدمت في الخلط الفيزيائي كانت كحول بولي فينيل و حمض الجولوكونيك وحمض الاكرليك. وقد بينت نتائج البحث أن الخلط الفيزيائي لصمغ الزانتان لم يكن قادرًا على زيادة اللزوجة على عكس التفاعل الكيميائي الذي استخدم فيه حمض الأكرليك.

بينت النتائج من تحليل فورشمير لقياس الأشعة تحت الحمراء وتحليل الرنين المغناطيسي النووي أن التركيب الكيميائي لصمغ الزانتان قد تغير. وبالتالي تحسنت كفاءة لزوجته مقارنة بصمغ الزانتان قبل المعالجة الكيميائية. على سبيل المثال: عند معامل إجهاد القص 0.1 لكل ثانية, كانت لزوجة صمغ الزانتان هي 587 باسكال. ثانية, بينما

ارتفعت إلى 2,200 باسكال. ثانياً لسمع الزانتان المعدل لنفس نسبة التركيز لكل منهما التي كانت 1,500 جزء في المليون ونفس درجة الحرارة التي أقيمت عندها التجربة.

وبالتالي، فإن التحسن الناتج في لزوجة الزانتان المعدل قد أثر على زيادة الإنتاج النفطي في تجربة الفيض الصخري. إن العينة الصخرية المستخدمة في تجارب الفيض كانت اسطوانة من الحجر الرملي بطول 12 بوصة وقطر 1.5 بوصة قسمت لعينتين كل منها بطول 6 بوصات كي تتم المقارنة بين الزانتان العادي والمطور بشكل صحيح. كان المحلول الملحي المستخدم في تعبئة العينتين الصخريتين وعملية الفص هو ماء مقطر مضاف إليه ملح صوديوم الكالسيوم بسنبة 3% أي ما يوازي 30,000 جزء في المليون. وكان النفط المستخدم في التجربة من نوع النفط العربي الخفيفة بلزوجة 19.8 سنتي بوز عند 25 درجة مئوية. للمرحلة الثانية من الإنتاج (الفيض المائي) أظهرت النتائج أن كلا الصخرتان لديهما نفس معامل الإنتاجية من النفط تقريباً ب44% و 43% من النفط الكلي الموجود للصخرة رقم 1 التي استخدم فيها الزانتان العادي والصخرة 2 التي استخدم فيها الزانتان المطور فيما بعد على التوالي. لتقييم نتائج استخدام صمغ الزانتان بنوعيه العادي والمعدل لتعزيز الإنتاج، تم قياس معامل الإنتاج لإحدى العينات الصخرية باستخدام صمغ الزانتان العادي والذي أظهر زيادة في معامل الإنتاجية بلغت نسبته 14%، بينما أظهر استخدام صمغ الزانتان المعالج كيميائياً قدرة على زيادة معامل الإنتاجية بمقدار 19%. وعليه، فإن هناك زيادة لا تقل عن 5% في معامل الإنتاجية عند استخدام صمغ الزانتان المعالج، وهي نسبة مهمة لتعزيز الإنتاج من المكامن النفطية.

ولاستكمال نتائج البحث، فإنه يوصى بأن يتم القيام بالمزيد من التجارب حول تعديل الزانتان العادي ودراسة مدى تأثير هذا التعديل على لزوجة الزانتان واستخدامه في عملية تحسين إنتاج المكامن النفطية واستخدامه في مجالات أخرى في الصناعات النفطية.

# CHAPTER 1

## INTRODUCTION

There is valuable oil that remains in the reservoir after primary and secondary recoveries; these represent approximately 10% and 40% of the total oil present, respectively. The purpose of enhanced oil recovery is to improve the amount of oil recovered via a process considered tertiary recovery. Polymer injection is one of the most common methods of enhanced oil recovery (EOR), due to its ability to improve viscosity and sweep efficiency.

An experimental study is presented here with the goal of modifying xanthan gum through a chemical process and scrutinizing the rheological properties and EOR potential of both xanthan gum and modified xanthan gum.

### **1.1 Background**

After secondary recovery is completed, the third stage of production – known as tertiary recovery – is applied. Tertiary recovery includes the use of miscible gases, chemicals, and thermal energy to recover the oil remaining after secondary recovery. However, not all reservoirs follow the same chronological sequence. This is especially true in cases of heavy crude oil, in which the tertiary process is usually engaged as the second operation (Green and Willhite, 1997). Because of disfavor in the petroleum industry, the term “tertiary recovery” was replaced with EOR. Therefore, the oil recovery processes are as follows: primary recovery, secondary recovery, and EOR processes. EOR operations include the injection of fluids, steam, or hot water into a reservoir and the use of thermal

energy through oil combustion within the reservoir rock. The most commonly used fluids in EOR processes are polymers, surfactants, and hydrocarbon solvents.

### 1.1.1 Green Polymer-Based EOR

One of the major EOR techniques is chemical flooding. The most popular chemical method is polymer flooding. There are many promising green polymers employed for EOR purposes such as schizophyllan, which has a very high thermal stability compared to chemical polymers (Gao, 2015). However, the cost is very high compared to other polymers on the market. Xanthan gum is considered one of the most popular and cheapest biopolymers. It has been used both in EOR and drilling operations. However, it has limitations in harsh conditions, and thus is not as popular as HPAM.

### 1.1.2 Using Polymers for EOR

The main use of a polymer is to increase water viscosity to avoid the fingering problem, a condition at the interface of two fluids such as oil and water wherein one bypasses the other as it moves along, creating an uneven or “fingered” profile. Polymers are added to water to increase its viscosity, controlling the mobility ratio. The mobility ratio is defined as the ratio of the displacing phase mobility (i.e., water) to the displaced phase mobility (i.e., oil), as given by Eq. 1.

$$N_M = \frac{\lambda_w}{\lambda_o} = \frac{\left[ \frac{K_{rw}}{\mu_w} \right]}{\left[ \frac{K_{ro}}{\mu_o} \right]} \quad (1)$$

The additional recovery from injecting polymers is usually 15% to 20% of the original oil in place (OOIP) after secondary recovery (Rellegadla, 2017). There are two kinds of polymers commonly utilized for mobility control in water flooding: partially hydrolyzed polyacrylamide (HPAM) and xanthan biopolymer. Since HPAM is chemically

manufactured, it pollutes the environment and has many other problems (e.g., produced water treatment and toxicity issues) stemming from the degradation products of the chemical materials (Xiong et al., 2018).

Xanthan gum was selected as the target of this research, because globally it is currently one of the most commonly used and versatile polysaccharides available (Jang et al., 2015). It is mostly made of D-glucose, D-mannose, D-glucuronic acid, and acetyl. Under proper conditions, it is produced by fermentation. Figure 1 shows the chemical structure of xanthan gum.

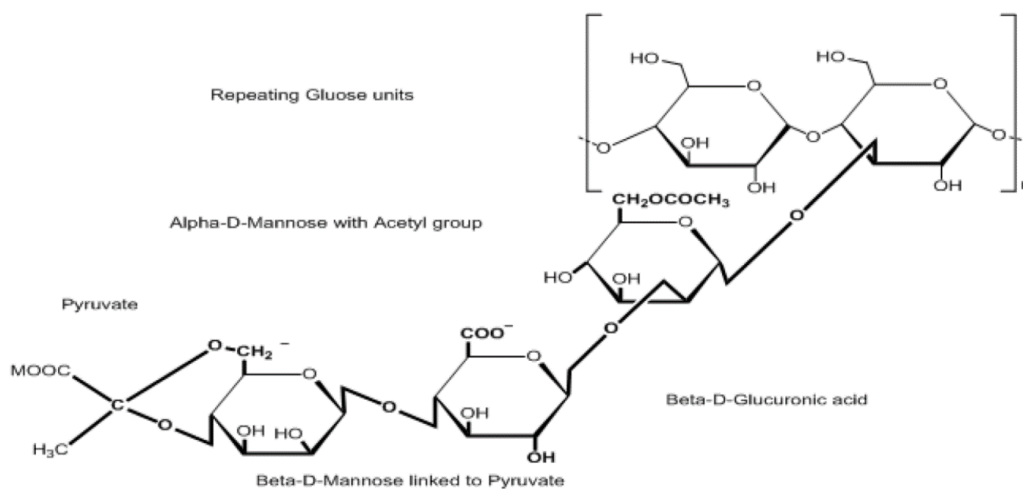


Figure 1: Chemical structure of xanthan gum (Jang et al., 2015).

Xanthan gum was chosen because it is considered one of the most popular biopolymers in the world (Jang et al., 2015). It is used in many fields, such as the food and cosmetic industries, among others. Xanthan gum offers many advantages, which are listed in Figure 2.

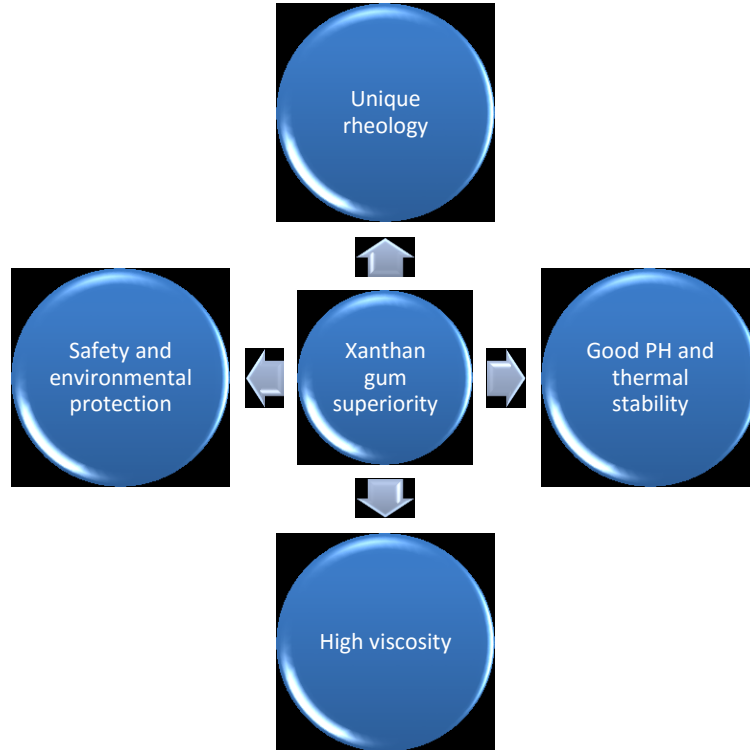


Figure 2: Advantages of xanthan gum (JIANLONG1).

## 1.2 Thesis Objectives

The aims of the research are to develop a green polymer from xanthan gum and explore the relationship between the rheological properties and EOR performances of xanthan gum and the developed polymer.

To achieve the objectives, the following steps were used:

- 1- Synthesize xanthan by adding acrylic acid.
- 2- Examine the synthesized xanthan's chemical structure by FT-IR and NMR spectra.
- 3- Investigate the rheological properties of xanthan and synthesized xanthan gum solutions at different temperatures in order to determine the level to which the synthesis process has been achieved.

- 4- Explore the relationships among EOR performance and xanthan and modified xanthan gums.

### **1.3 Overview of Experimental Work**

The goal of this thesis was to investigate the role of green polymers (i.e., xanthan and modified xanthan gums) in Green Enhanced Oil Recovery (GEOR). To fulfill these objectives, xanthan gum was modified by both chemical and physical methods. Second, the rheologies of the two gums were compared. Lastly, core flooding experiments were conducted to investigate their respective performances.

#### **1.3.1 Chemical and Physical Modifications**

A main disadvantage of using xanthan gum in EOR is its limitations in harsh conditions, where pressures and temperatures are high. Therefore, this thesis investigated enhancing xanthan viscosity through physical and chemical alterations. Consequently, the mobility ratio decreased and recovery increased. The chemical modification was examined by FT-IR and NMR analyses to study the changes in xanthan's chemical structure.

#### **1.3.2 Rheology Measurements**

After the modifications were made, the viscosity of the modified xanthan gum was compared to the viscosity of normal xanthan in order to test for any improvement. The viscosities were measured by varying the temperature at different shear rates.

#### **1.3.3 Core Flood Experiments**

The xanthan and modified xanthan gum performances were determined by core flood experiments. In this study, two experiments were conducted to examine the obtained oil

recovery of two green polymers: (1) xanthan gum and (2) chemically modified xanthan gum.

## **1.4 Chapters Descriptions**

This thesis consists of five chapters. Chapter 1 introduces the subject and objectives of this thesis. Chapter 2 is a literature review and identifies gaps in the existing research. Chapter 3 illustrates the methodology and materials used in the experiments. Chapter 4 presents and discusses the results. Chapter 5 highlights the conclusions and recommendations.

## CHAPTER 2

### LITERATURE REVIEW

The most popular polymers used in EOR are chemical-based polymers. These polymers often cause environmental pollution, either by precipitating in the reservoir or returning back with produced fluids that require additional treatment to separate. Green polymers offer a solution to certain environmental problems and also are better able to face harsh conditions. In this literature review, research done on modifications to xanthan gum for EOR purposes is presented.

#### 2.1 Previous Work

Avery et al. (1986) analyzed cross-linked xanthan gum with chromium ions, claiming that xanthan gel formed because of ionic bonding between the chrome and carboxyl groups on xanthan molecules (see Figure 3). This weak bonding kept its pseudo-plasticity and improved cross-link strength. The gel was found to have a very high shear stability, as shown in Figure 4. This gel is used to treat injection well flow profiles as the highly permeable zones shoot water towards production wells, causing quick breakthrough. The gel diverts the resulting water to under-swept oil zones. From five years of Mobil's filed experiences in North America (i.e., Louisiana), the researchers discovered that the xanthan/Cr gel became unstable above 71<sup>0</sup>C (160<sup>0</sup>F).

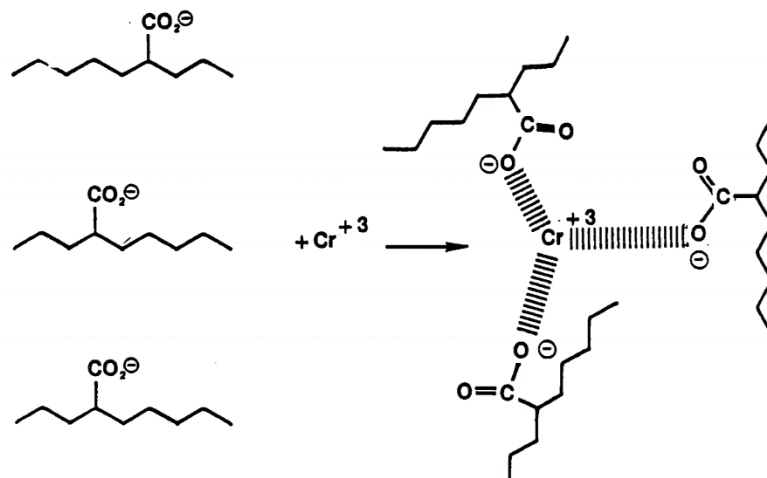


Figure 3: Xanthan/Cr (III) ionic bonding (Avery 1986).

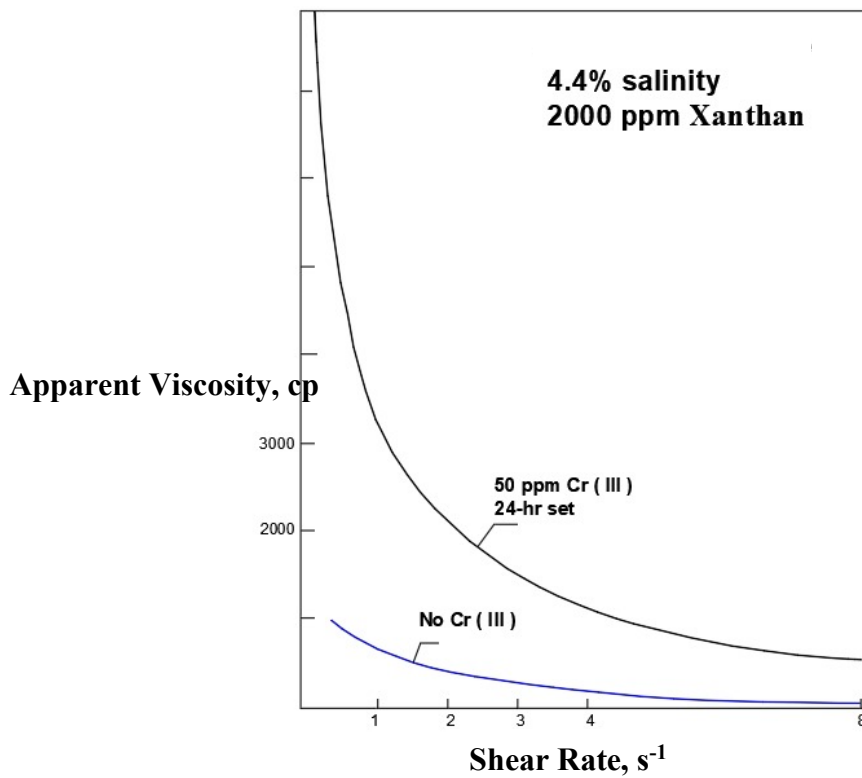


Figure 4: Xanthan/Cr (III) viscosity vs. shear rate (Avery 1986).

Chang et al. (1988) attempted to improve xanthan viscosity by cross-linking it with chromium ions, finding that at 2,000 ppm of xanthan and 100 ppm of chromium, the

viscosity increased, as compared to 2,000 ppm of xanthan (see **Error! Reference source not found.**). Furthermore, at 3,000 ppm of xanthan and a low shear rate, the viscosity decreased; then, the rate of change became less, meaning the shear thinning decreased (see Figure 6). Figure 7 shows how the viscosity of the xanthan was investigated with changes in concentration at 75<sup>0</sup>F (23.9<sup>0</sup>C).

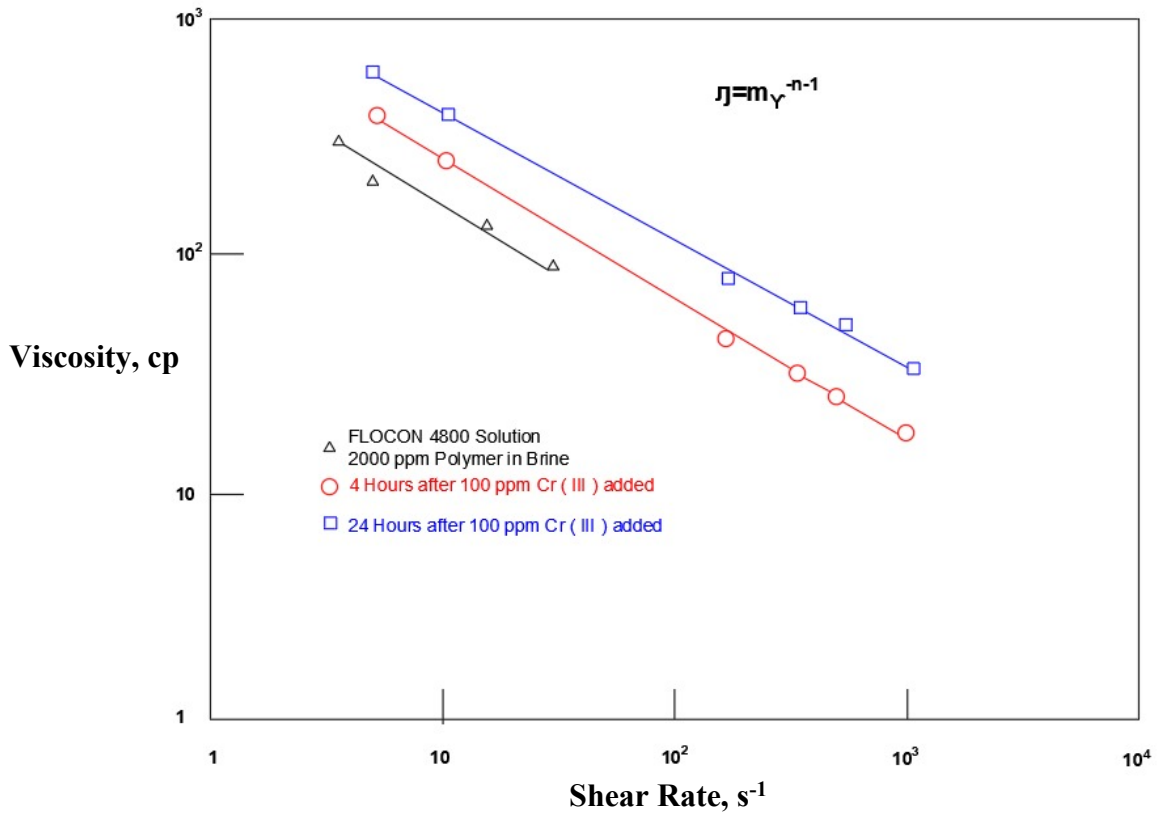


Figure 5: Xanthan/Cr (III) viscosity vs. shear rate, 3,000 ppm (Chang 1988).

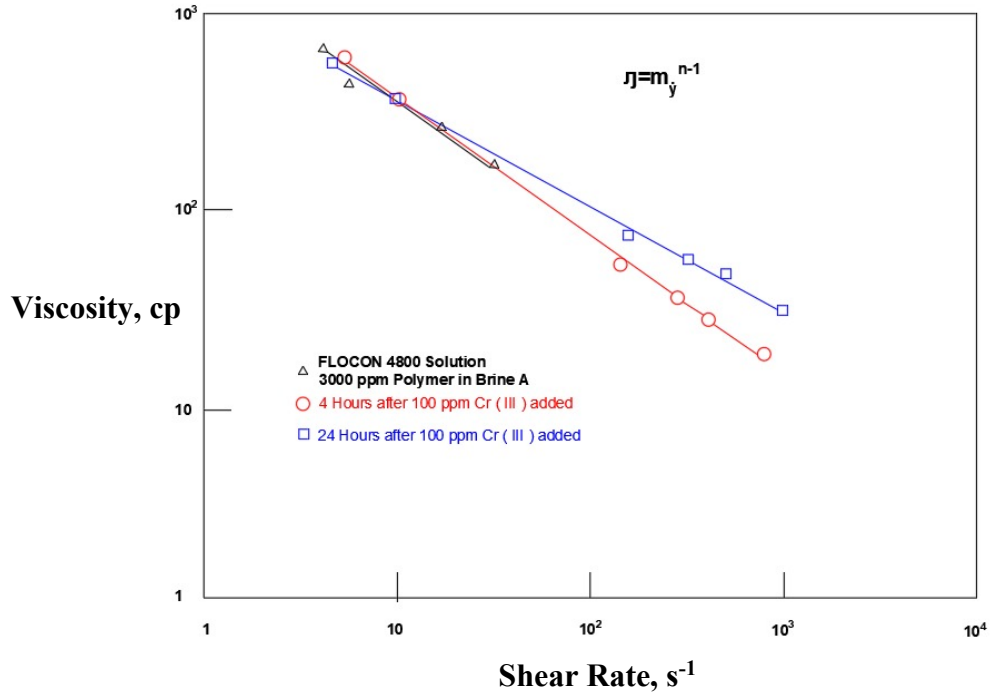


Figure 6: XG/Cr (III) viscosity vs. shear rate, 2,000 ppm (Chang 1988).

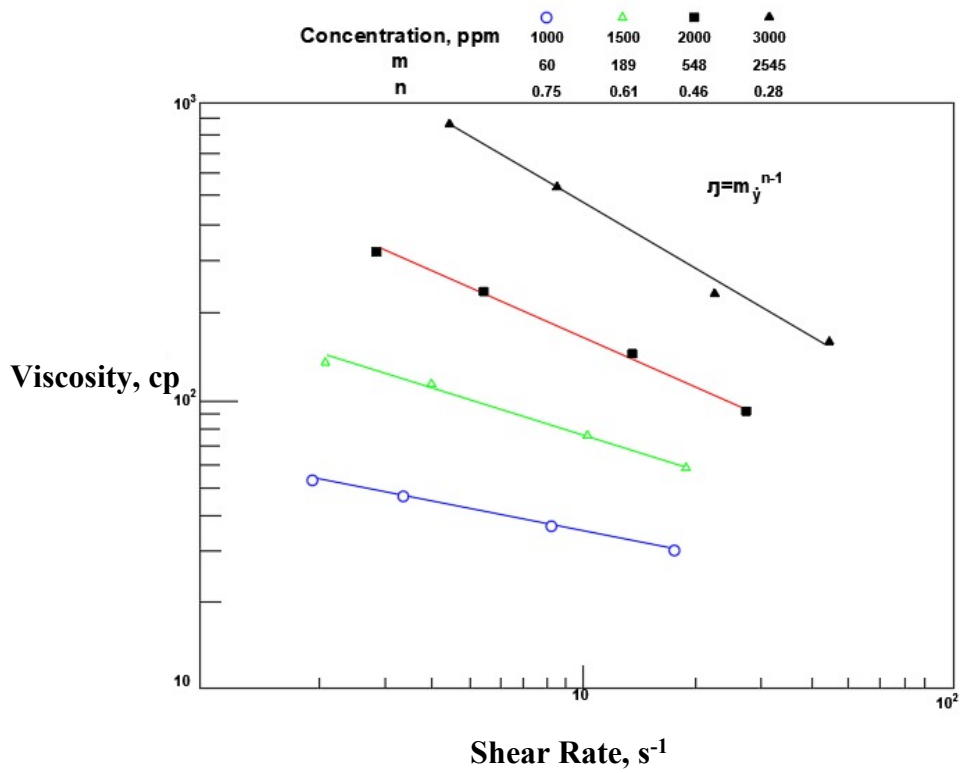


Figure 7: Change in xanthan gum concentration vs. shear rate (Chang 1988).

Eggert et al. (1992) studied permeability reduction in unconsolidated sand packs via xanthan gel and cross-linked chromium. The gel exhibited two unique properties: swelling and syneresis. The swelling was caused by the gel's ability to adsorb the solvent, causing the volume to increase. Conversely, syneresis is a shrinkage in gel volume due to expulsion of the solvent portion upon aging of the gel. This is usually caused by continued crosslinking. The gel illustrated up to 71% syneresis as a bulk sample, and was effective in maintaining permeability reduction in unconsolidated sand packs. In contrast, the swelling gel increased up to 45% in volume and was less effective in maintaining permeability reduction. The concentration used in this study was 2,000 ppm xanthan gum and 25 to 200 ppm Cr (III). In addition, the author investigated changes in permeability with changes in the pH of the solution, finding that sand pack permeability was inversely proportional to the pH of the solution.

Broseta et al. (1995) studied the adsorption of scleroglucan and xanthan for 100% saturated brine and residual oil-saturated cores. In the residual oil case, the adsorption decreased sharply in oil wet porous media. Conversely, adsorption slightly increased in water wet media in the presence of oil.

Su et al. (2003) modified xanthan gum to improve its dissolution rate, using formaldehyde in the modification. The formaldehyde worked to reduce intermolecular interactions. Consequently, the gelatinous layer did not form, or if it did, the molecules left the surface of the particle quickly, and hence the dissolution rate increased compared to normal xanthan gum. The FT-IR and X-ray diffraction spectra showed that the molecular structure of the xanthan gum had been changed (see Figure 8 and Figure 9).

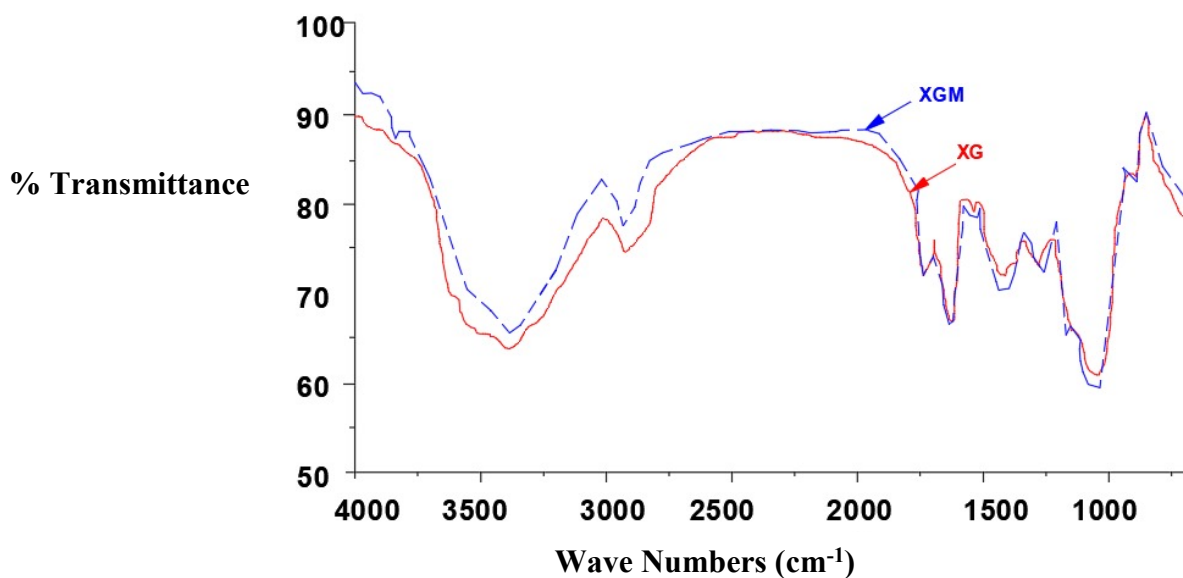


Figure 8: FT-IR spectra of XGM and XG (Su 2003).

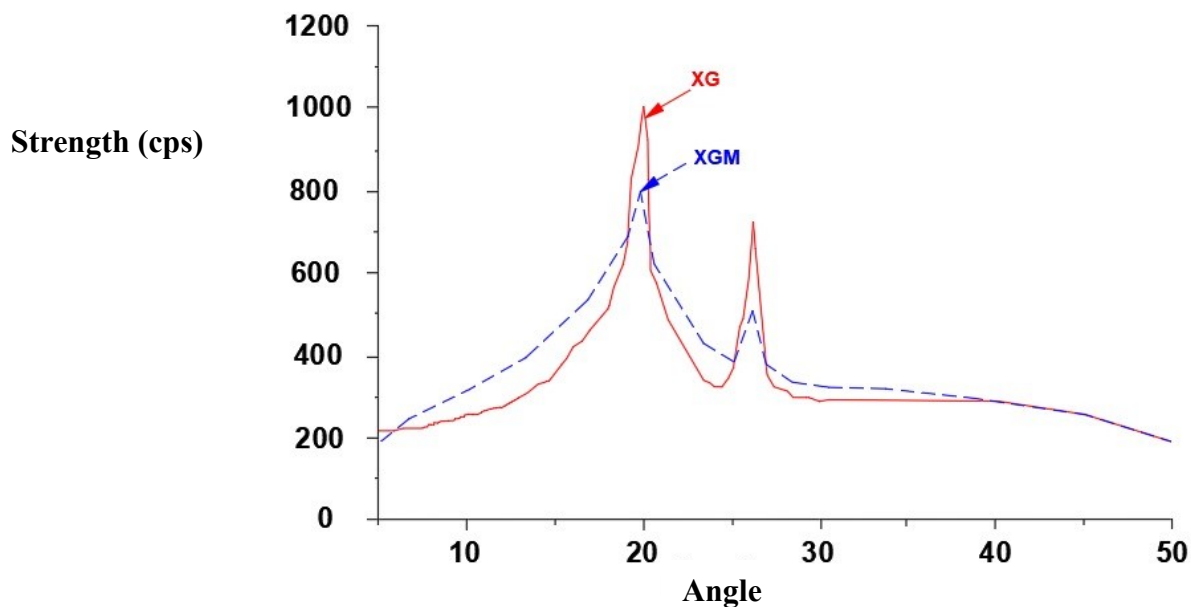


Figure 9: X-ray diffraction spectra of XGM and XG (Su 2003).

Reddy et al. (2012) modified xanthan gum and scleroglucan for cement purposes, adding the following organic carbonates: ethylene carbonate (EC), propylene carbonate (PC), butylene carbonate (BC), dierhl carbonate (DEC), and glycerin carbonate (GC). Figure 10

shows a comparison between the types of xanthan viscosity with their respective concentrations.

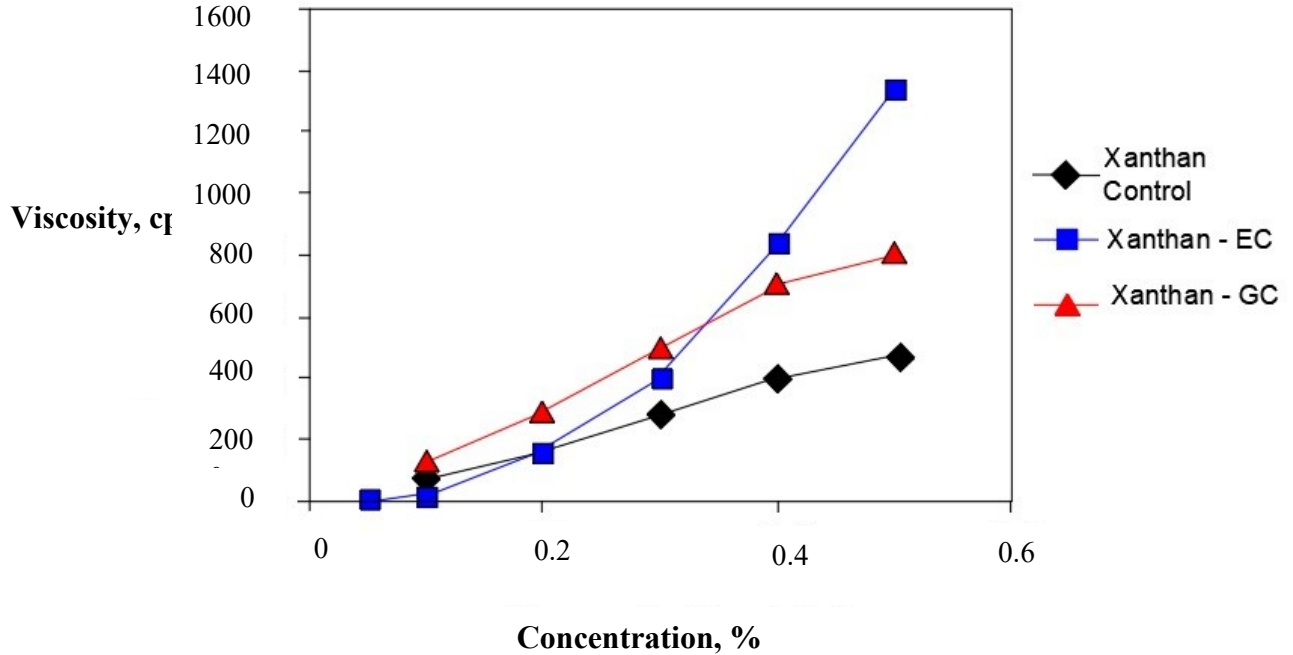


Figure 10: Viscosity vs. polymer concentration composition (Reddy 2012).

Sun et al. (2013) investigated improved recovery via an exopolysaccharide polymer (a kind of xanthan gum), finding that the recovery of crude oil from two cases of sand packed columns increased by 3% and 11% with low and high permeabilities, respectively.

Wei et al. (2014) added a surfactant (i.e.,  $\beta$ -cyclodextrin) to xanthan and studied the resulting rheological parameters and flow behavior in porous media. These researchers found that the novel self-assembling biopolymer (SAP) system offered higher stability in terms of viscosity over time, as compared to xanthan gum (see Figure 11).

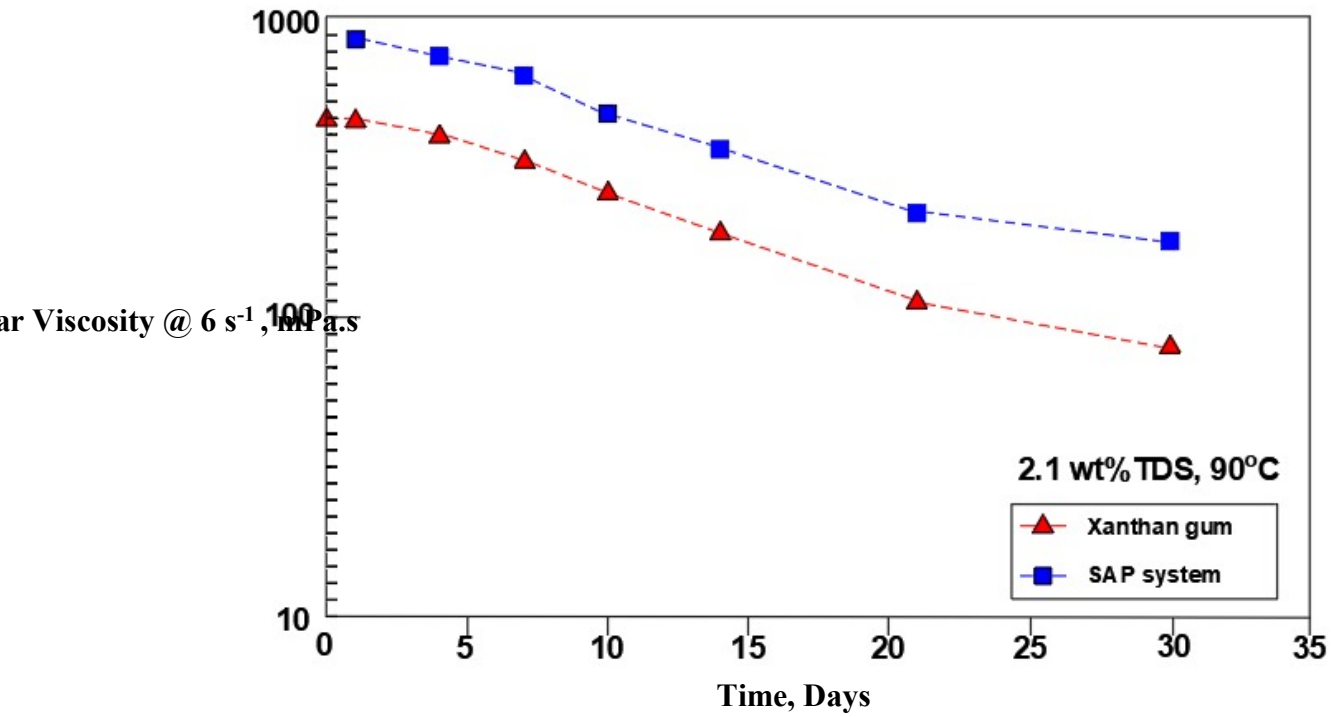


Figure 11: Xanthan and xanthan with surfactant viscosities vs. shear rate (Wei 2014).

In addition, they studied the resistance (RF) and residual resistance (RRF) factors of the polymer in a core flood experiment (see Figure 12 and Figure 13).

RF:

$$RF = \frac{\Delta P (\text{polymer})}{\Delta P (\text{water})}$$

RRF:

This indicates the magnitude of irreversibility of the permeability reduction.

$$RRF = \frac{\Delta P (\text{water after polymer})}{\Delta P (\text{water before polymer})}$$

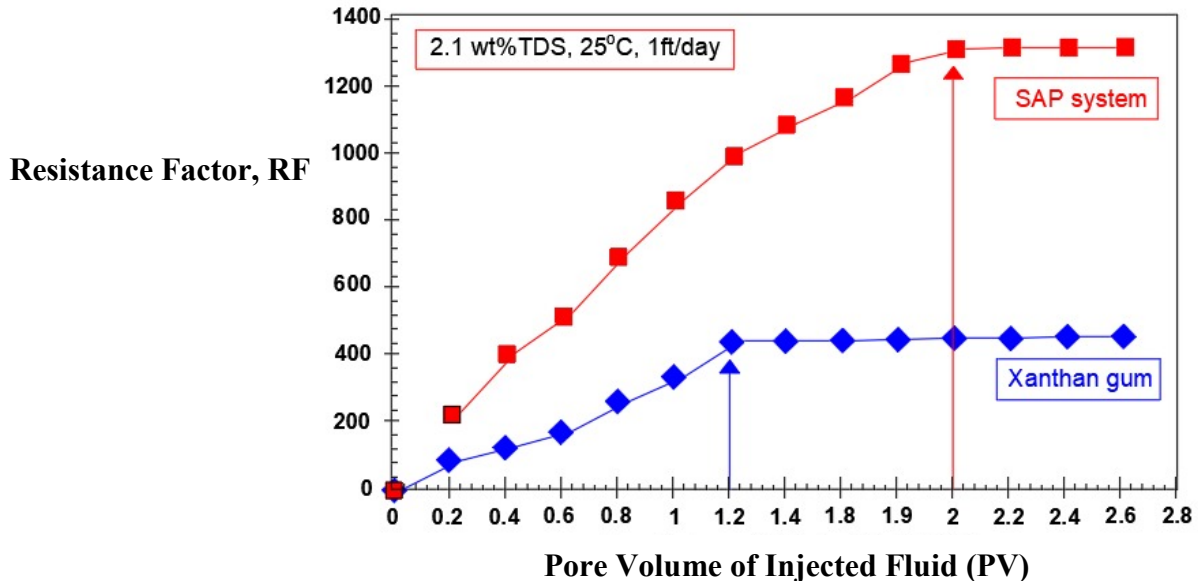


Figure 12: RF vs. pore volume (Wei 2014).

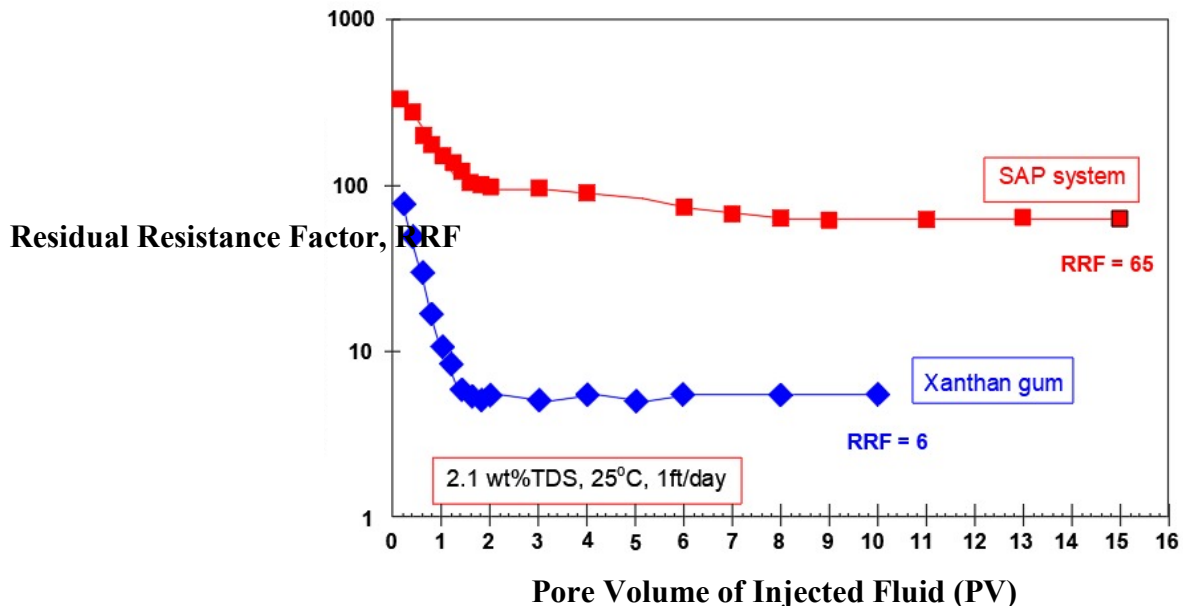


Figure 13: RRF vs. pore volume (Wei 2014).

Bernd et al. (2015) compared shizophyllan, xanthan, and HPAM in terms of rheological stability over time (see Figure 14).

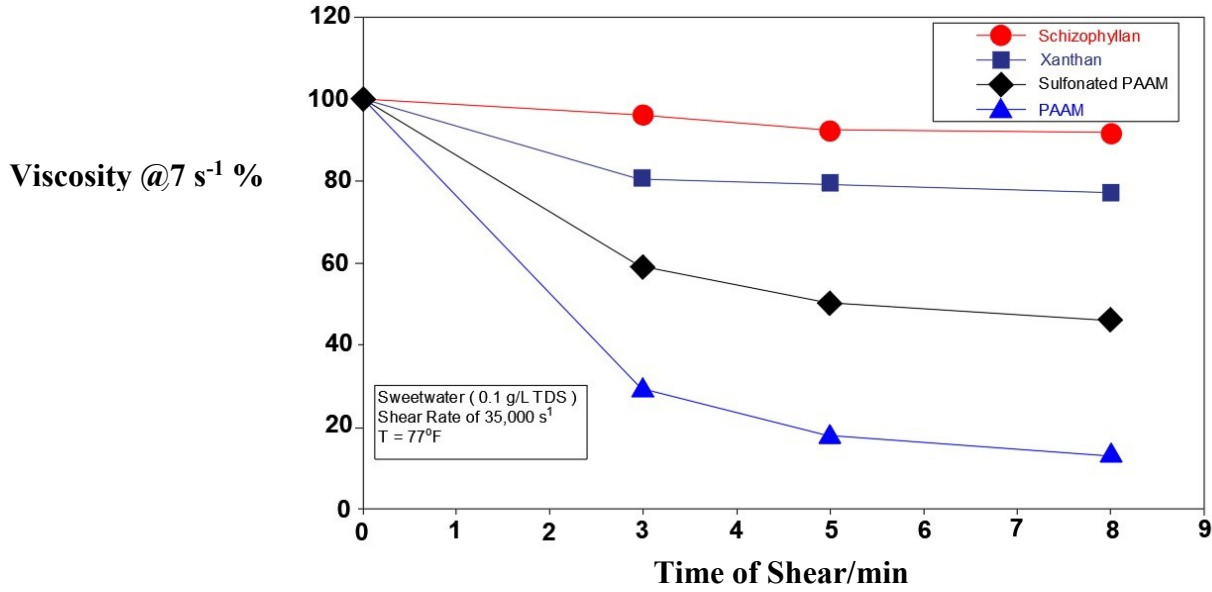


Figure 14: Comparison of shear stabilities of different polymers (Bernd 2015).

Gao (2015) compared changes in viscosity among three polymers (i.e., schizophyllan, xanthan, and HPAM) in response to changes in temperature (see Figure 15).

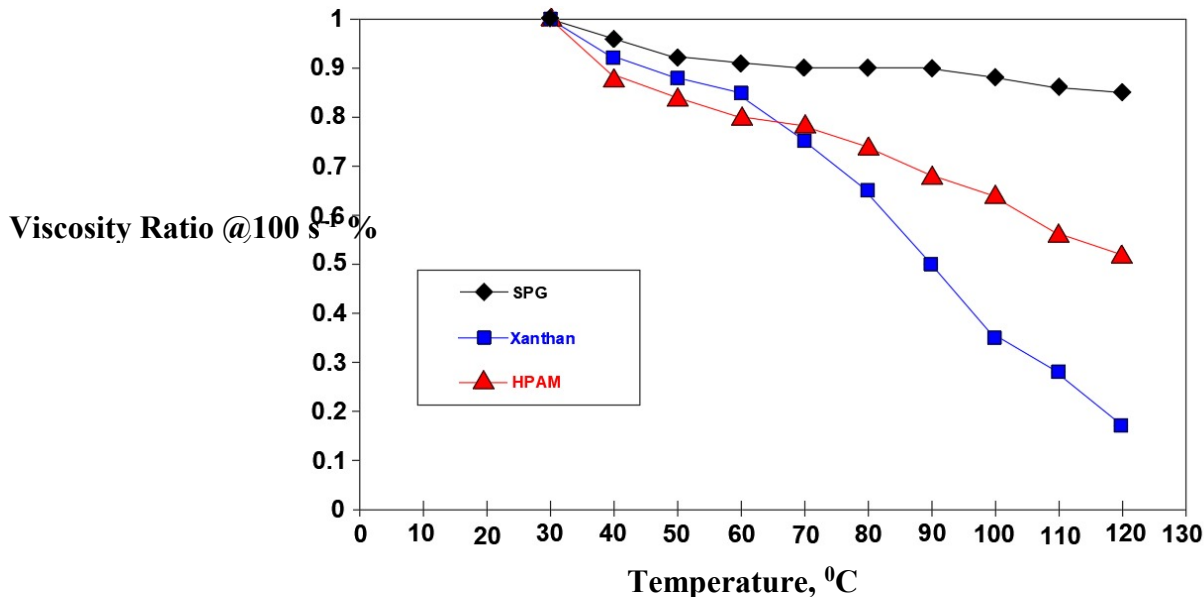


Figure 15: Polymer viscosities at different temperatures (Gao 2015).

Necla et al. (2015) treated xanthan gum solutions with high-pressure homogenization (HPH) to provide alternative treatments for enzymatic and chemical modifications at

25<sup>0</sup>C. These researchers considered the rheological properties of normal Xanthan gum and treated samples in order to understand the consequences of physical modifications over time. They found that physical modifications offered very low recovery in terms of viscosity, indicating that the changes obtained by high shear treatments are irreversible (see Figure 16).

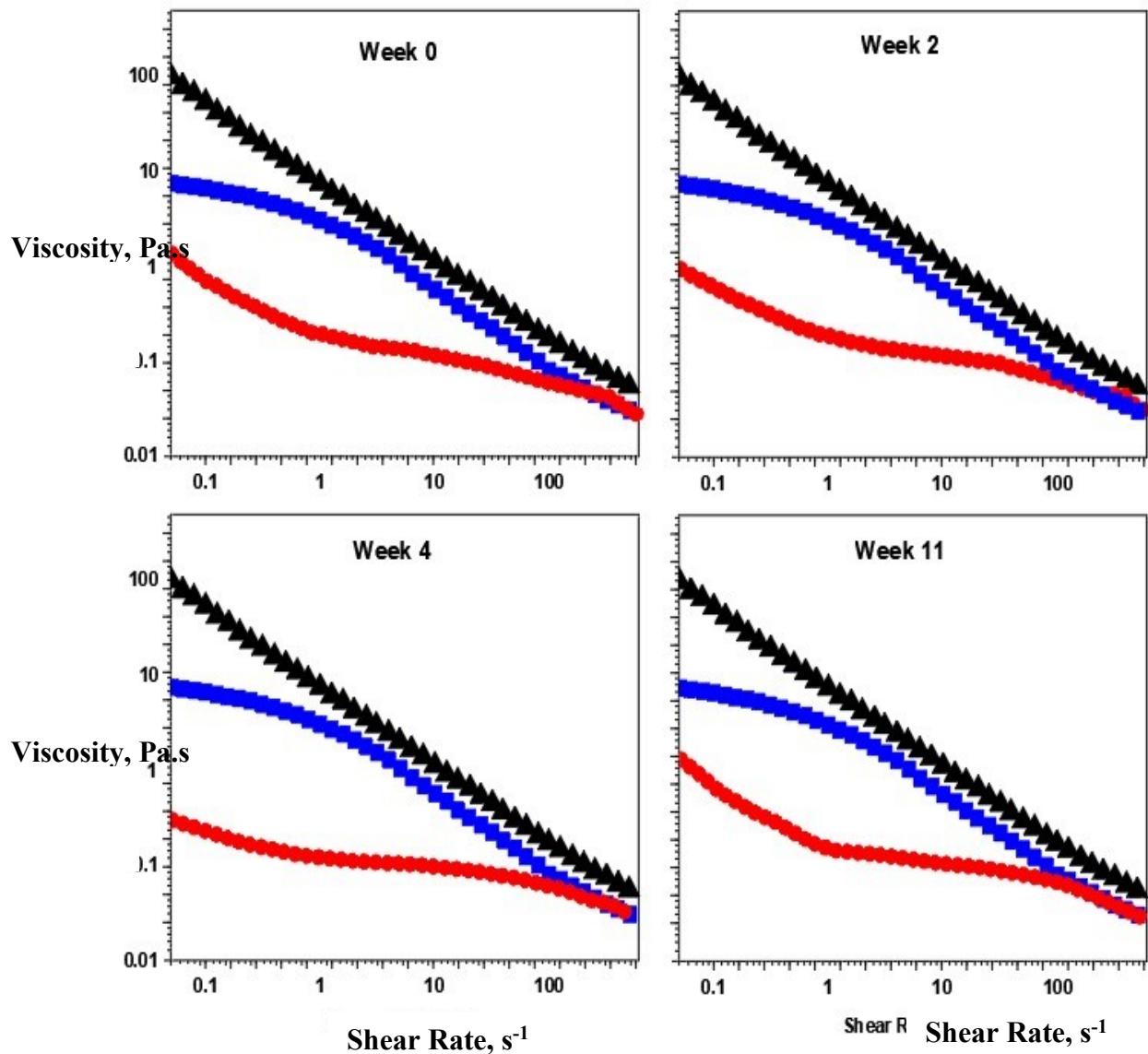


Figure 16: Viscosity vs. Shear rates (Necla 2015).

Jordan et al. (2015) modified xanthan gum using locust bean gum (LBG) in the presence of silicon dioxide nanoparticles. These researchers characterized the rheological responses for xanthan gum solutions and studied the impacts of polymer/particle interactions with changes in nanoparticle concentration. The concentration they used for their polymers was 1% per each polymer solution and a 1:1 ratio of xanthan and LBG. This ratio resulted in a 1% w/v total polymer concentration with nanoparticle concentrations varying from 1% to 10% by weight. In their work, no salts were added and the pH was neutral at 7. They found that the modified solution's viscosity increased. For example, at a  $10 \text{ s}^{-1}$  shear rate, the xanthan viscosity was around 3 cp, while it was approximately 6 cp for modified xanthan gum. Moreover, the viscosity of the xanthan gum clearly improved by adding 10%  $\text{SiO}_2$  nanoparticles. This was caused by the interaction between silanol groups on the surface of the silicon dioxide and carboxylic groups ( $\text{COOH}$ ) with the trisaccharide side chains through hydrogen bonding within the xanthan. The addition of 1% silica nanoparticles did not affect the behavior of the solution in terms of viscosity. Conversely, at 10%  $\text{SiO}_2$ , the viscosity increased sharply.

Wei et al. (2015) conducted an experimental study that investigated the relationships among rheological properties and flow in porous media during enhanced oil recovery, using the following three polymers: xanthan gum, HPAM, and HMSPAM. For porous media, they used granular pack composed of glass beads with an average size range of 80 to 200  $\mu\text{m}$ . The permeability was around 3,500 md and porosity was approximately 40%. For the rheological analysis, at lower shear rates, the xanthan gum exhibited greater viscosity than did the HPAM or HMSPAM. The reverse was true at higher shear rates. However, for recovery under the same applied conditions, xanthan gum and HMSPAM

recovered around 15% more of the IOIP than did the HPAM, due to their high mobility control abilities. The researchers claimed that the control capacity of the HMSPAM's mobility was governed by a permeability reduction, while the xanthan case was more likely governed by viscoelastic properties, to some extent leading to low adsorption and high mechanical stability (i.e., a piston-like flood). The recovery results are summarized in Table 1 and Figure 17.

**Table 1: Oil Recovery Results**

Flood Type	HPAM	Xanthan	HMSPAM
Water flood	34.7%	33.3%	34.5%
Polymer flood	33.5%	49.4%	30.7%
Post-water flood	0.7%	1.8%	17.5%
Cumulative	68.9%	84.5%	82.7%

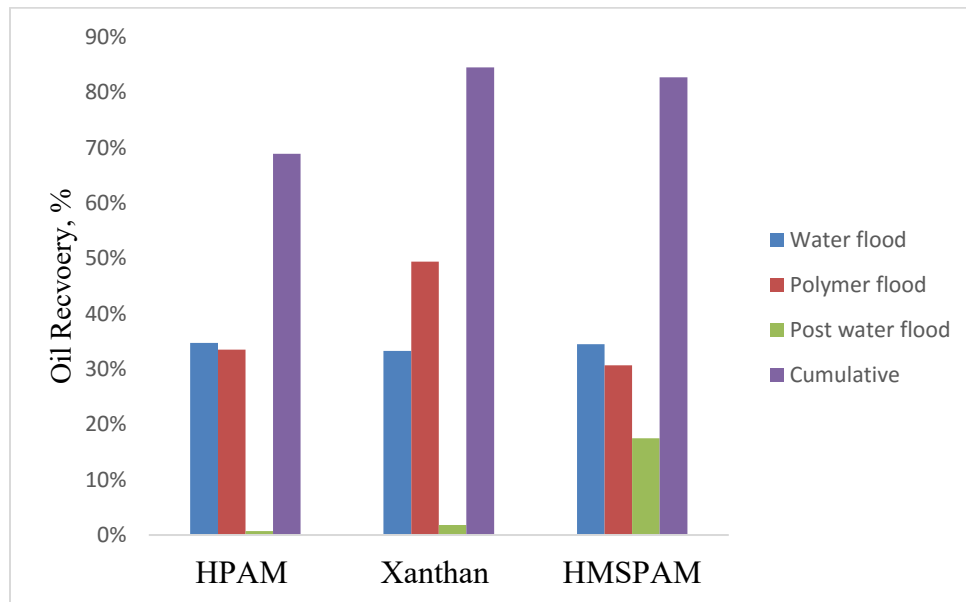


**Figure 17: Oil recoveries from three polymer floods (Wei et al., 2015).**

Jang et al. (2015) compared xanthan gum viscosities with different salinities used in the recovery of heavy oil. First, they studied changes in xanthan viscosity resulting from

increasing the xanthan concentration and salinity. For porous media floods, they used glass beads with a 36.9% porosity and 3,790 md permeability. The viscosity of the crude oil was 45 cp and the flow rate was 4 ml/min. The oil recoveries for xanthan with 3% NaCl and 10% NaCl were almost the same, with differences in recovery only occurring at the early stages of polymer injection. They also compared recoveries obtained from xanthan gum and HPAM polymers (see Table 2).

**Table 2: Comparison of Xanthan and HPAM Recoveries (Jang et al., 2015).**

	Water Flooding	HPAM 3 wt%	Xanthan 3 wt%	Xanthan 10 wt%
Water flood recovery	39.0%	24.0%	24.2%	24.5%
EOR recovery	-	37.9%	44.9%	42.9%
Cumulative	39.0%	61.9%	69.1%	67.4%
Inj PV	3	0.6	0.6	0.6

Wang et al. (2016) modified xanthan gum via esterification with poly(maleic anhydride/1-octadecene) (PAMO) in order to improve viscosity through shearing and thermal effects. They called the new polymer PX. They characterized PX and XG by FT-IR, NMR, and static light scattering. FT-IR analysis emphasized a change in the chemical structure of the normal xanthan. The PX samples showed a highly enhanced absorption as a result of the new ester bond carboxylic acid group that was generated. From a thermal gravimetric analysis (TGA), the thermal stability of the XG and PX samples were almost the same, and the change was almost negligible (see Figure 18 and Figure 19).

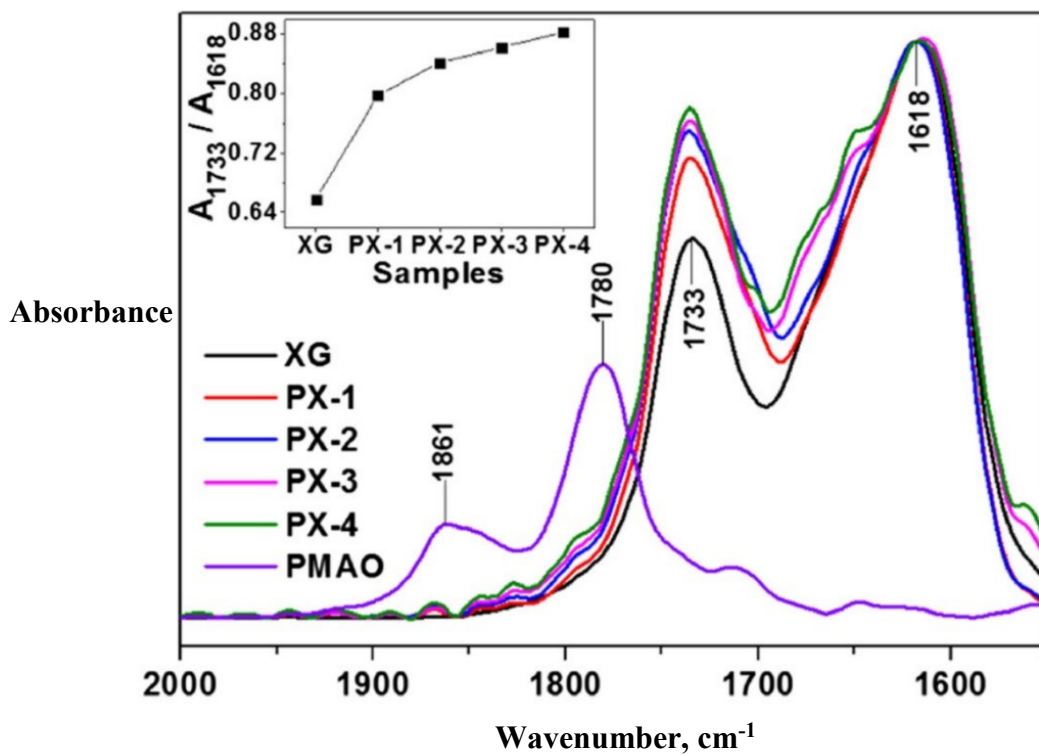


Figure 18: FT-IR spectra of XG, Px sample, and PMAO (Wang 2016).

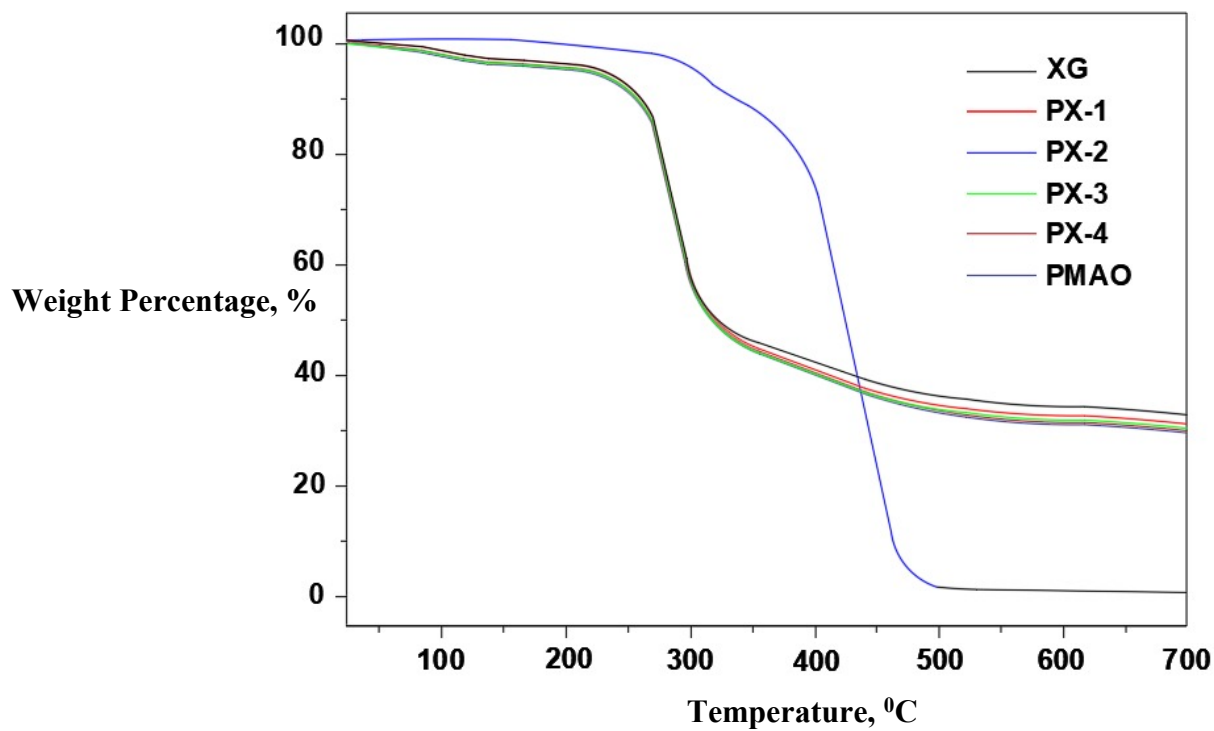


Figure 19: TGA plots for xanthan, PX, and PMAO (Wang 2016).

Due to the linkage and enhancement of the hydrophobic association, the PX samples obtained better viscosities than did the xanthan gum, as shown in Figure 20.

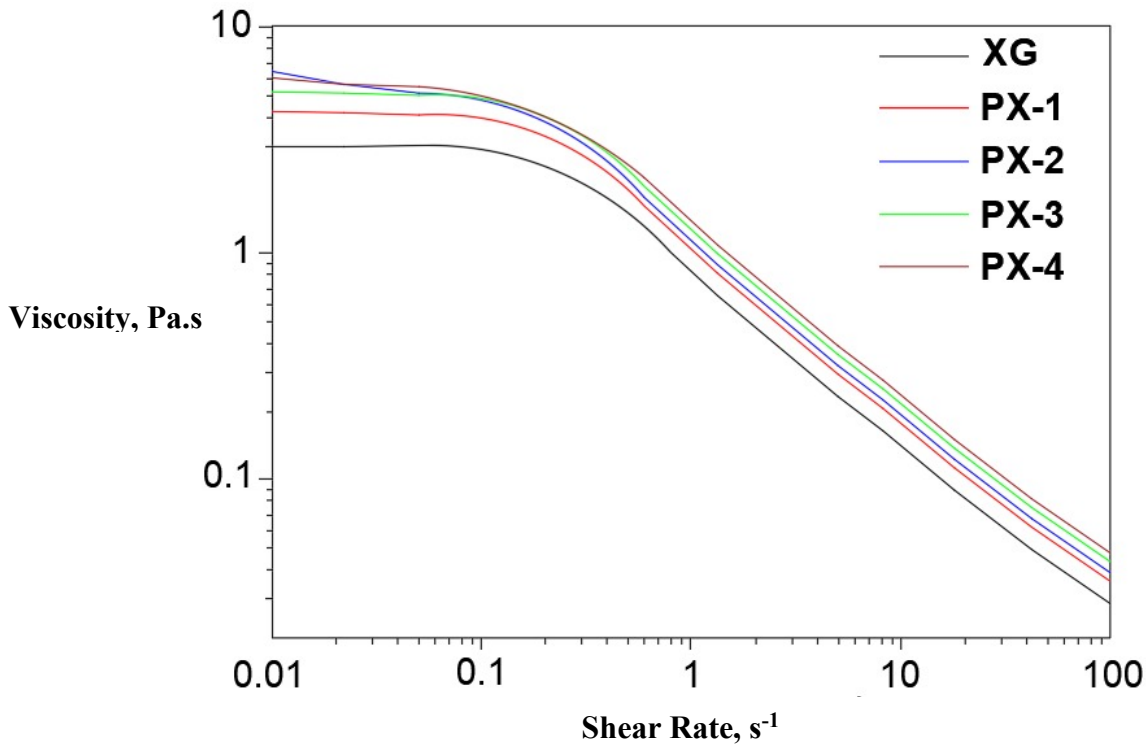


Figure 20: Viscosity vs. shear rate, 2,000 ppm at 25°C (Wang 2016).

Esraa and Attia (2016) investigated the effect of xanthan solution slug size on oil recovery. The optimum slug size was found to be 0.6 pore volume (PV), as shown in Figure 21. These researchers also investigated the optimum xanthan solution concentration for use in EOR, claiming it should be 500 ppm. The additional recovery they obtained from 500 ppm of xanthan and 3.5% NaCl was 12% of the IOIP. The recovery obtained by water flooding (i.e., secondary recovery) was 51% and the total recovery after xanthan flooding (i.e., tertiary recovery) was 63% of the IOIP.

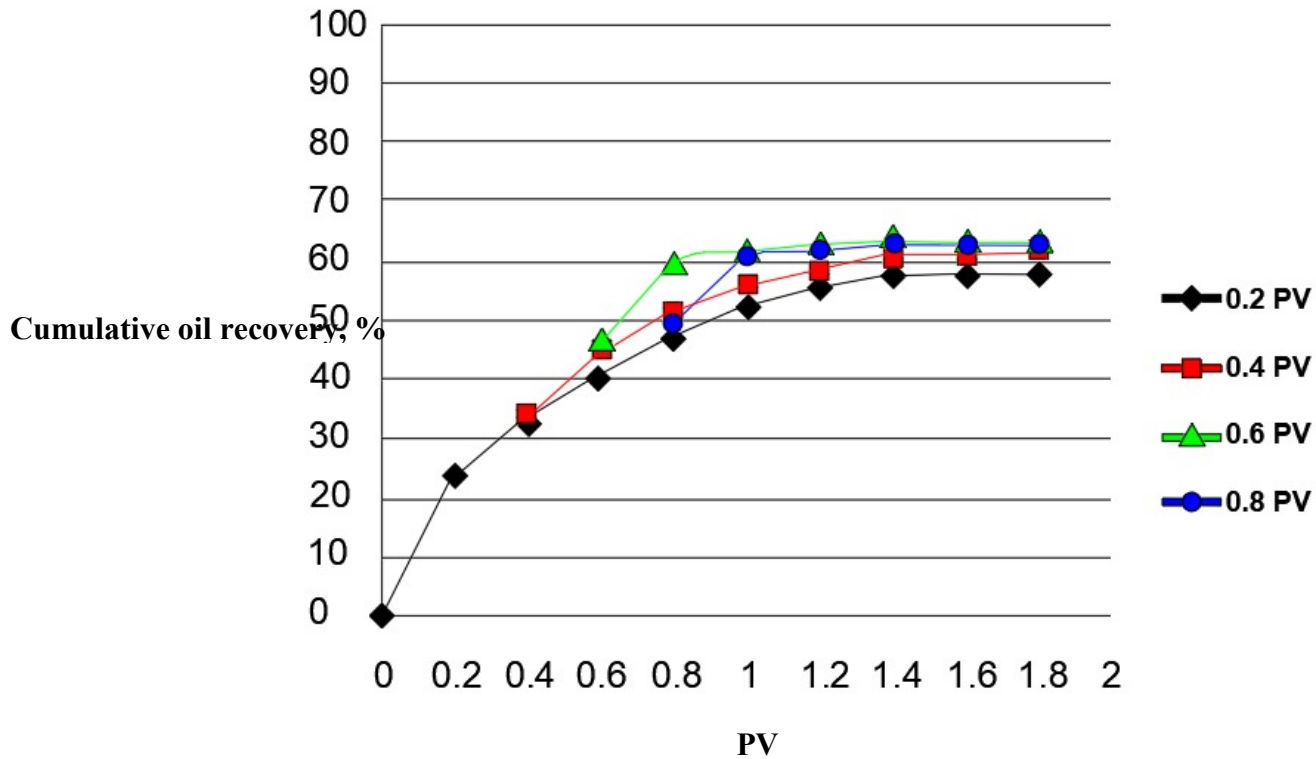


Figure 21: Effect of slug size on recovery (Esraa 2016).

Yangang et al. (2017) conducted a rheological study of xanthan, stating that at 68°C the xanthan solution displayed non-Newtonian behavior and strong shear thinning. The xanthan lost 40% of its initial value at this temperature (i.e., 68°C).

Corredor et al. (2018) developed the viscosity of xanthan gum by adding surface-modified silica nanoparticles, either through chemical or physical interaction. These researchers found that when SiO<sub>2</sub> nanoparticles were added to the xanthan gum solution, the silica surface adsorbed some polymer chains through either hydrophobic interaction or hydrogen bonding. These chains positively influenced the stability of the nanoparticles by effective steric repulsion. The interaction between the silica nanoparticles and xanthan gum occurred through hydrogen bonding between the COOH of the silica and carboxyl

groups on the xanthan gum. Consequently, the viscosity of the xanthan increased, as shown in Figure 22. The concentrations used in this research were 0.4% for xanthan and 2% for silica.

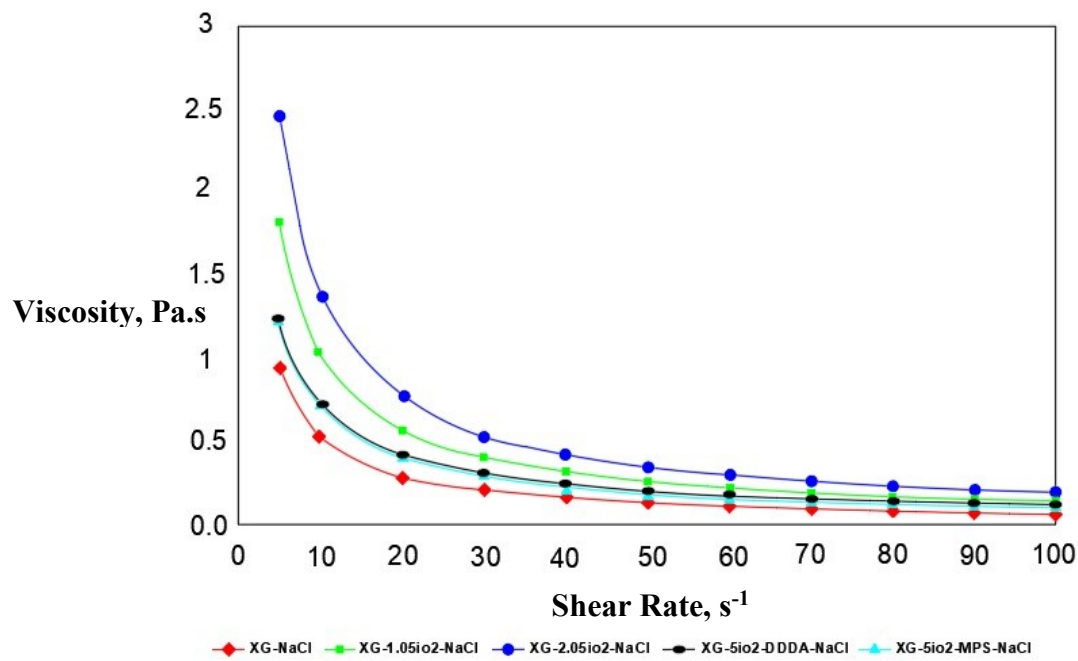


Figure 22: Viscosity of XG nanopolymer vs. shear rate (Corredor 2018).

## 2.2 Summary of Literature Review and Knowledge Gap

### 2.2.1 Literature Review Summary

Table 3 summarizes the previous research, which involving the use of Xanthan gum in EOR, and its modifications to improve its properties and applications.

**Table 3 Literature Review Summary**

<b>Author</b>	<b>Title</b>	<b>Procedure</b>	<b>Results</b>
<b>Avery, 1986</b>	Use of Cross-linked Xanthan Gels in Actual Profile Modification Field Projects	Modified xanthan by crosslinking with chromium ions to form a gel	Obtained gel had a very high shear stability
<b>Chang, 1988</b>	Selective Emplacement of Xanthan/Cr(III) Gels in Porous Media	Improved xanthan viscosity by crosslinking with chromium ions	The viscosity's rate of changing the viscosity was lessened, meaning shear thinning decreased
<b>Eggert, 1992</b>	Experimental Measurement of the Persistence of Permeability Reduction in Porous Media Treated with Xanthan/Cr(III) Gel Systems	Studied permeability reduction in unconsolidated sand packs due to xanthan gel by crosslinked chromium	Swelling and syneresis were observed; swelling was observed because the gel adsorbed the solvent and thus its volume increased
<b>Broseta, 1995</b>	Polymer Adsorption/Retention in Porous Media Effects of Core Wettability and Residual Oil	Conducted flood tests on sandstone cores to study the effects of the presence of oil and core wettability on polymer adsorption/retention	With residual oil, adsorption decreased sharply for oil wet cores, and slightly increased for water wet cores in the presence of oil
<b>Su, 2002</b>	Chemical Modification of Xanthan Gum to	Used formaldehyde to modify xanthan gum to	Dissolution rate increased compared to normal xanthan gum; FT-IR and X-ray

	Increased Dissolution Rate in Carbohydrate Polymers	improve dissolution rate	diffraction spectra showed changes in the xanthan gum's molecular structure
<b>Reddy, 2012</b>	Chemical Modification of Biopolymers to Design Cement Slurries with Temperature-Activated Viscosification	Modified xanthan gum for cementing purposes via organic carbonates, including: ethylene carbonate, propylene carbonate, butylene carbonate, diethyl carbonate, and glycerin carbonate	Modified polymer showed higher viscosities, and acidic materials did not increase the solubility of the modified polymers
<b>Sun et al., 2013</b>	Construction and Evaluation of an Exopolysaccharide Producing Engineered Bacterial Strain by Protoplast Fusion for Microbial Enhanced Oil Recovery	Investigated improved recovery through an exopolysaccharide polymer	Recovery of crude oil from two sand packed columns increased by 3% and 11% for low and high permeabilities, respectively
<b>Wei et al., 2014</b>	Evaluation of Two New Self-assembly Polymeric Systems for Enhanced Heavy Oil Recovery	Added $\beta$ -cyclodextrin, a surfactant, to xanthan and studied the rheological parameters and flow behavior in porous media	The surfactant/polymer viscosity increased, as did the resistance factor
<b>Bernd et al., 2015</b>	Field Testing the Polysaccharide Schizophyllan: Results of the First Year	Compared schizophyllan, HPAM, and xanthan gum viscosity stability values over time	Emphasized that schizophyllan is a promising biopolymer for EOR in harsh reservoir conditions
<b>Gao, 2015</b>	Application of a Novel Biopolymer to Enhanced Oil	Used schizophyllan for EOR; compared changes in viscosity among schizophyllan, xanthan,	Schizophyllan had the highest viscosity of the three polymers, and when used in flooding, it gave more than

	Recovery	and HPAM, with changes in temperature.	20% additional recovery
<b>Necla et al., 2015</b>	Mechanically Modified Xanthan Gum: Rheology and Polydispersity Aspects	Treated xanthan gum solutions with high-pressure homogenization	The physical modification yielded a very low recovery in terms of viscosity, indicating that the changes obtained by high shear treatments were irreversible
<b>Wei et al., 2015</b>	Flow Characteristics of Three Enhanced Oil Recovery Polymers in Porous Media	Investigated the relationships among rheological properties and flow in porous media-enhanced oil recovery of xanthan gum, HPAM, and HMSPAM	Xanthan gum and HMSPAM recovered around 15% of the IOIP in total, more than HPAM, due to their high mobility control abilities
<b>Jang et al., 2015</b>	Enhanced Oil Recovery Performance and Viscosity Characteristics of Polysaccharide Xanthan Gum Solution	Compared xanthan gums with different salinities for enhanced heavy oil recovery	Salinity affected xanthan viscosity; recoveries from 3% and 10% NaCl were almost the same
<b>Jordan et al., 2015</b>	Rheology of Dispersions of Xanthan Gum, Locust Bean Gum, and Mixed Biopolymer Gel with Silicon Dioxide Nanoparticles	Modified xanthan gum using locust bean gum in the presence of silicon dioxide nanoparticles	Xanthan viscosity clearly improved with 10% SiO <sub>2</sub> nanoparticles as a result of the interaction through hydrogen bonding between the silanol groups on the surfaces of the silicon dioxide and carboxylic groups (COOH) located on the trisaccharide side-chains in the xanthan

<b>Wang et al., 2016</b>	Synthesis and Characterization of Modified Xanthan Gum using Poly(maleic anhydride/1-octadecene)	Modified xanthan gum by esterification with poly(maleic anhydride/1-octadecene) to improve viscosity through shearing and thermal effects	FT-IR analysis emphasized a change in the chemical structure of the normal xanthan; PX samples showed highly enhanced absorption because of a new ester bonds carboxylic acid group generated
<b>Esraa &amp; Attia, 2016</b>	Optimum Polymer Concentration in EOR	Investigated the effects of xanthan solution concentration and slug size on oil recovery	Optimum slug size for oil recovery was found to be a 0.6 pore volume; optimum xanthan concentration for EOR was 500 ppm
<b>Yangang, 2017</b>	Dendrimer-Based Demulsifiers for Polymer Flooding Oil-in-Water Emulsions	Conducted a rheological study of xanthan	At 68 <sup>0</sup> C, the xanthan solution displayed non-Newtonian behavior and strong shear-thinning; xanthan viscosity loss reached 40 % of its initial value at this temperature
<b>Corredor et al., 2018</b>	Improving Polymer Flooding by Addition of Surface Modified Nanoparticles	Developed the viscosity of xanthan gum by adding surface-modified silica nanoparticles, resulting in either a chemical or physical interaction	When SiO <sub>2</sub> nanoparticles were added to xanthan gum solution, the silica surface adsorbed some polymer chains through hydrophobic interaction or hydrogen bonding; these chains positively influenced the stability of the nanoparticles by effective steric repulsion

### **2.2.2 Knowledge Gap**

From this literature review, it can be seen that the use of xanthan gum in EOR has recently increased. However, only limited research has been conducted on green EOR. Consequently, to the best of our knowledge there is a gap in terms of using acrylic acid to modify xanthan gum for EOR purposes. This work examines the possibility of improving the performance of xanthan gum in EOR by adding acrylic acid. Core flood experiments were conducted to study the effects of this modification.

## CHAPTER 3

### METHODOLOGY

This research presents an experimental study illustrating the relationships among the rheological properties and enhanced oil recovery (EOR) performance of xanthan gum and modified xanthan gum polymers.

This chapter discusses the materials and methods used in this research.

#### 3.1 Materials

The materials used for this work are outlined below.

##### 3.1.1 Brine

The brine used in the core flood experiments was 3% NaCl (30,000 ppm of the total weight). From previous lab experiments, it was determined that a 3% salinity is the minimum concentration required to prevent swelling in sandstone cores.

##### 3.1.2 Crude Oil

The oil used in this research was Arabian light oil, with a 31.14 API and 0.87 g/cc density when measured at 23<sup>0</sup>C (i.e., room temperature). The viscosity was 19.8 cp at 25<sup>0</sup>C.

##### 3.1.3 Xanthan Gum

Xanthan gum is an anionic polysaccharide polymer produced by fermentation. It is composed of a  $\beta$ -(1 $\rightarrow$ 4)-D-glucopyranose glucan backbone with side chains of (1 $\rightarrow$ 3)- $\alpha$ -D-mannopyranose-(2 $\rightarrow$ 1)- $\beta$ -D-glucuronic acid-(4 $\rightarrow$ 1)- $\beta$ -D-mannopyranose on

alternating residues. Approximately half of the terminal mannose residues are 4,6-pyruvated, while most of the inner mannose residues are 6-acetylated (Sworn, 2009). The xanthan gum used in the present research was obtained from Sigma Aldrich. Its chemical structure is depicted in Figure 23.

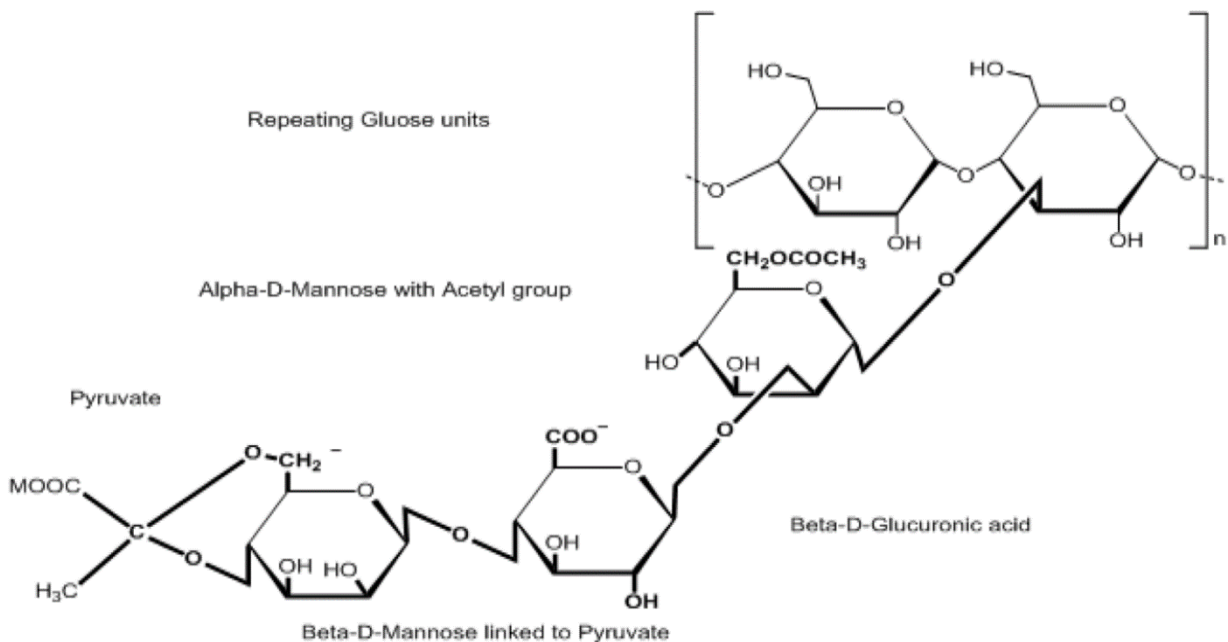


Figure 23: Chemical structure of xanthan gum (Sworn, 2009).

### 3.1.4 Acrylic Acid

Acrylic acid is hygroscopic, brittle, and colorless in nature, with a boiling point of nearly 141°C. At temperatures between 200°C and 250°C, it loses water and becomes an insoluble cross-linked polymer anhydride. The solubility of dried PAA in water increases with a rise in temperature (Sigmaaldrich), as shown in Figure 24.

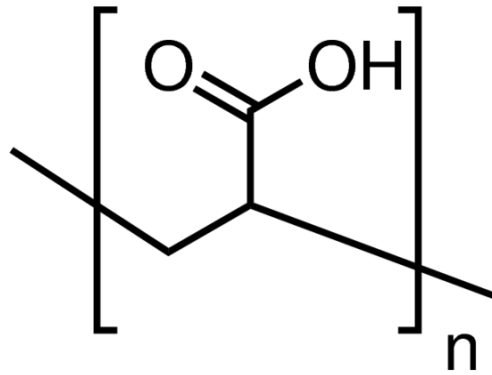


Figure 24: Chemical structure of acrylic acid (Sigmaaldrich).

### 3.1.5 Dimethylaminopropyl

This catalyst was used in the chemical reaction; it was acquired from SOMATCHO.

## 3.2 Experimental Procedure

The experiments were conducted using the concept of a chemical reaction between xanthan gum and acrylic acid. A rheological analysis was also performed. Finally, the xanthan and modified xanthan gum recoveries were compared via core flood experiments. The experimental work is described below.

### 3.2.1 Solution Preparation

First, to illustrate the change of xanthan viscosity, a solution with 0.5% xanthan was prepared with distilled water. This allowed us to study the polymer's behavior at different temperatures (i.e., 25<sup>0</sup>C, 40<sup>0</sup>C, 50<sup>0</sup>C, 60<sup>0</sup>C, and 80<sup>0</sup>C) at varying shear rates. The polymer was prepared by mixing xanthan with distilled water and stirring for 24 hours at 400 RPM. After that, the gum was prepared with 2% NaCl brine to simulate reservoir conditions, since the water used in the fields is brine (see Figure 25). Based on the literature, the xanthan concentration used in the core flood experiments was 1,500 ppm.



Figure 25: Magnetic stirrer.

### 3.2.1.1 Polymer Synthesis:

#### a. Physical Blending:

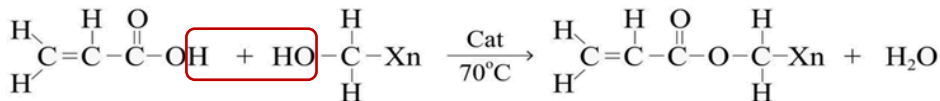
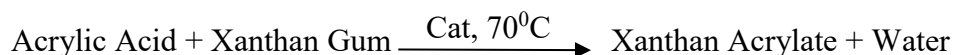
In this method, Xanthan gum solution is being physically mixed with acrylic acid and gluconic acid respectively.

#### b. Chemical Modification:

##### 1- Stoichiometry:

The stoichiometry balance between Xanthan gum and acrylic acid is the following:

First, Xanthan gum chemical formula:  $C_{35}H_{49}O_{29}$  and it has a molar mass of 701g. For acrylic acid, the chemical formula is  $C_3H_4O_2$  and it has 56g in molar mass. Therefore, the chemical reaction between Xanthan gum and acrylic acid is conducted by forming a chemical bond between carbon atom from Xanthan gum and oxygen atom in acrylic acid. In addition to that, a hydrogen atom from acrylic acid joins the hydroxyl group (OH) from Xanthan gum forming a water molecule as following:



(2)

## 2- Reaction Procedure

Xanthan gum was chemically modified using acrylic acid as following:

- 1- Dissolve 1g of Xanthan gum in 120 mL water under magnetic stirring for 22 h.
- 2- Heat up to a temperature of 70 °C under stirring of the Xan solution.
- 3- Add acrylic acid (67 mg) drop-wise to the solution
- 4- Add N-[3-(dimethylaminopropyl)]-N-ethylcarbodiimide hydrochloride (196 mg) to the solution and continue stirring 24 h.
- 5- Add 150ml acetone to the mixture and gently stir to precipitate the polymer.
- 6- Filter the solution to separate the polymer.
- 7- Rinse the product alternatively 4/5 times with ethanol/water mixture (ethanol 75 ml + water 25 ml).
- 8- Rinse the product again using only ethanol (100 ml).

9- Dry the product in a vacuum oven at 30°C.

### 3.2.2 Rheological Properties Measurements

The first step in investigating changes in the chemical structure of the polymer was to study changes in the rheological properties. A rheometer was used to measure changes in viscosity with changes in shear rate at different temperatures up to 80°C, which was the limit of the equipment. The instrument is depicted in Figure 26.



Figure 26: Rheology meter measuring up to 80°C.

### 3.2.3 Core flooding

Core flood experiments were conducted in the Core Flooding Laboratory at King Fahd University of Petroleum and Minerals (KFUPM). The aim of the core flood experiments was to duplicate reservoir conditions and test the EOR performance. A 12-inch buff

Berea sandstone core 1.5 inches in diameter was divided into two 6-inch cores to make the results comparable.

### **3.2.3.1 Sample Preparation**

A 12-inch Berea sandstone core was selected for the core flood experiments because of the homogenous nature of its porosity and permeability. The sample preparation steps are described below.

#### **3.2.3.1.1 Core Cutting**

The core was cut into two 6-inch cores to allow for reasonable comparisons in the core flood experiments. Thus, the porosity and permeability were similar and the EOR results comparable.

#### **3.2.3.1.2 Brine Saturation**

To prepare the core samples for flooding with xanthan and modified xanthan gums, they had to be 100% saturated with 3% NaCl brine. A vacuum saturation setup was used to saturate the sample. The setup consisted of a core holder cell, vacuum pump, and injection high-pressure pump. [Figure 27](#) shows the instrument. It was used as follows.

- a. First, a dried core sample was put into the core holder cell and kept under vacuum for 45 min to evacuate the air from the sample.
- b. Second, the inlet valve was opened to let the brine solution fill the core holder.
- c. Next, a pressure gauge was connected to the outlet valve.

- d. Then, the pressure pump was connected to the inlet valve to increase the pressure up to 2,500 psi inside the cell; hence, the saturation process was conducted.
- e. The cell was kept for 24 hours under pressure to make sure the core was fully saturated.



Figure 27: Vacuum saturation setup, vacuum pump, and injection pump.

### 3.3.1 Core flood experiment

A core flooding machine was used to saturate the cores with oil and perform the core flood experiments, the goal of which was to study the improvement in oil recovery obtained by using Xanthan and modified Xanthan gum. A schematic diagram of the experimental set up is shown in Figure 28.

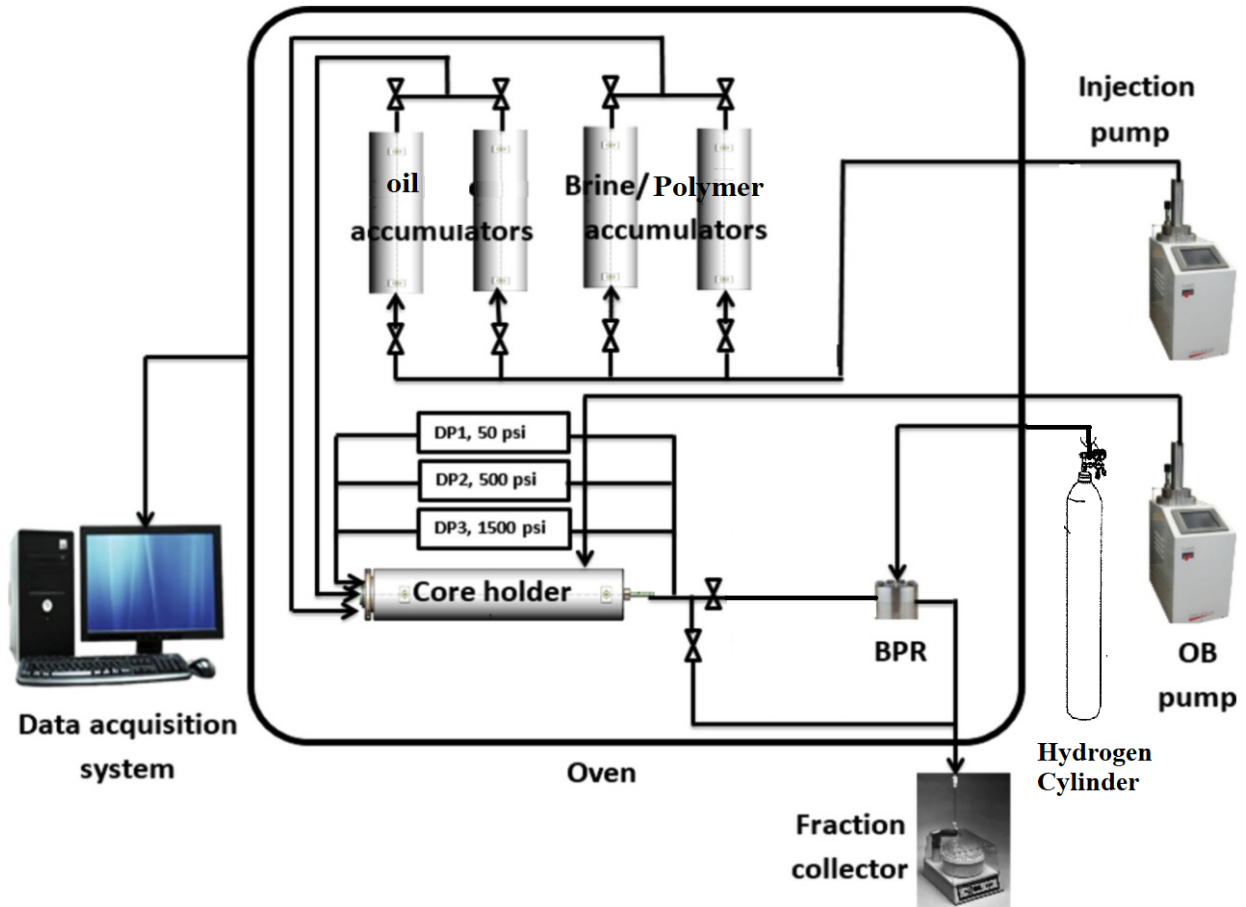


Figure 28: Core Flooding System

The experiment sequence was as follows:

### 3.3.1.1 Porosity and Permeability Calculation

After the sample was 100% saturated with brine, porosity was calculated as outlined below.

- a. The dry sample weight was measured.
- b. After brine saturation, the sample weight was again measured.

c. Then, the brine weight in the sample was calculated as: brine weight = saturated sample weight - dry sample weight.

d. To obtain the porosity, the volume of the sample was calculated as:

$$\text{core volume} = \text{area of base} \times \text{length}$$

$$= \pi \times d^2 / 4 \times L$$

e. Lastly, the porosity was calculated as: porosity = pore volume / brine sample volume.

To measure the permeability, the sample was put in the core flooding machine to flood the sample with 3% NaCl brine at different rates. The porosity and permeability calculations can be found in the Appendix.

Table 4 summarizes the porosity and permeability results.

**Table 4: Core Properties**

<b>Core plug</b>	<b>Length (cm)</b>	<b>Diameter (cm)</b>	<b>Pore volume (cc)</b>	<b>Dry weight (gm)</b>	<b>Porosity (%)</b>	<b>Permeability (md)</b>
1	15.32	3.8	20.5	363.4	19.58	102.66
2	15.09	3.8	20.25	362.3	19.78	107.30

### 3.3.1.2 Oil Saturation

1. After the sample was 100% saturated with brine, it was taken to the core flooding machine to measure the brine permeability and be saturated with oil.

2. After measuring the permeability, the core was flooded by oil with a 0.87 cc/g density and API of 31.14 at a rate of 0.5 cc/min. Three pore volumes of oil were injected to make sure no additional water was produced.
3. After that, the sample was kept in an oven for an aging time of 3 days at 50<sup>0</sup>C and 1,000 psi to simulate reservoir conditions.
4. The fluids produced were collected for each core in order to calculate the oil saturation. The values were 60.22% and 59.49% for Samples 1 and 2, respectively.

### **3.3.1.3 Water and Polymer Flooding**

- After 3 days of aging, water flooding was conducted. This was followed by polymer flooding.
- The injection rates for both the water and polymer were kept constant at 0.5 cc/min.
- The polymer concentration used for both the xanthan and modified xanthan gums was 1,500 ppm with 3% of NaCl.

The sequence of the flood experiments was as follows.

brine → xanthan gum → brine

The same sequence was used for the developed polymer.

brine → modified xanthan gum → brine

## CHAPTER 4

# RESULTS AND DISCUSSIONS

### 4.1 FT-IR and NMR Analysis

The Fourier Transform-infrared spectrum (FT-IR) is a well-known method for detecting similarities and/or differences in compound chemical structures. In this section, the FT-IR analysis that was performed on both the xanthan and modified xanthan gums is described in order to investigate the chemical modification.

#### 4.1.1 FT-IR Analysis

The FT-IR spectrum of acrylic acid (see Figure 29) shows a band at  $1698\text{ cm}^{-1}$ , which refers to the C = O stretch, followed by bands at 1,635, 1,239, 1,048, 981, 925, 813, and  $648\text{ cm}^{-1}$ , which correspond to the C = C stretch, CH in-plane bend, CH<sub>2</sub> rocking, out-of-phase CH<sub>2</sub> wag, out-of-plane CH bend, out-of-plane OH bend, CH<sub>2</sub> twist, and CO<sub>2</sub> in-plane bend, respectively. The FT-IR spectrum for the xanthan gum (see Figure 30) shows absorption peaks at  $3,277\text{ cm}^{-1}$ , which are due to the O–H axial deformation; a similar phenomenon at  $2,850\text{--}2,950\text{ cm}^{-1}$  is due to symmetric and asymmetric stretching vibrations of the C–H group in the methyl and methylene groups. The bands at  $1,710\text{ cm}^{-1}$  are due to C = O stretching vibrations, while bands nearer to  $1,601\text{ cm}^{-1}$  are due to axial deformation of the C–O of the enols. The FT-IR spectrum for the modified xanthan gum (see Figure 31) shows peaks identical to those of the xanthan gum. Additionally, a new peak appeared at  $1,645\text{ cm}^{-1}$ , assigned to C = C, which came from the acrylic acid (see

Figure 32). This confirmed a successful modification of the xanthan gum by the acrylic acid.

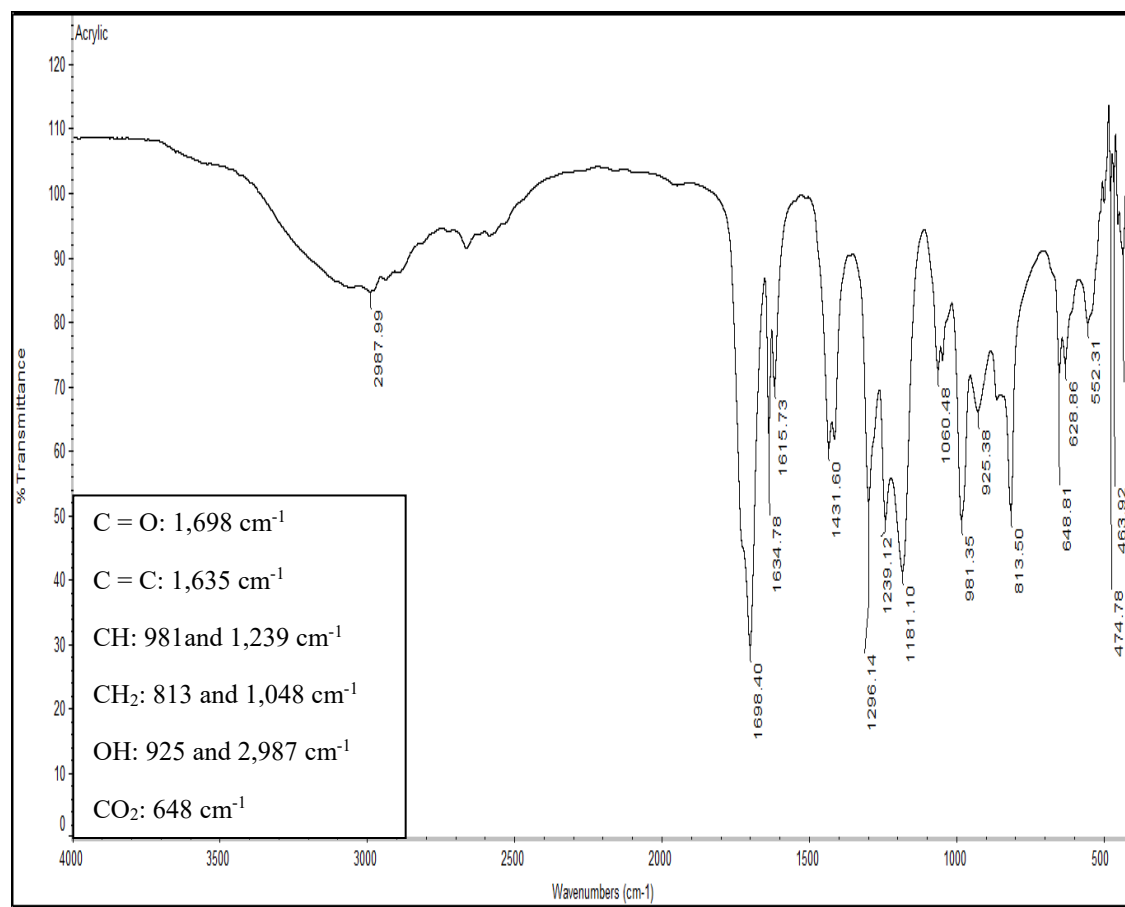


Figure 29: FT-IR spectrum of acrylic acid.

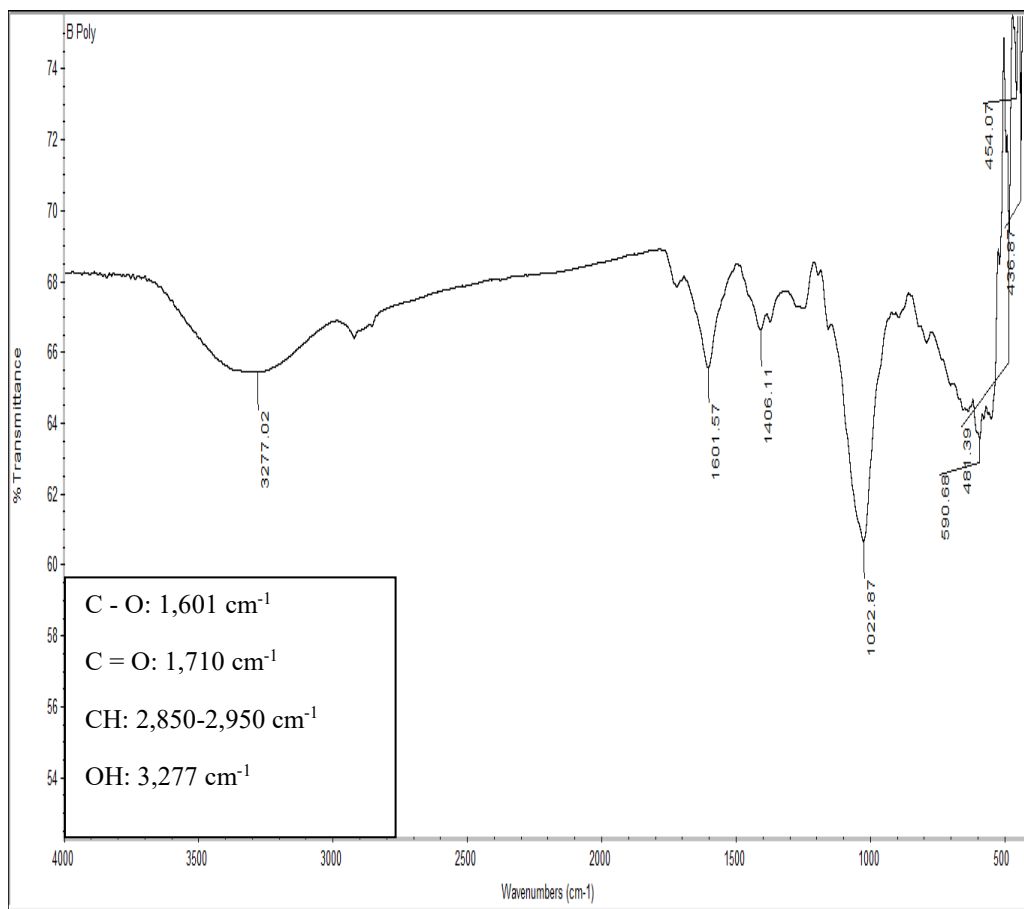


Figure 30: FT-IR spectrum of xanthan gum.

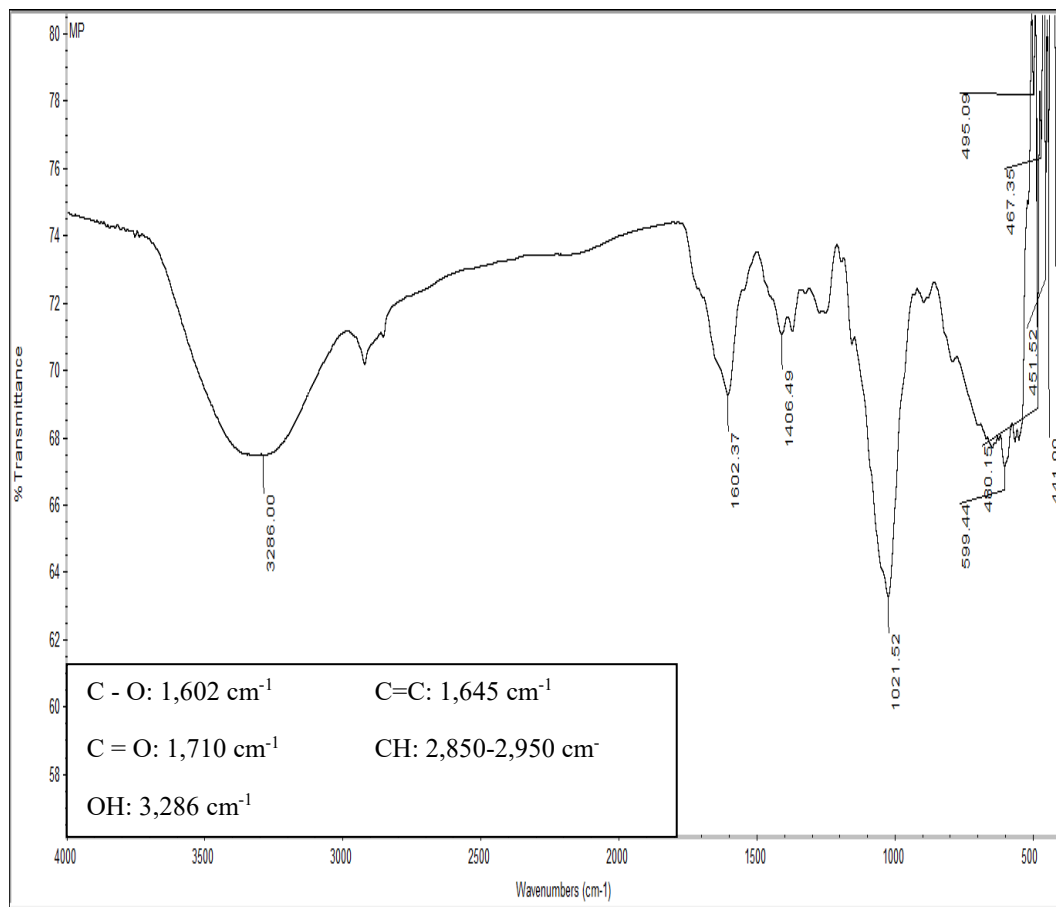


Figure 31: FT-IR spectrum of modified xanthan gum.

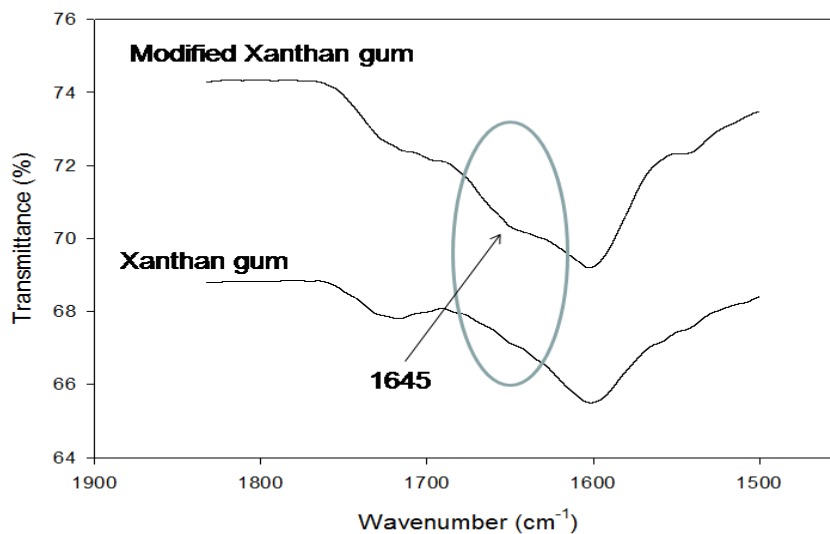


Figure 32: FT-IR spectra of two polymers.

#### 4.1.2 NMR Analysis

The <sup>1</sup>H-NMR spectrum of the xanthan gum displayed chemical shifts at  $\delta$  ppm = 1.33 (s, 3H, terminal (-CH<sub>3</sub>) group of pyruvate) and 1.53 (s, 3H, terminal -CH<sub>3</sub> group of the acetyl group in  $\alpha$ -D-mannose); the chemical shifts at  $\delta$  ppm = 2.1 correspond to (-OH and -CH<sub>2</sub>) groups of anhydro-glucose units of xanthan (see Figure 33). The <sup>1</sup>H-NMR spectrum of the modified xanthan gum displayed similar values. Additionally, a few new peaks appeared at 5.80, 6.02, and 6.41 ppm (see Figure 34). These new peaks appeared due to the new bonds with the acrylic acid. Both the FT-IR and NMR analyses confirmed a new modified xanthan polymer.

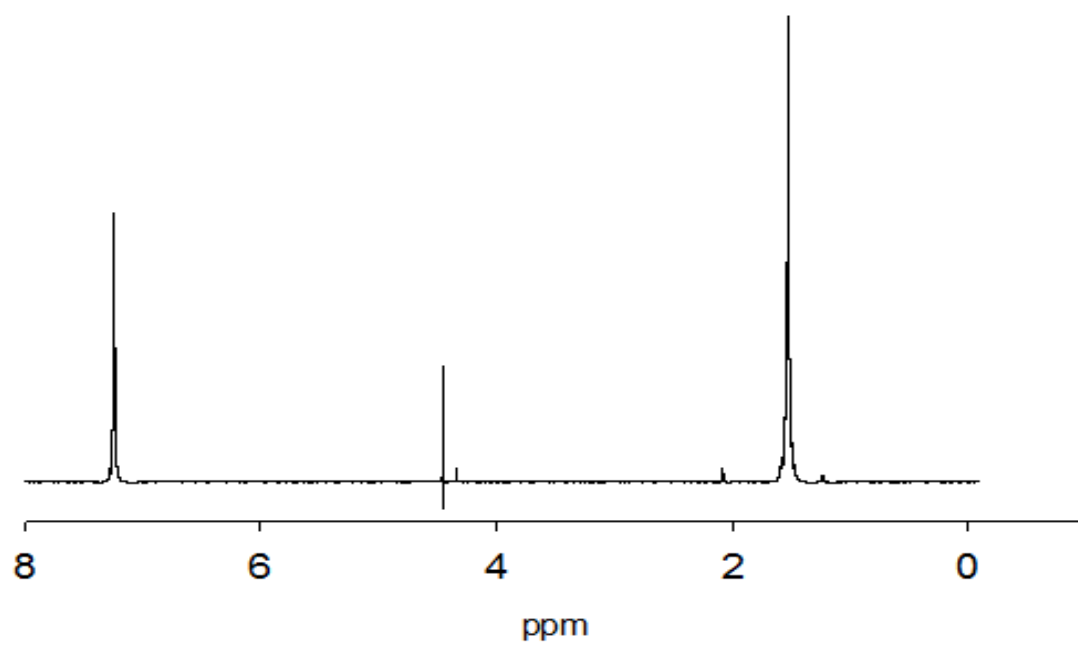


Figure 33: 1H NMR spectrum of xanthan gum.

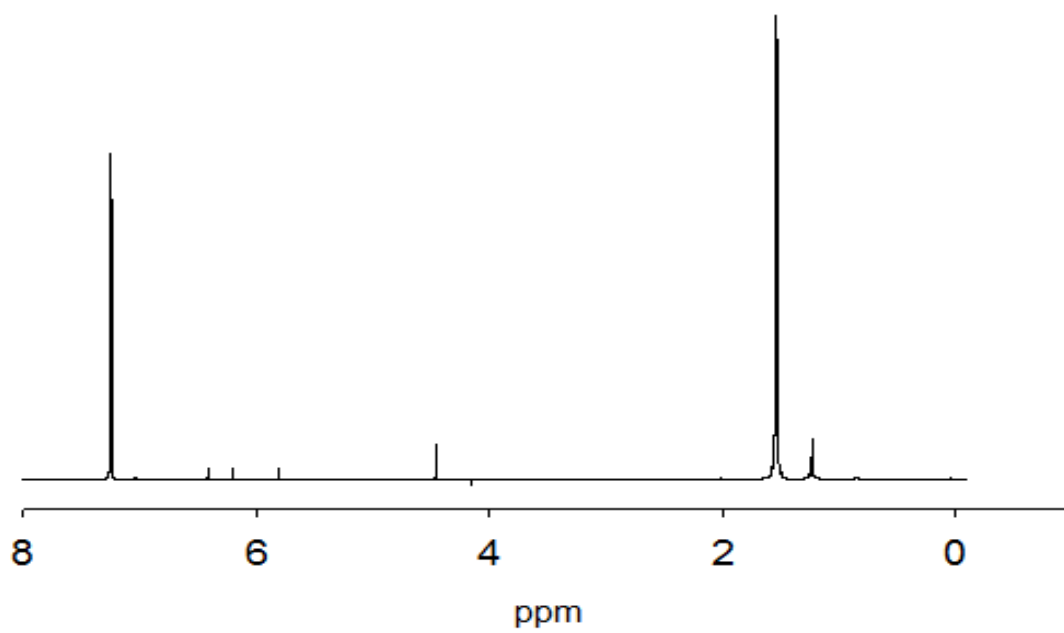


Figure 34: 1H NMR spectrum of modified xanthan gum.

## **4.2 Rheological Properties Results**

Xanthan viscosity is considered the main factor in evaluating the effectiveness of a polymer flood, since the main goal of adding polymers to water is to increase its viscosity and thus decrease the mobility ratio. The result is that the water sweep efficiency increases. Two main factors that affect polymer viscosity are temperature and solution salinity. Their effects are discussed in this section, in addition to the effects of blending the xanthan gum with PVA, gluconic acid, and acrylic acid. Moreover, the effect of chemical modification on xanthan viscosity is explained.

### **4.2.1 Effect of Temperature**

The change in viscosity of the xanthan gum was investigated by varying the temperature at different shear rates, as shown in Figure 35. The temperature was adjusted to: 25<sup>0</sup>C, 40<sup>0</sup>C, 50<sup>0</sup>C, 60<sup>0</sup>C, 70<sup>0</sup>C, and 80<sup>0</sup>C. For each test, 25 ml of xanthan solution was used. It was observed that as the temperature increased, the solution viscosity decreased. For example, at a shear rate of 1 s<sup>-1</sup>, the solution viscosity was measured at 5 cp and 1.8 cp at 25<sup>0</sup>C and 80<sup>0</sup>C, respectively.

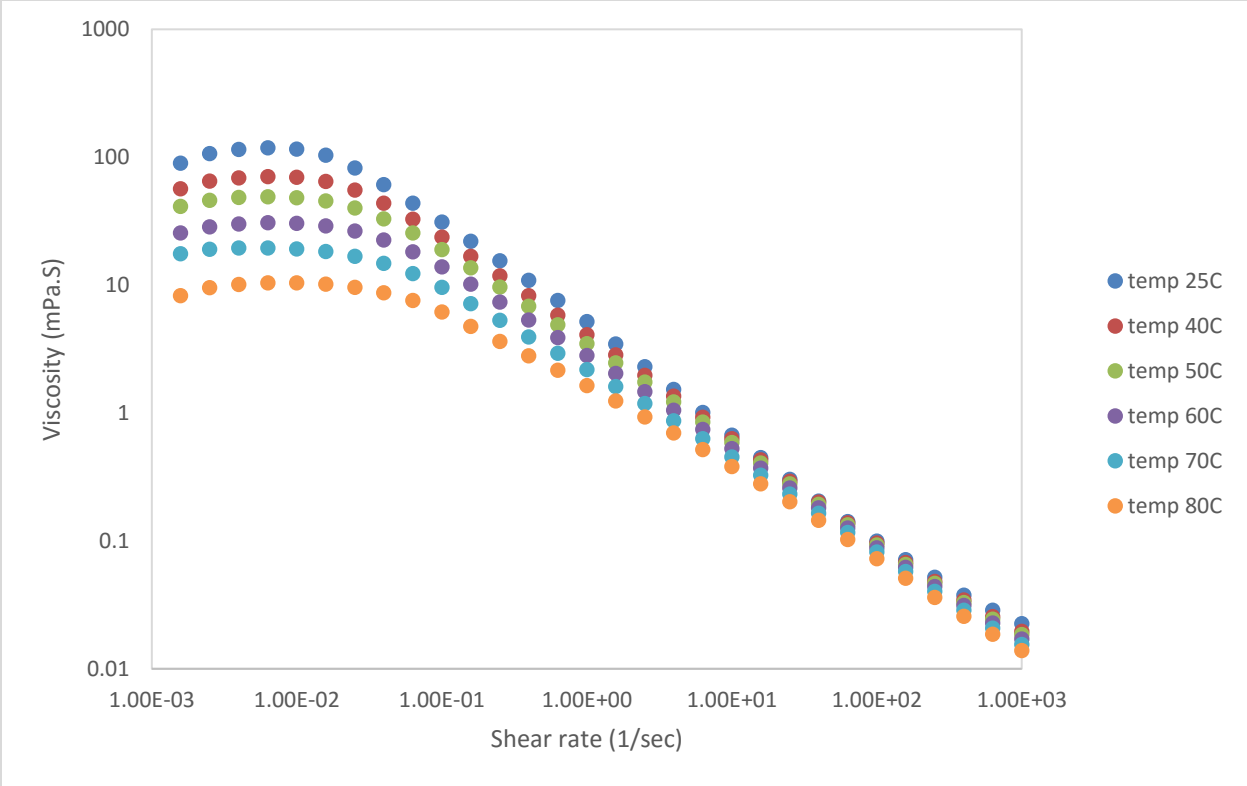


Figure 35: 0.5% xanthan viscosity vs. shear rate at different temperatures.

After analyzing the viscosity change from  $0.1 \text{ s}^{-1}$  to  $1,000 \text{ s}^{-1}$ , we found that at a given temperature, the change in viscosity with the shear rate was a power related as described in Figure 36.

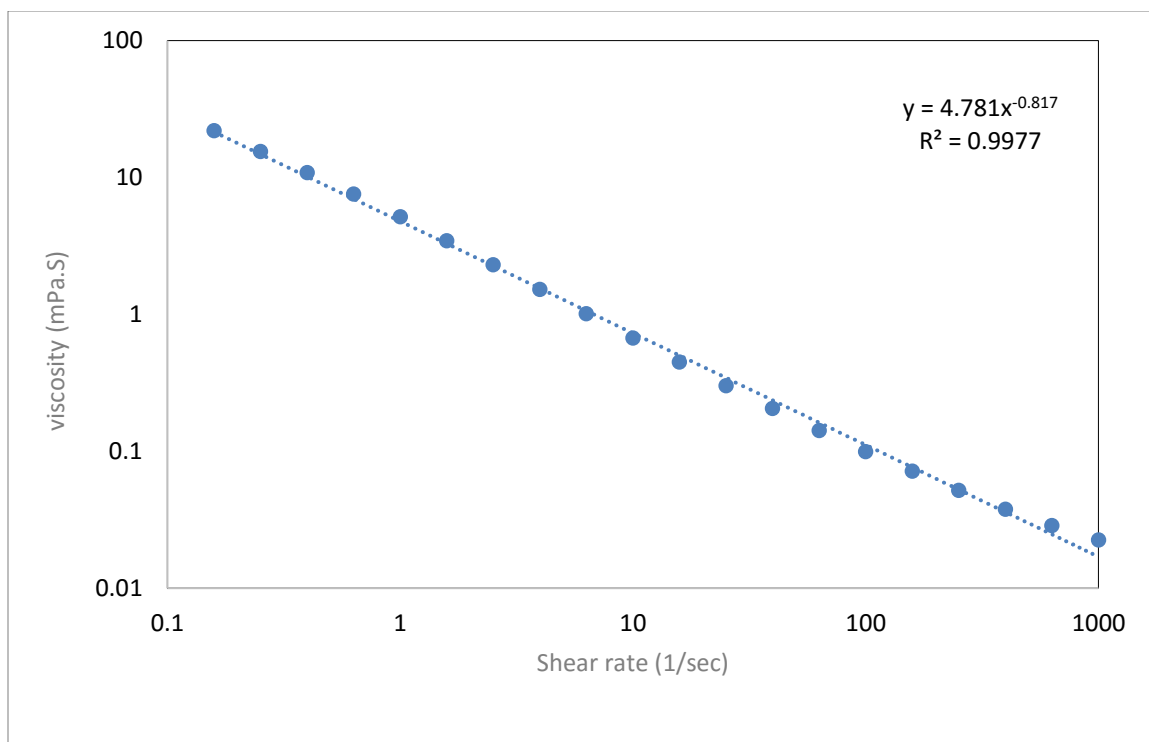


Figure 36: 0.5% xanthan gum viscosity vs. shear rate at 25°C.

#### 4.2.2 Effect of Salinity

To study the effect of salinity at a given temperature, 2% NaCl was added to 1% total weight of xanthan gum, and the viscosities were measured at different shear rates. From the experiments, it was determined that up to moderate temperatures (i.e., 50°C) and at lower applied shear rates, adding NaCl had a noticeably negative impact on the viscosity of the gum, as shown in Figure 37. However, as the shear rate increased, the effect of the NaCl was minimized and the viscosity appeared to almost be the same as if no NaCl was added, as shown in Figure 38. For example, at 50°C and a 0.01 1/sec shear rate, the gum viscosity was 48.34 mPa.S; the viscosity of the gum with the NaCl was 36.12 mPa.S. The Newtonian viscosity region was observed at a low shear rate (i.e., 0.04 S<sup>-1</sup>). Moreover, as the temperature increased, the effect of the added salt decreased until it was almost negligible at 80°C, as shown in Figure 39.

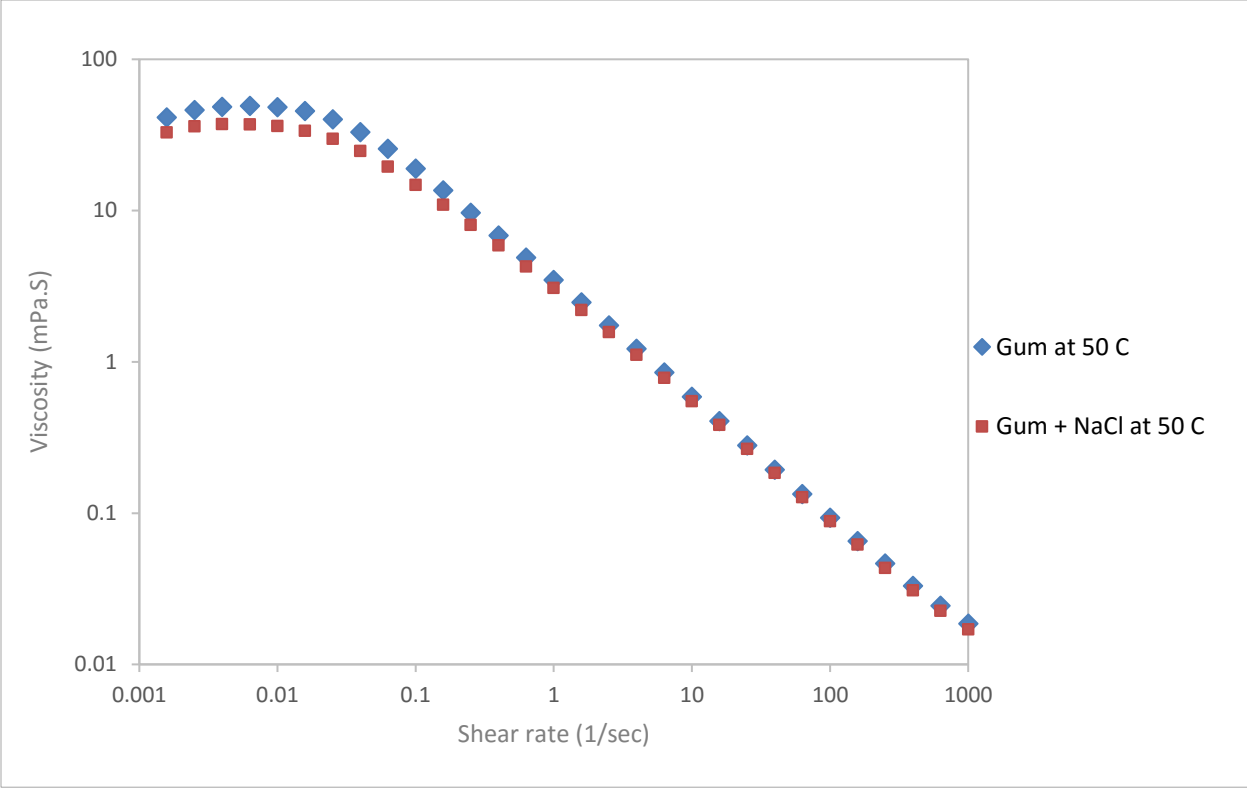


Figure 37: Effect of adding NaCl to 0.5% xanthan viscosity vs. shear rate at 50°C.

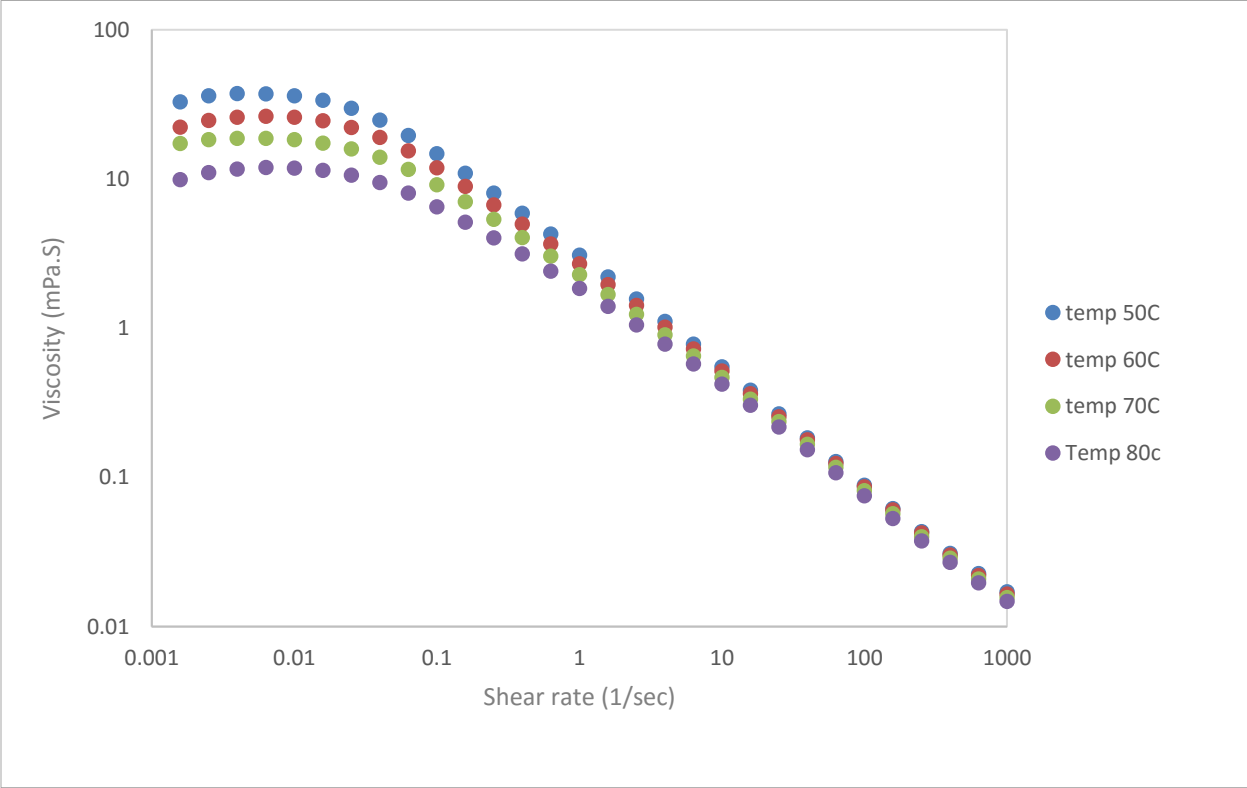


Figure 38: 0.5 % xanthan (2 wt% NaCl) vs. shear rate at different temperatures.

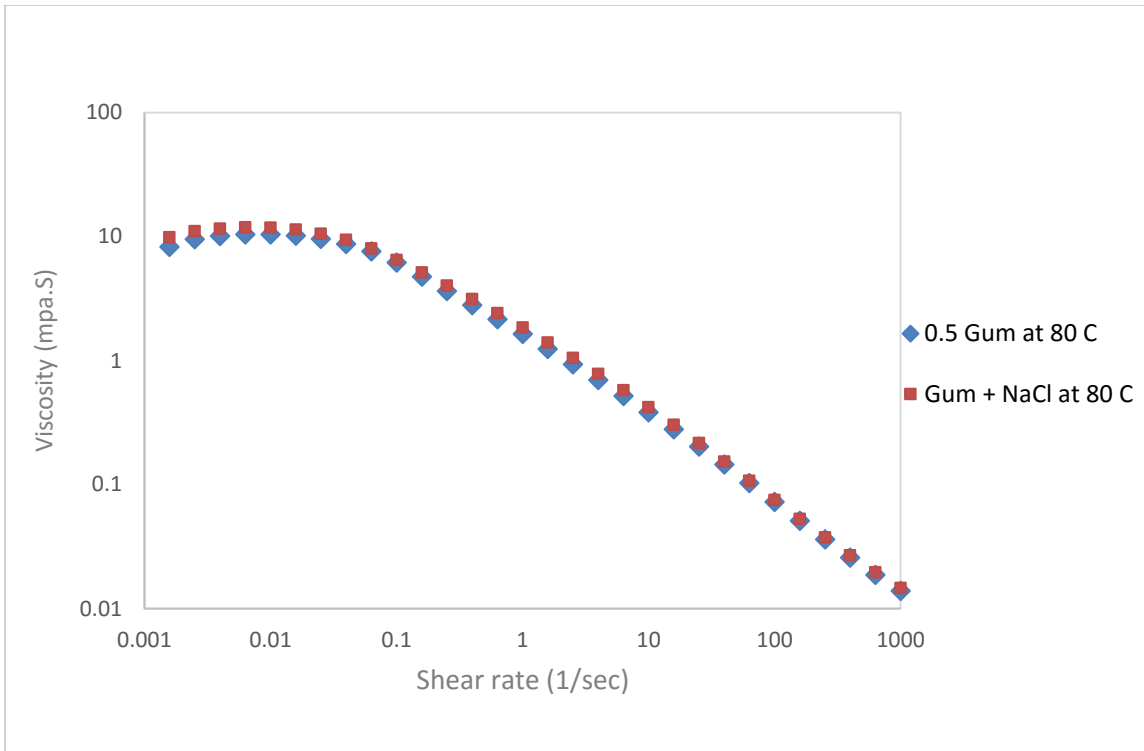


Figure 39: Effect of adding NaCl to 0.5% xanthan viscosity vs. shear rate at 80°C.

#### 4.2.3 Effect of Polyvinyl Alcohol

Temperature was kept constant to study the effect of adding polyvinyl alcohol (PVA) to the viscosity of xanthan gum at varying shear rates. From the experiments, it was determined that adding PVA resulted in a minor increase in xanthan viscosity. For example, at 50°C and a 1,000 1/sec shear rate, the gum viscosity was 0.018 mPa.S, while for the gum with PVA added, the viscosity was 0.020 mPa.S, as shown in Figure 40 and Figure 41. In addition, at 80°C and a 0.01 1/sec shear rate, the gum's viscosity was 10.41 mPa.S, while the gum with PVA had a viscosity of 11.37 mPa.S, as shown in Figure 42. However, the change in viscosity was very small and considered negligible.

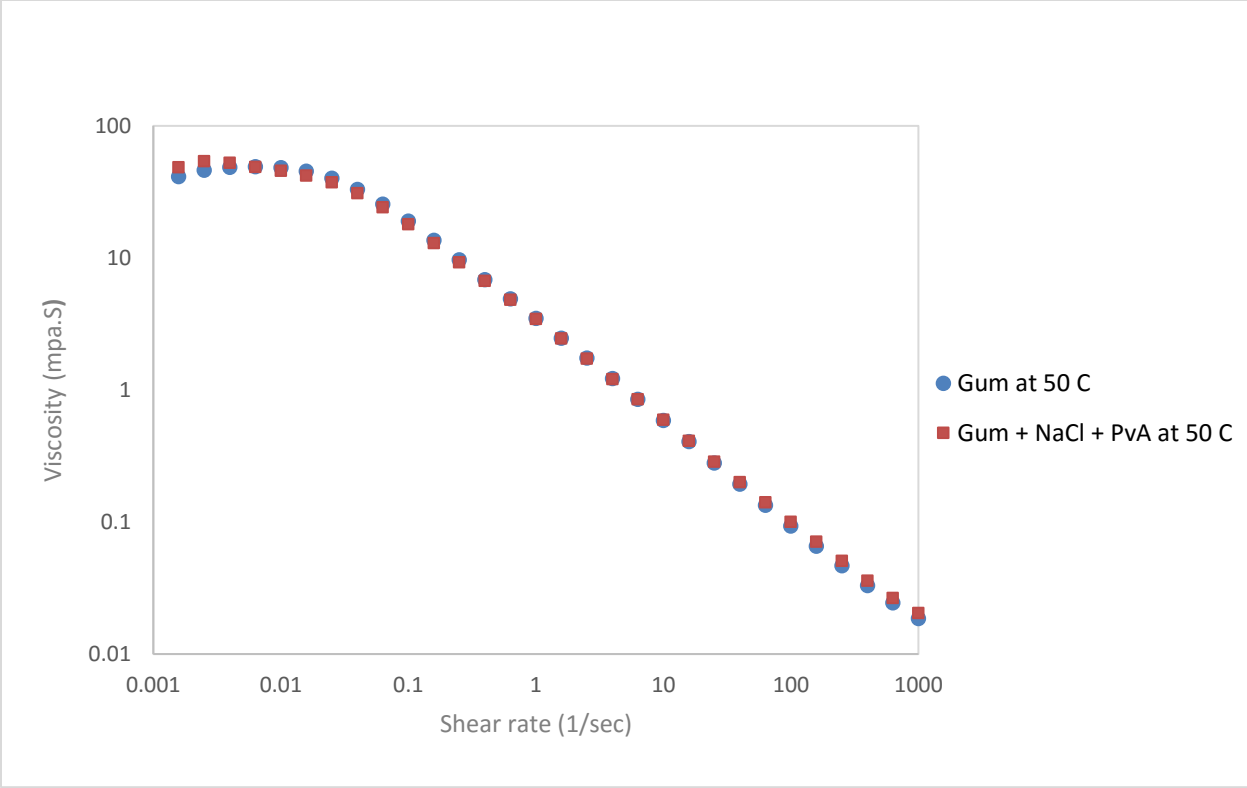


Figure 40: Effect of adding PVA to 0.5% xanthan viscosity vs. shear rate at 50°C.

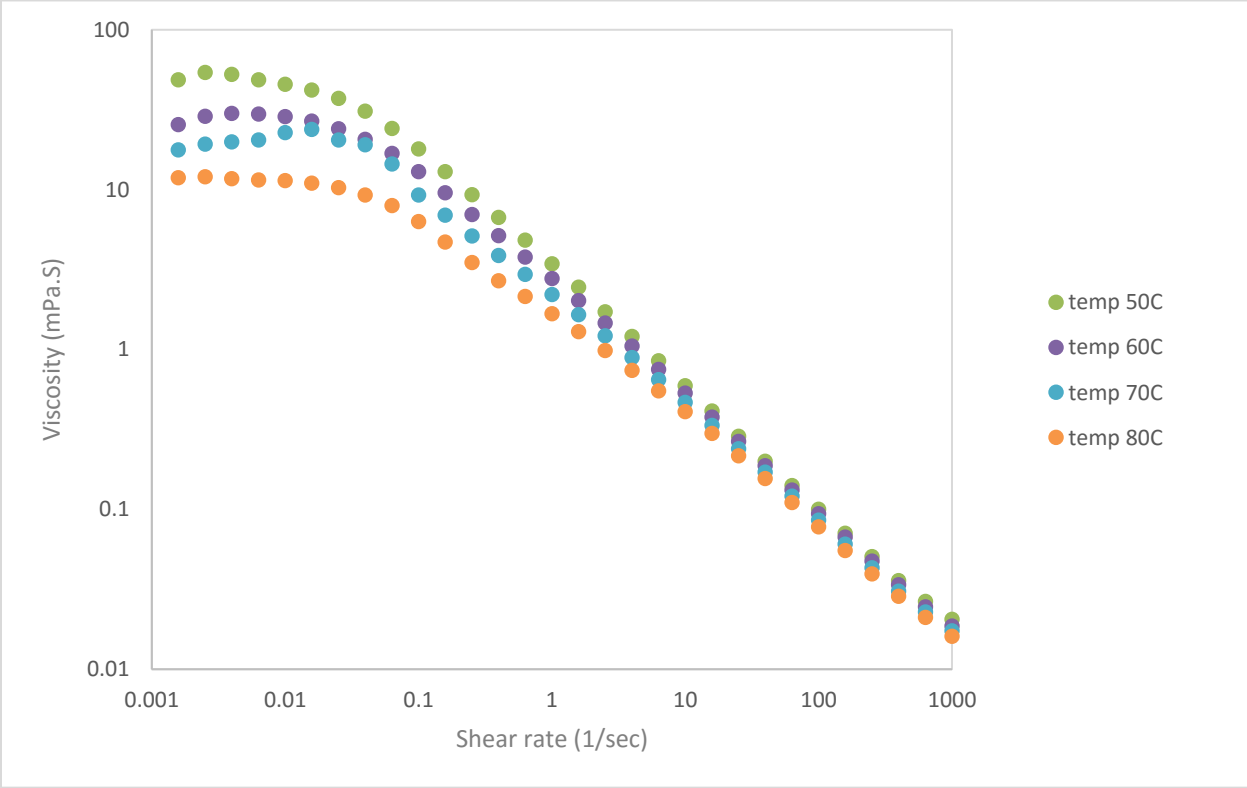


Figure 41: 0.5% Xan viscosity vs. Shear rate + 0.5% PVA at different temperatures.

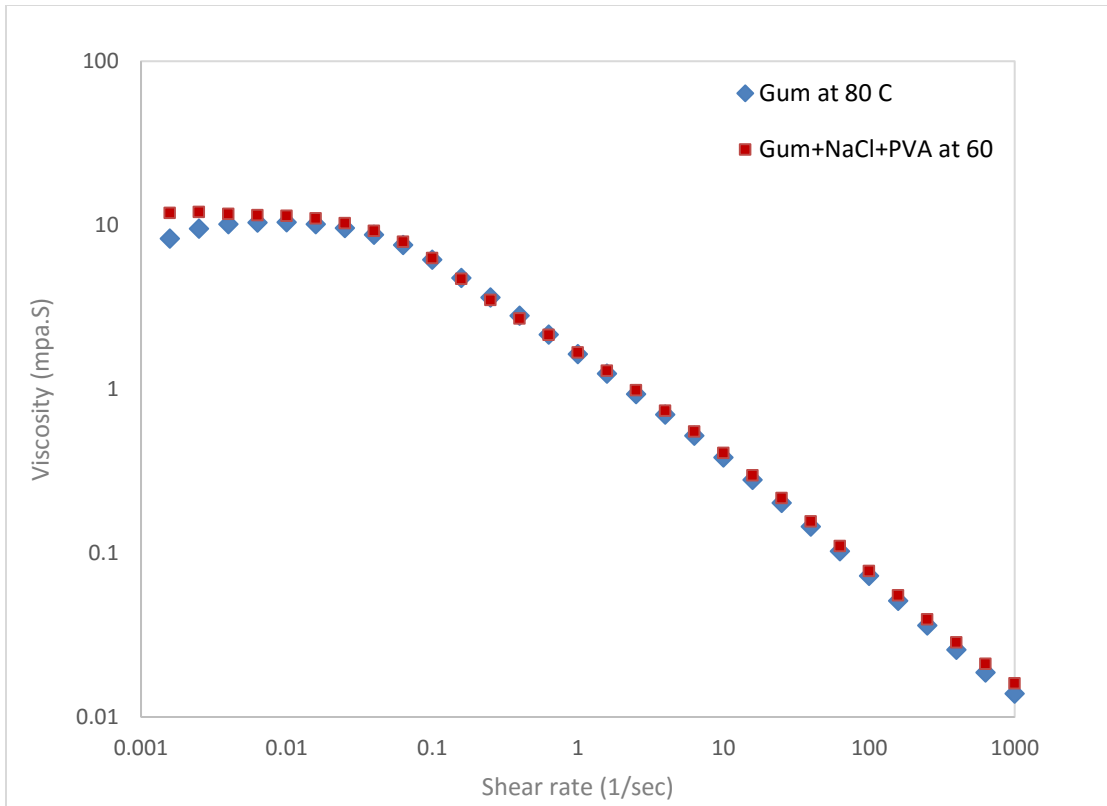


Figure 42: Effect of adding PVA to 0.5% Xan viscosity vs. Shear rate at 80°C.

#### 4.2.4 Effects of Temperature, Salinity, and PVA on Xanthan Viscosity

The viscosity of the xanthan gum was inversely proportional to the temperature and shear rate. Moreover, experiments were conducted to study the effect of NaCl on the viscosity of the solution, in order to simulate the properties of injected water. It was found that adding salts (i.e., 2%) slightly decreased the viscosity of the xanthan solution. Furthermore, the results show that adding PVA barely increased the polymer's viscosity, to the point that the change was negligible.

### **4.2.3 Blending Xanthan with Gluconic and Acrylic Acids and the Effect on Viscosity**

Xanthan gum has been mixed with acids to investigate the effect of physical mixing on viscosity. Sometimes the blending process improved the intended property (viscosity in the present research). The work done in this regard was as follows.

#### **4.2.3.1 Blending of Gluconic Acid and Xanthan Gum**

Gluconic acid has a carboxyl group in its chemical structure, which is why it was chosen for blending. It was expected to connect to the xanthan gum's chemical chain and increase the strength of the bonds among the molecules; as a result, the viscosity would increase. This might happen with a chemical reaction. However, blending the xanthan gum with gluconic acid at the same concentration ratio (i.e., 1:1) slightly decreased the viscosity of the gum, as shown in Figure 43. The concentration used in the experiment was 1,500 ppm.

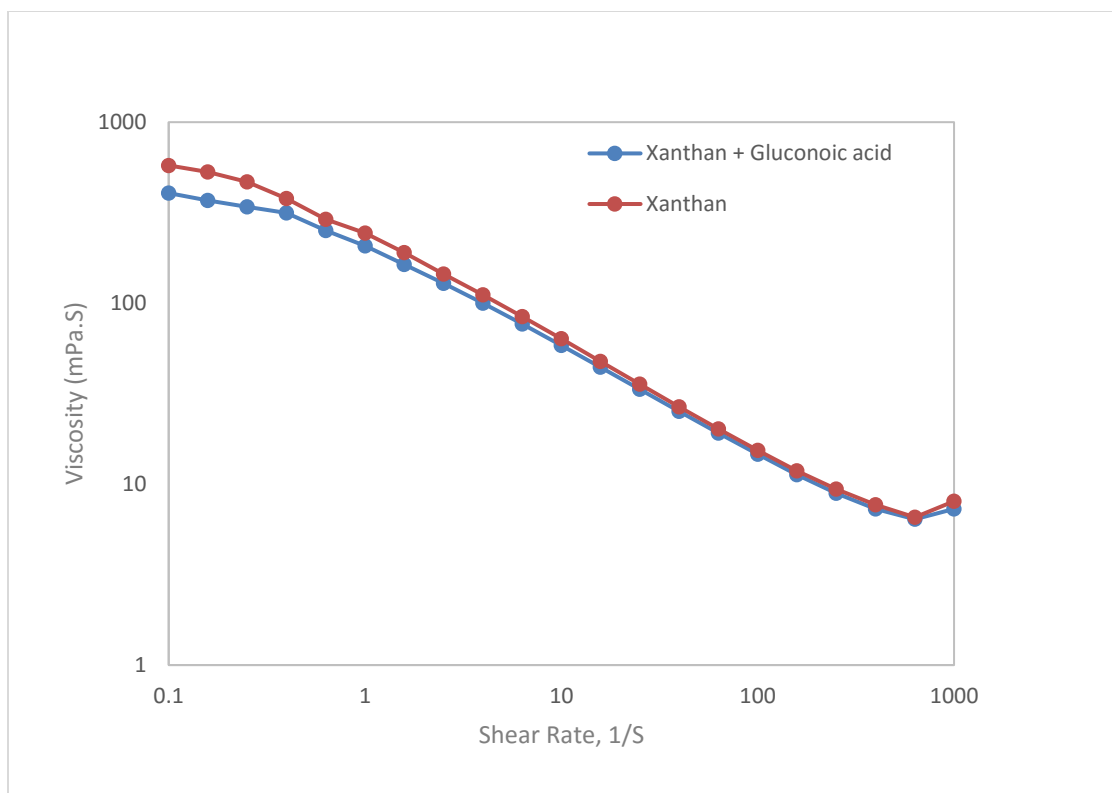


Figure 43: 1,500 ppm Xan and Xan + gluconic acid viscosities vs. shear rate at 25°C.

#### 4.2.3.2 Blending of Acrylic Acid and Xanthan Gum

It was observed that mixing xanthan gum with acrylic acid did not increase the viscosity of the solution. It decreased the viscosity as the concentration of acrylic acid increased, as shown in Figure 44 and 45. The xanthan concentration used in the experiments was 1,500 ppm. The ratios of xanthan to acrylic acid used in the experiments were 1:1, 1:3, and 1:4, as shown in Figure 46 and Figure 47. As the concentration of acrylic acid was increased in the blending process, the viscosity of the solution decreased. This reduction in viscosity resulting from adding the acrylic acid was the result of a non-reaction between the xanthan and acid. Therefore, due to this non-reaction, the mixed solution was diluted because the acid was in liquid form and hence decreased the viscosity.

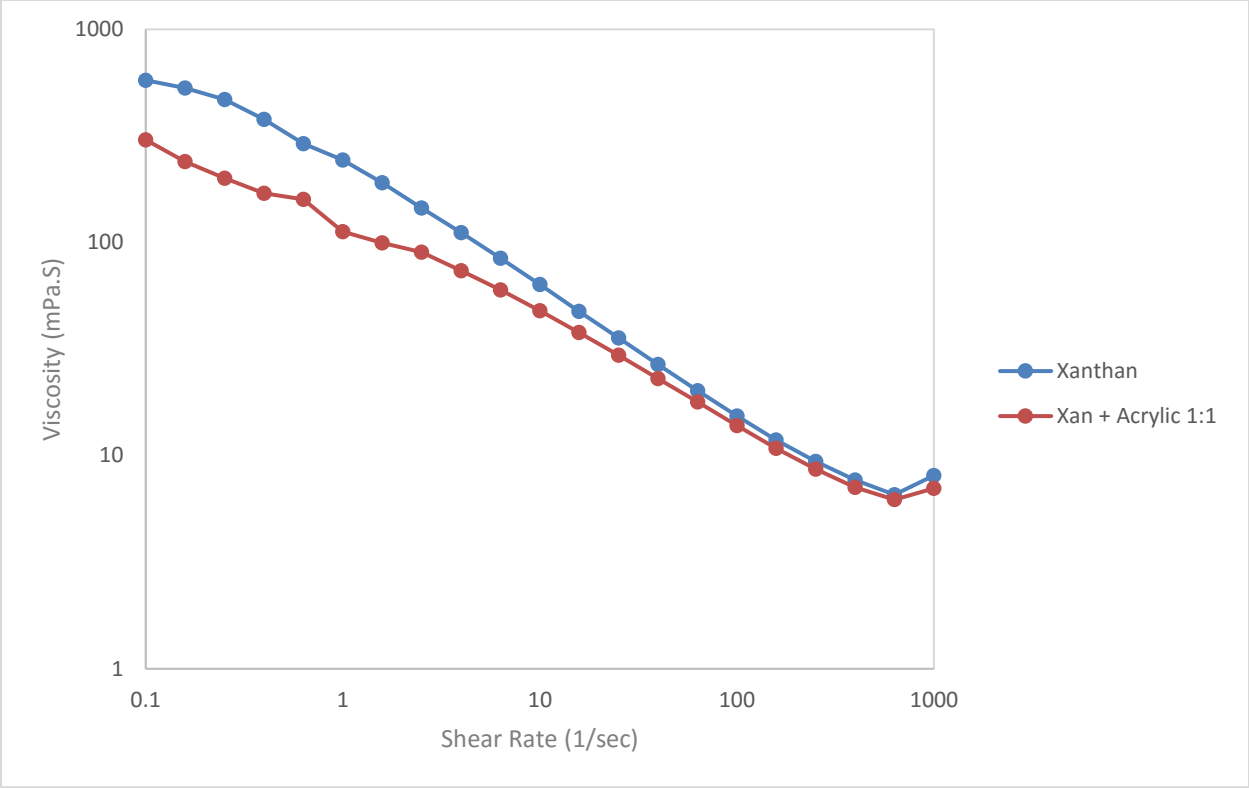


Figure 44: 1,500 ppm Xan and Xan + acrylic acid viscosities vs. shear rate at 25°C.

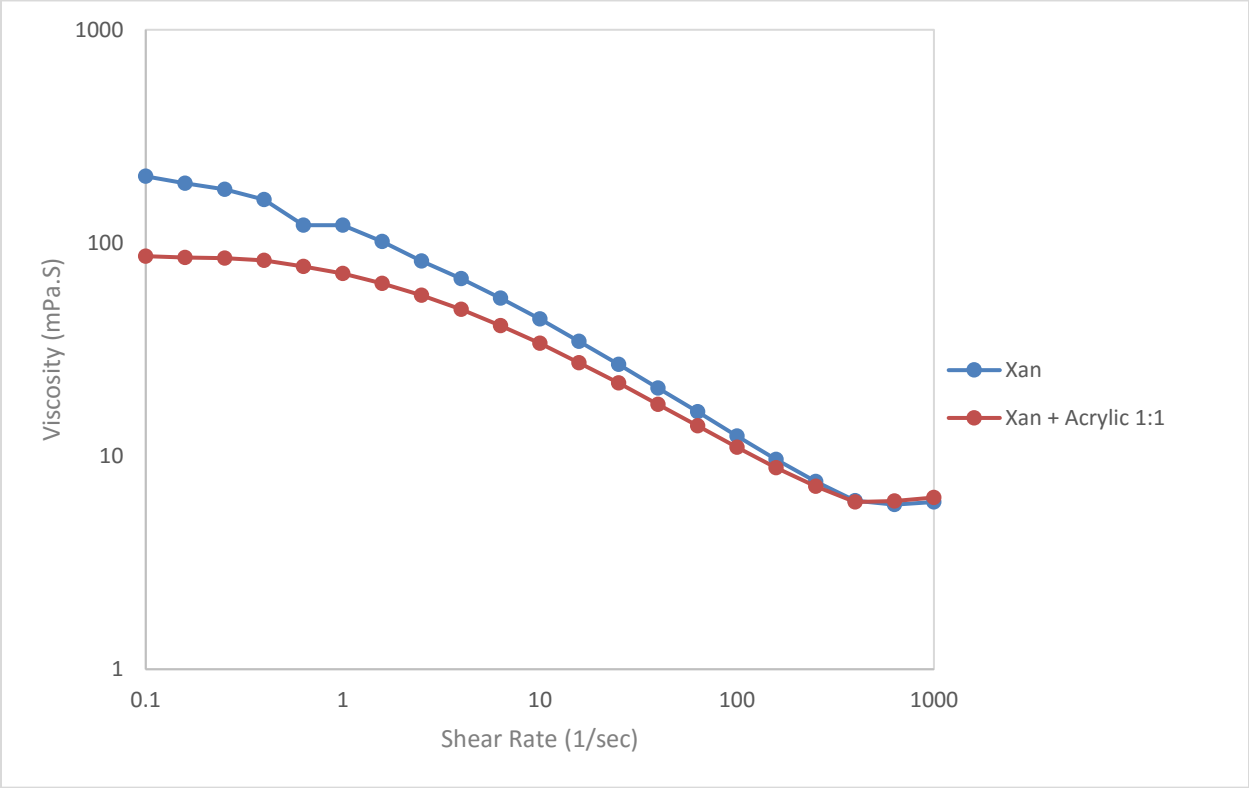


Figure 45: 1,500 ppm Xan and Xan + acrylic acid viscosities vs. shear rate at 50°C

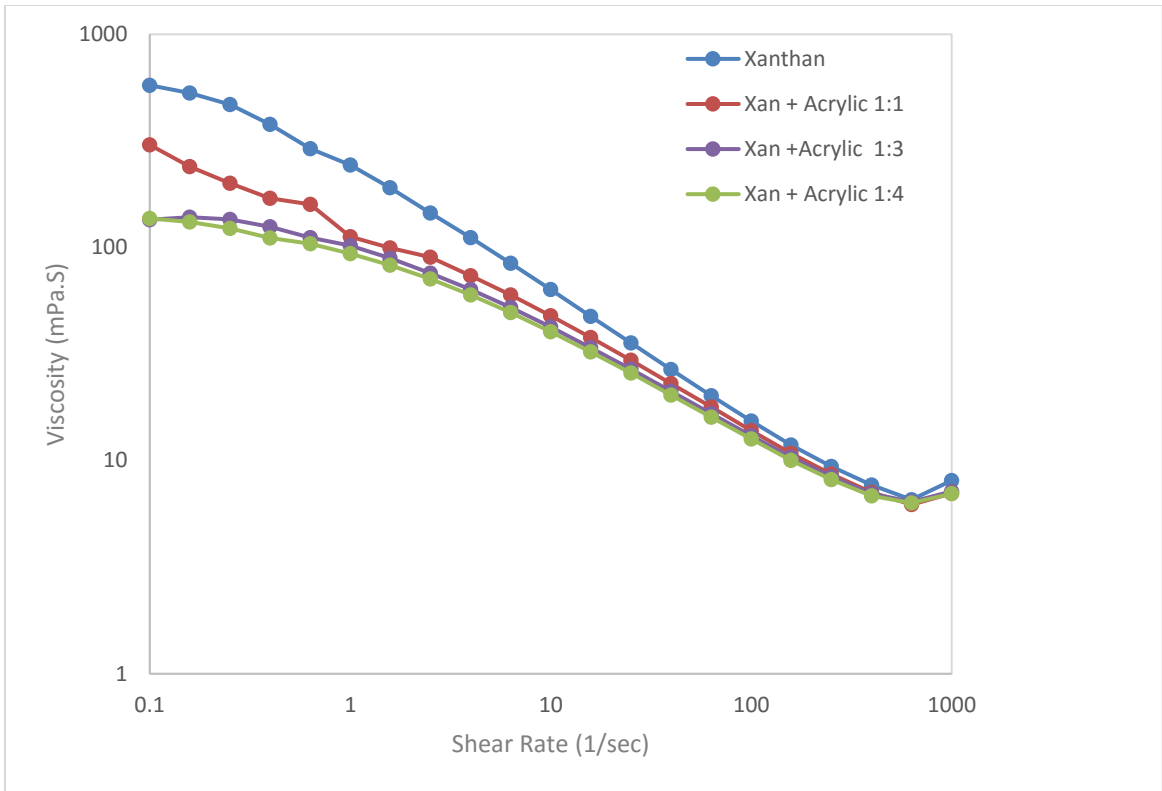


Figure 46: 1,500 ppm Xan & acrylic acid (blending) viscosities vs Shear rate at 25°C.

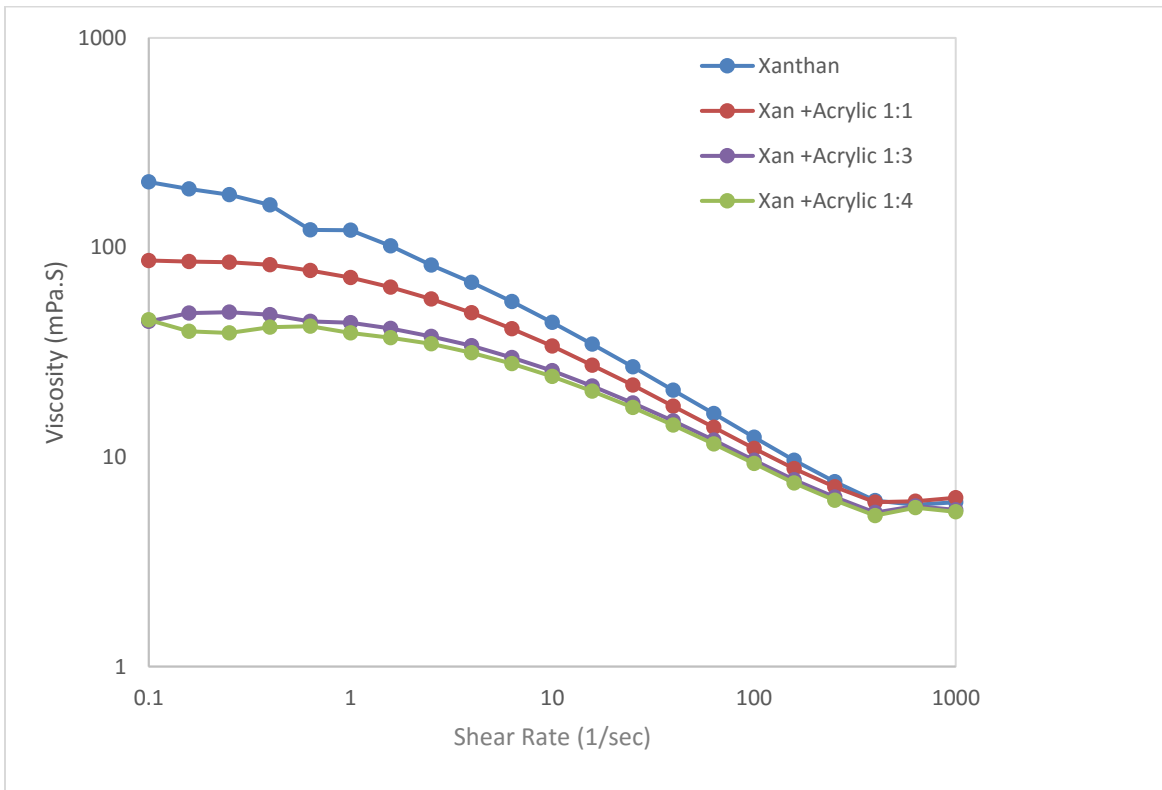
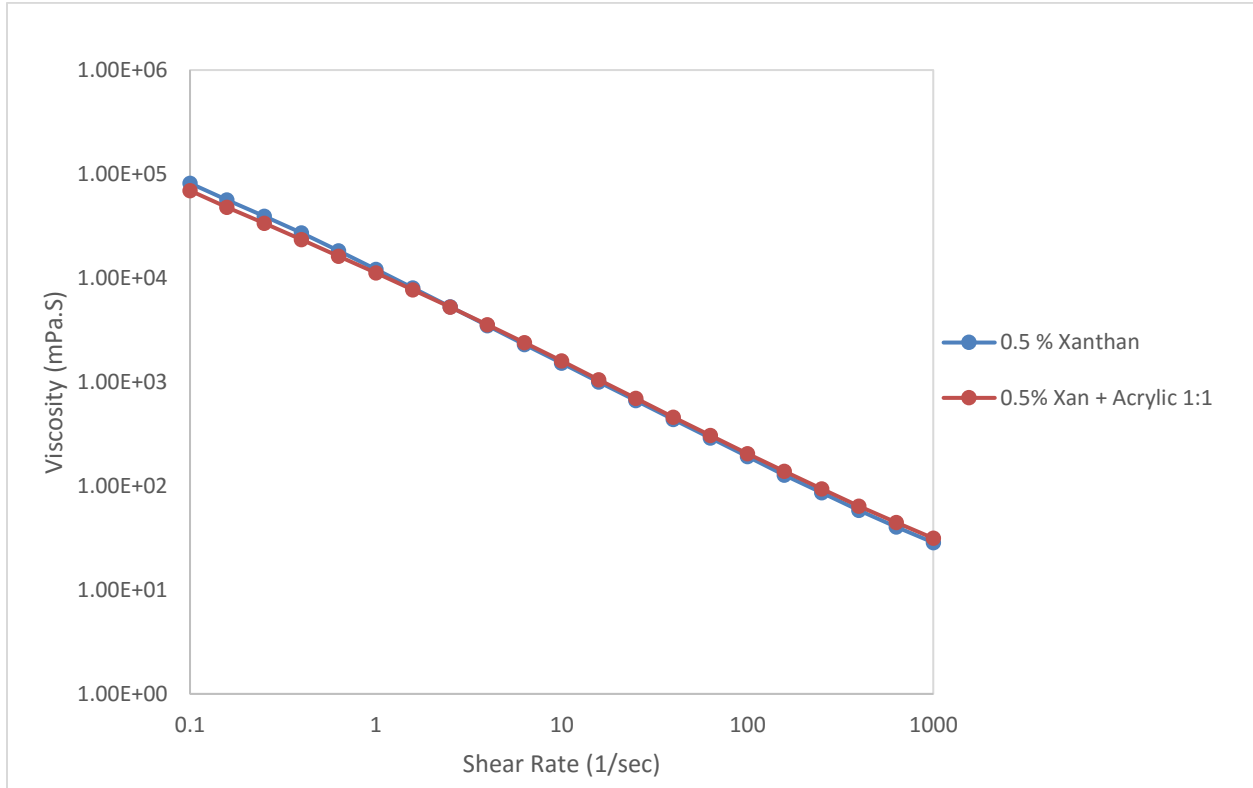


Figure 47: 1,500 ppm Xan & acrylic acid (blending) viscosities vs Shear rate at 50°C.

The blending processes were done for higher concentrations of xanthan and acrylic acid (i.e., a 1% concentration) to double check the results (see Figure 48).



**Figure 48: 0.5 % Xan and acrylic acid (blending) viscosities vs. shear rate at 50°C.**

For the higher concentrations, the change in viscosity was not noticeable because the dilution effect of the acrylic acid was very small compared to the high viscosity of the xanthan gum.

#### **4.2.4 Chemically Modified Xanthan Gum**

The xanthan was modified with acrylic acid in a chemical reaction, as described in Chapter 3. The chemically modified xanthan gum new polymer (NP) analysis results are described below.

##### **4.2.4.1 Viscosity Effect**

Experiments analyzing and illustrating the viscosities of the NP and xanthan gum were conducted for 1,500-ppm concentrations of both, as shown in Figure 49 and 50. From the plots, it is clear that the NP showed a higher viscosity value than did the xanthan at the same shear rate. This improvement in viscosity was due to a chemical reaction with the acrylic acid that connected the hydroxyl group to the xanthan bonds and made them stronger. Therefore, the viscosity increased.

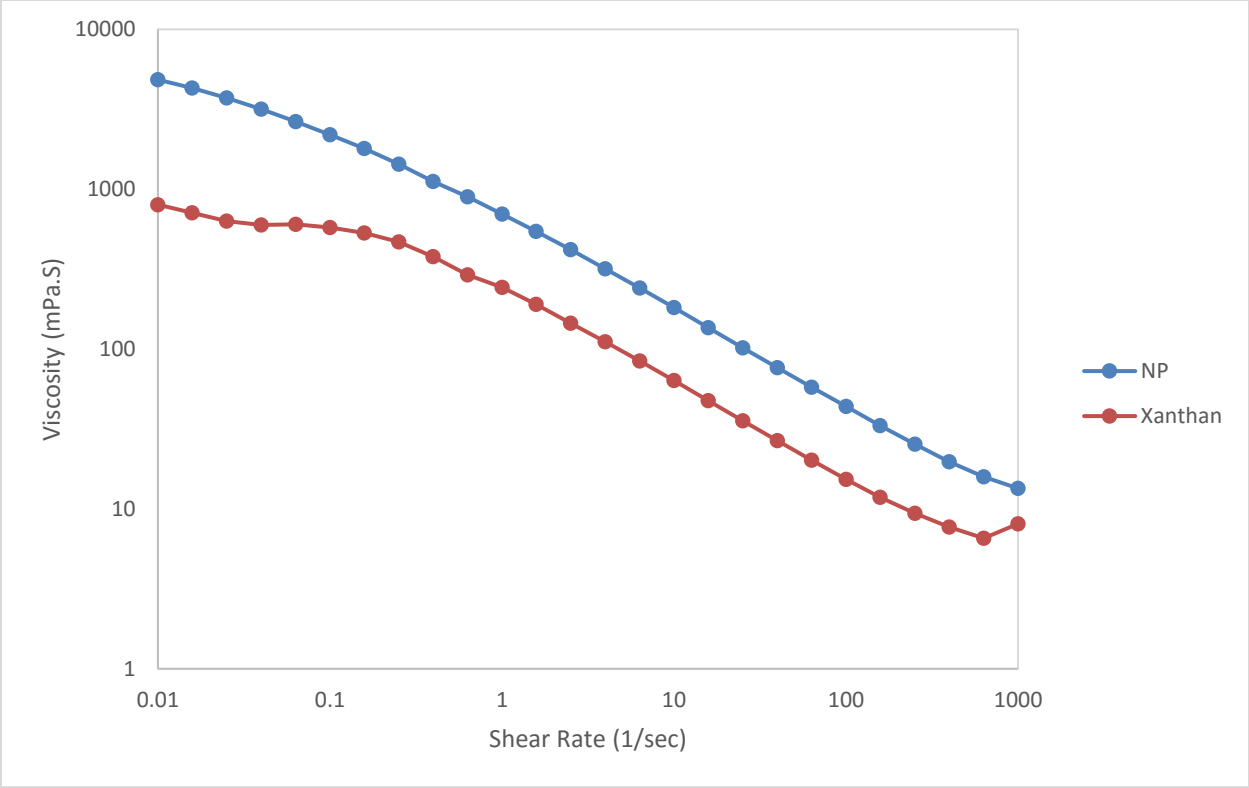


Figure 49: NP and xanthan viscosities vs. shear rate at 25°C.

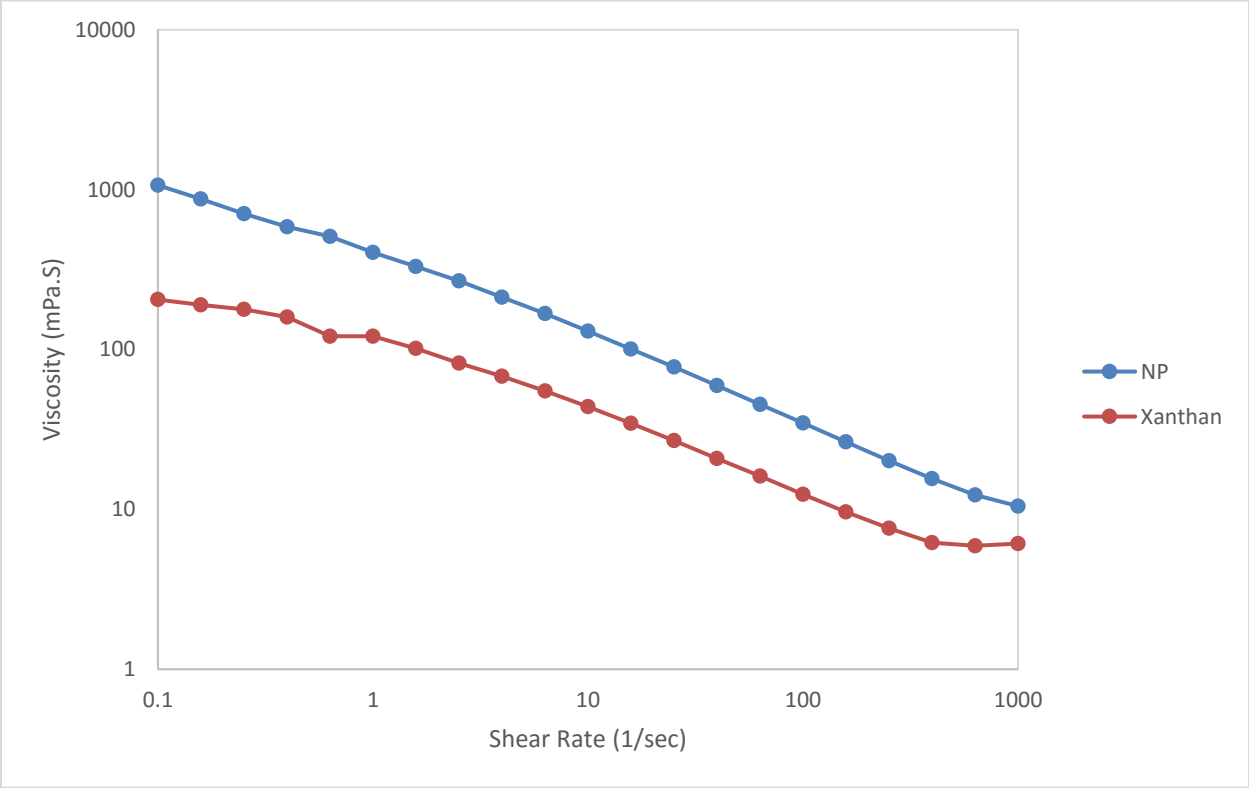


Figure 50: NP and xanthan viscosities vs. shear rate at 50°C.

#### 4.2.4.2 Temperature Effect

The new polymer offered a higher stability in terms of viscosity with the change in temperature, as shown in Figure 51 and Figure 52. For example, at a  $0.1 \text{ s}^{-1}$  shear rate, the viscosities of the xanthan gum were 578 and 205 mPa.S at  $25^{\circ}\text{C}$  and  $50^{\circ}\text{C}$ , respectively. The NP viscosities were 2,200 and 1,070 mPa.S at  $25^{\circ}\text{C}$  and  $50^{\circ}\text{C}$ , respectively. The reduction in xanthan viscosity was around 65%. For the NP, the decrease in viscosity was around 50%. Even at a  $10 \text{ s}^{-1}$  shear rate, the xanthan gum's viscosities were 63.5 and 44 Pa.S at  $25^{\circ}\text{C}$  and  $50^{\circ}\text{C}$ , respectively. For the NP, they were 182 and 130 Pa.S at  $25^{\circ}\text{C}$  and  $50^{\circ}\text{C}$ , respectively. The decrease in xanthan viscosity was around 30%. For the NP, the decrease in viscosity was around 20%.

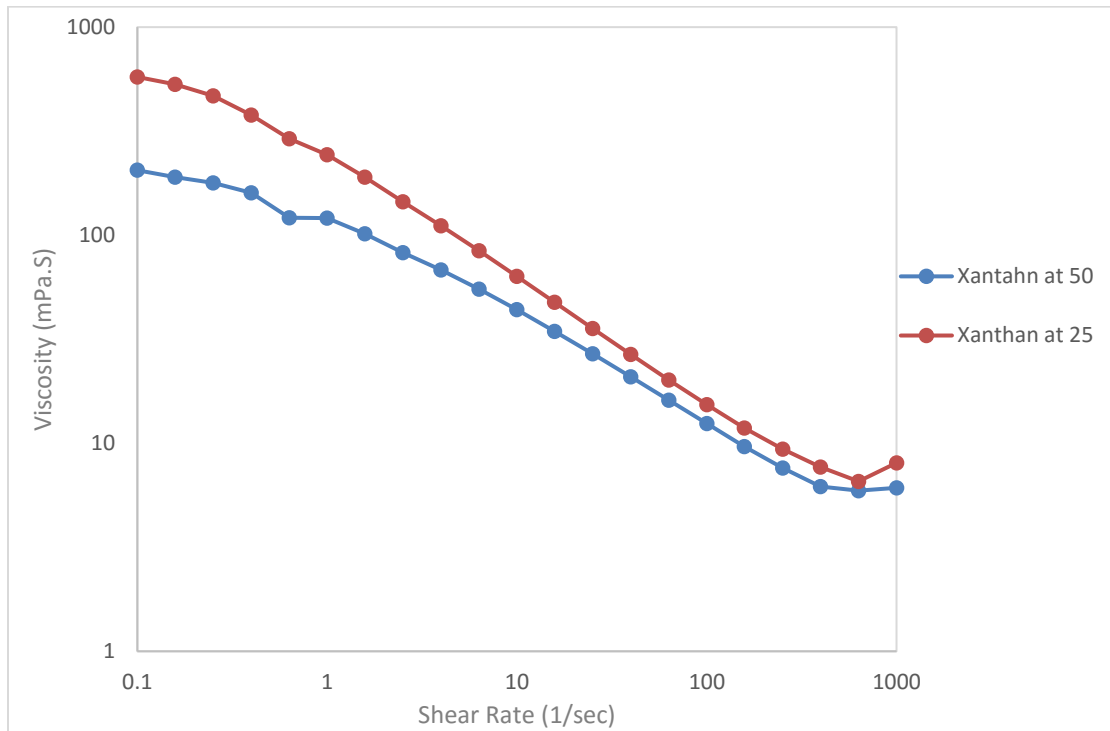


Figure 51: Xanthan viscosity vs. shear rate at  $25^{\circ}\text{C}$  and  $50^{\circ}\text{C}$ .

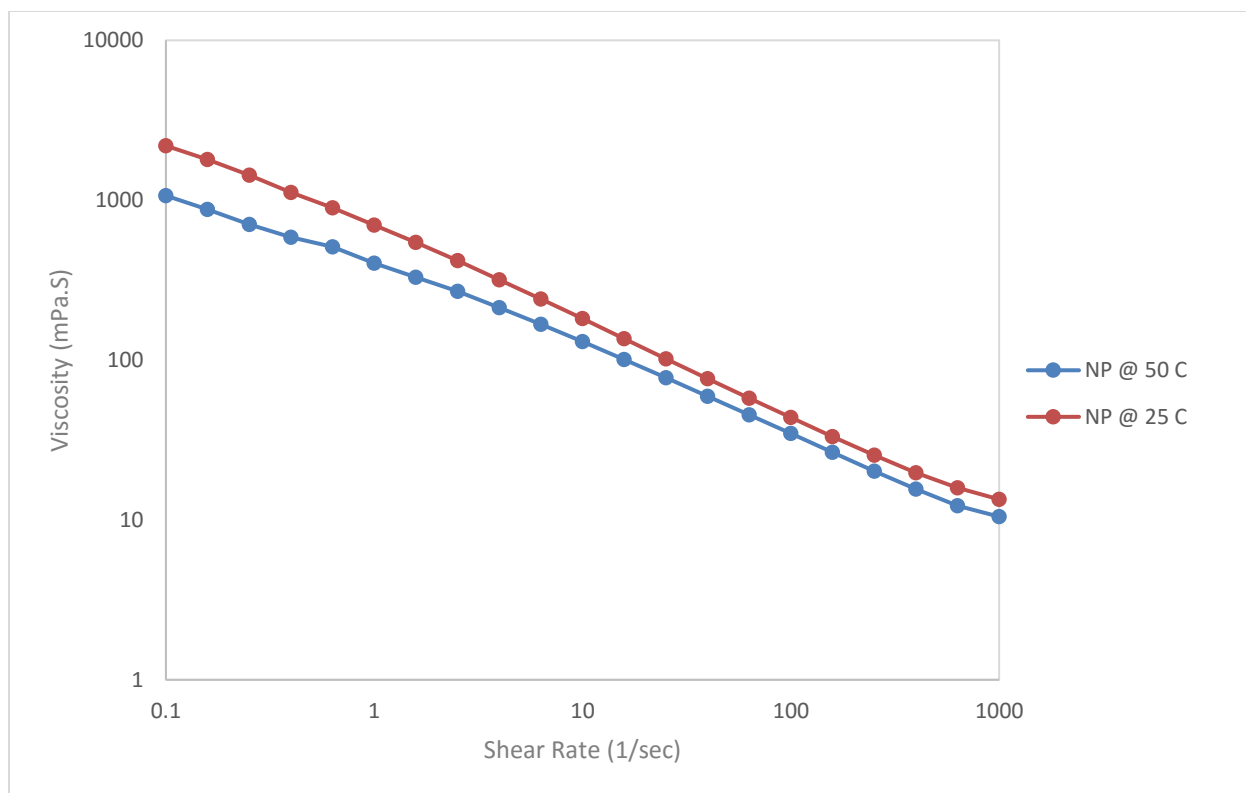


Figure 52: NP viscosity vs. shear rate at 25°C and 50°C.

It is evident from the rheological experiments that of the physical and chemical modifications, only the latter succeeded in increasing the xanthan's viscosity. Consequently, a comparison between the xanthan gum and NP was conducted via core flood experiments to investigate which of the two offered more recovery.

#### 4.2.4.3 Sample 2 of Modified Xanthan gum Analysis

To continue the rheological analysis for modified Xanthan gum, and since the first sample was totally consumed, a new patch was prepared following the same procedures. The sample was used to analyze chemical and rheological properties. FT-IR, NMR, salinity and temperature effects are discussed in the following:

- a. FT-IR and NMR Analysis

To investigate the salinity effect in the chemically modified xanthan gum, 5%, 10% and 15% of NaCl are added to the solution. Figure 53 and Figure 55 show the FT-IR and NMR of the new sample. Both spectra illustrated differences in the chemical structures (see Figure 30 and Figure 33), which confirmed that the chemical reaction took place producing a new substance. For example, in FT-IR spectrum the O–H axial deformation peaks in Xanthan gum was at  $3,277\text{ cm}^{-1}$ , while it was at  $3,431\text{ cm}^{-1}$  for FT-IR spectra. In addition to that, bands nearer to  $1,601\text{ cm}^{-1}$  was due to axial deformation of the C-O in Xanthan gum spectra, it was around  $1,632\text{ cm}^{-1}$  for sample 2 FT-IR spectra (See Figure 54). These changes implied that the reaction had happened.

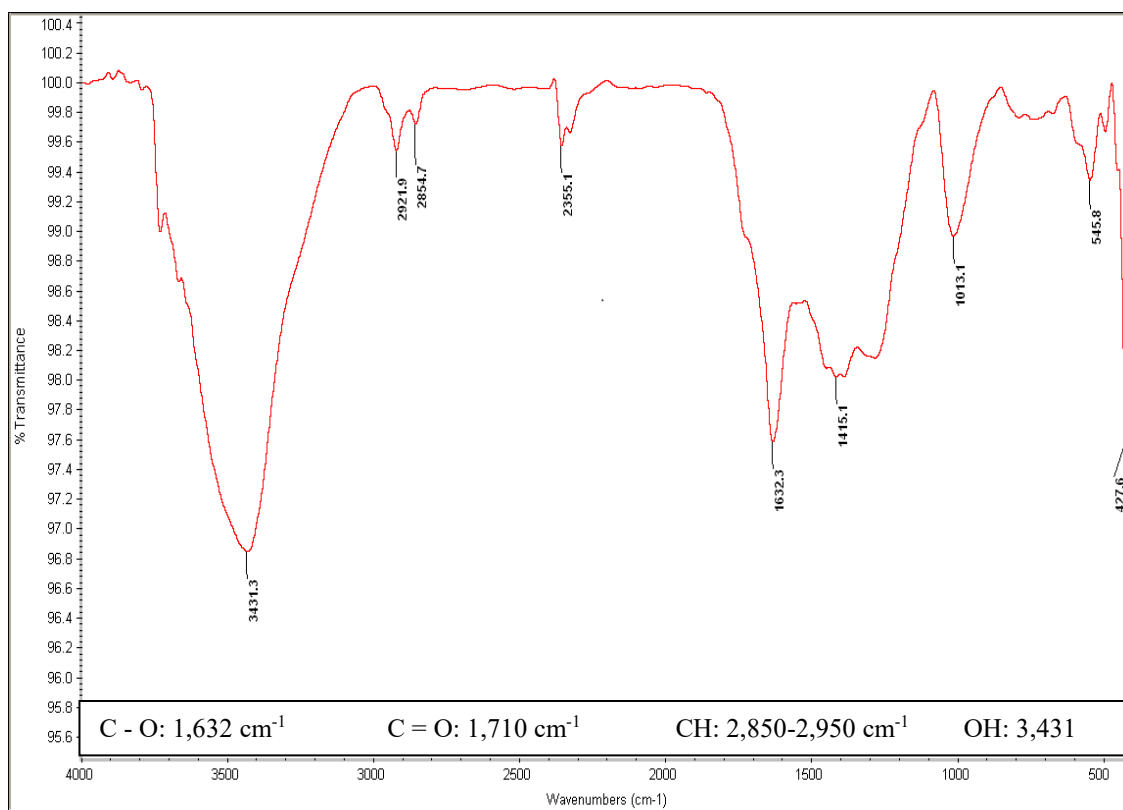


Figure 53: FT-IR spectrum of modified xanthan gum (sample No. 2)

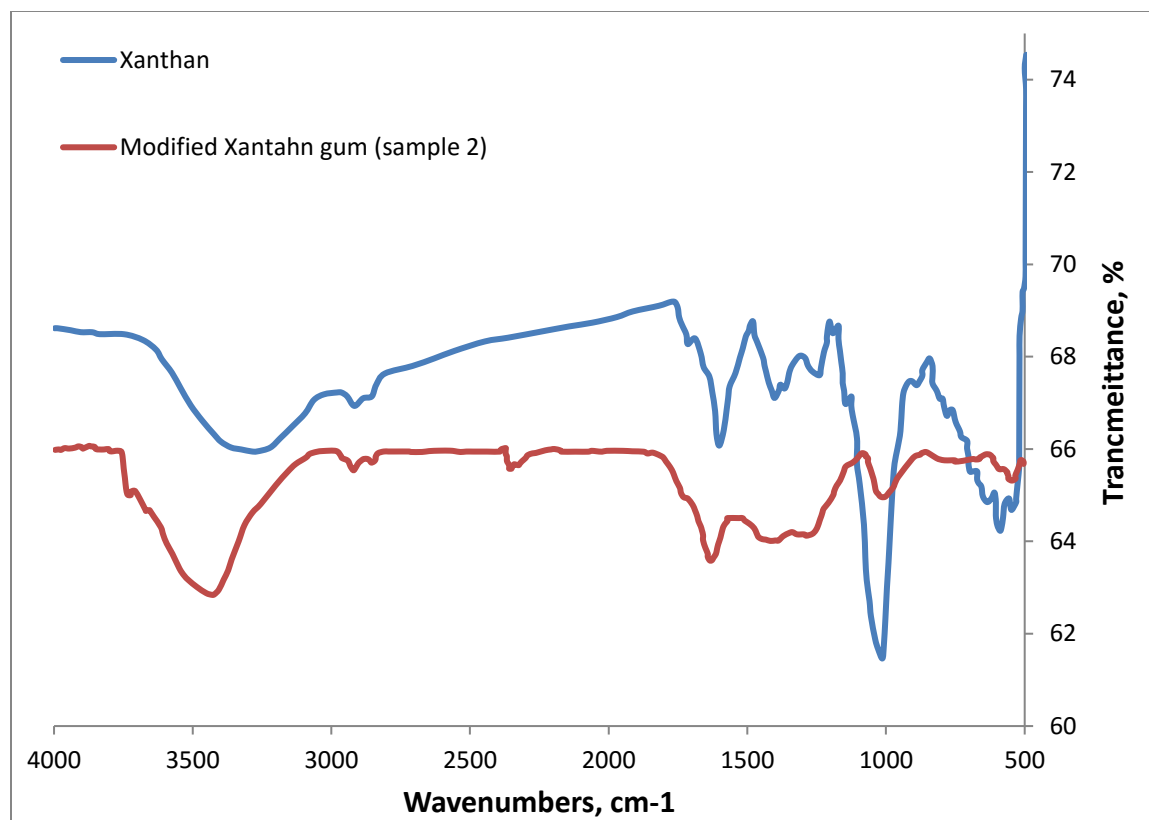


Figure 54: Comparison between Xanthan gum and Sample 2 FT-IR spectrum

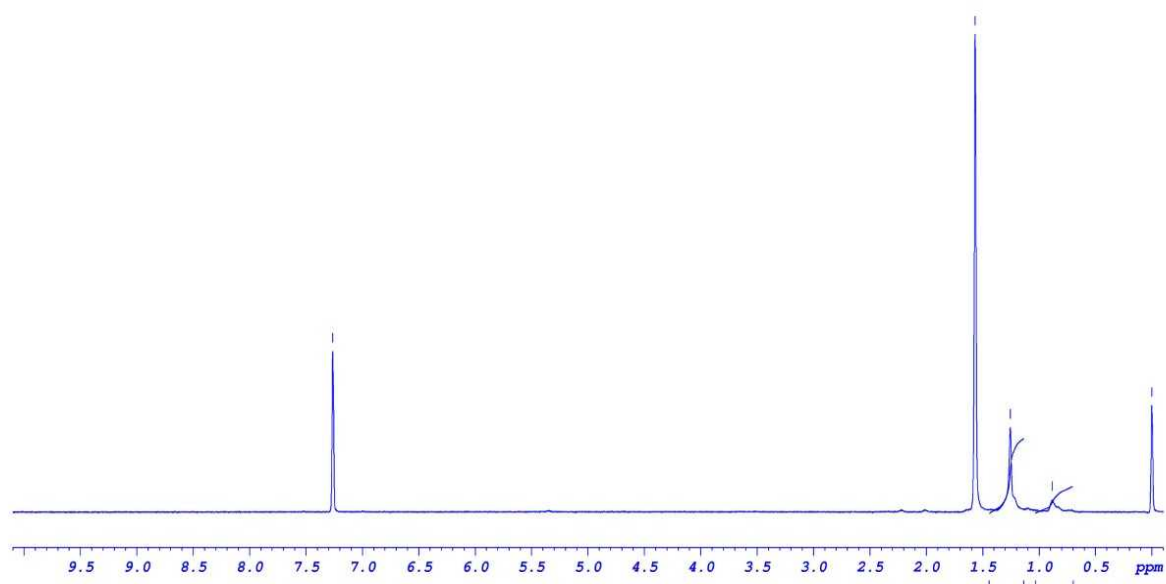


Figure 55: <sup>1</sup>H NMR spectrum of modified Xanthan gum (sample number 2)

### b. Salinity Effect

For salinity effect investigation, Figure 56 shows the effect of adding NaCl with different concentrations to the solution viscosity. From the plot, it is clear that above 5% NaCl concentration, the effect of salinity on Xanthan solution viscosity is very small and could be negligible.

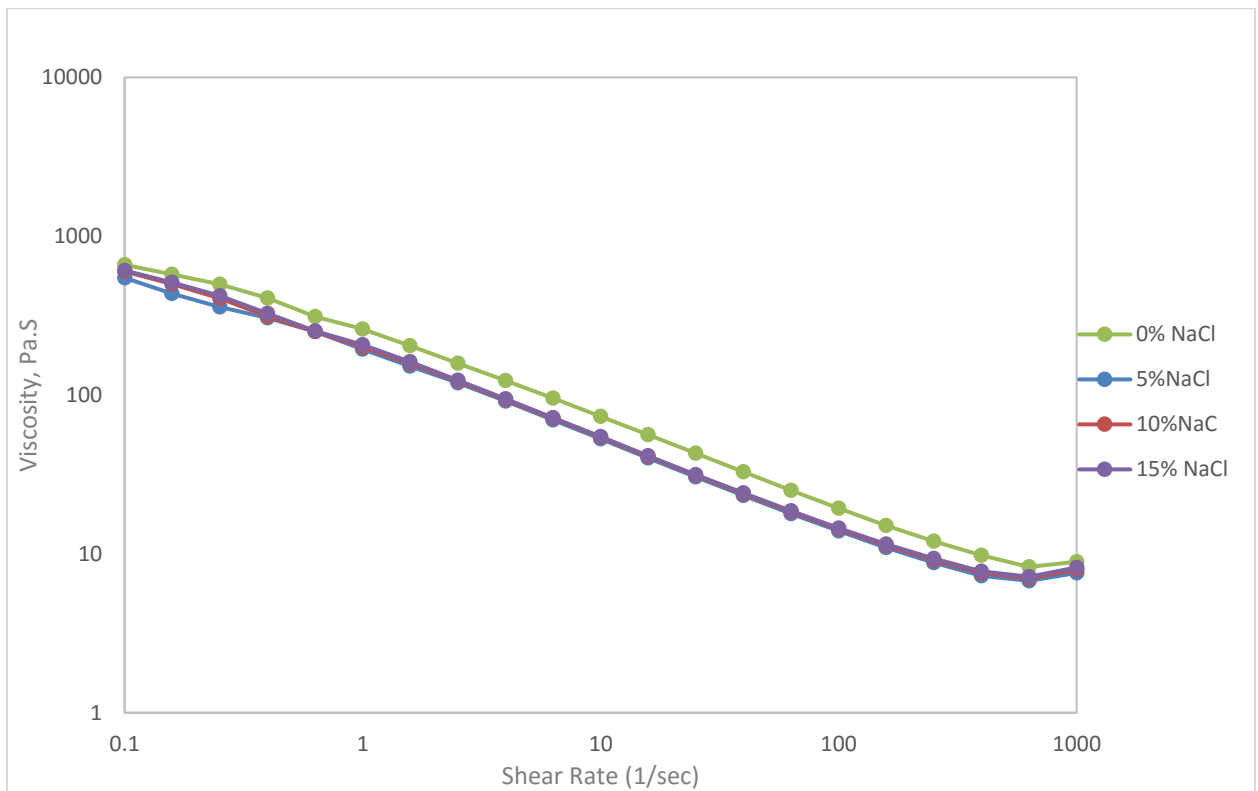


Figure 56: Salinity effect on Xanthan viscosity

### c. Temperature Effect

The effect of higher temperature (60 and 70<sup>0</sup>C) on the solution viscosity were conducted as shown in Figure 57. The viscosities of the modified Xanthan at 60<sup>0</sup>C and 70<sup>0</sup>C are

very close to each other, which could conclude that, at higher temperature, the effect of the temperature on the solution viscosity becomes smaller.

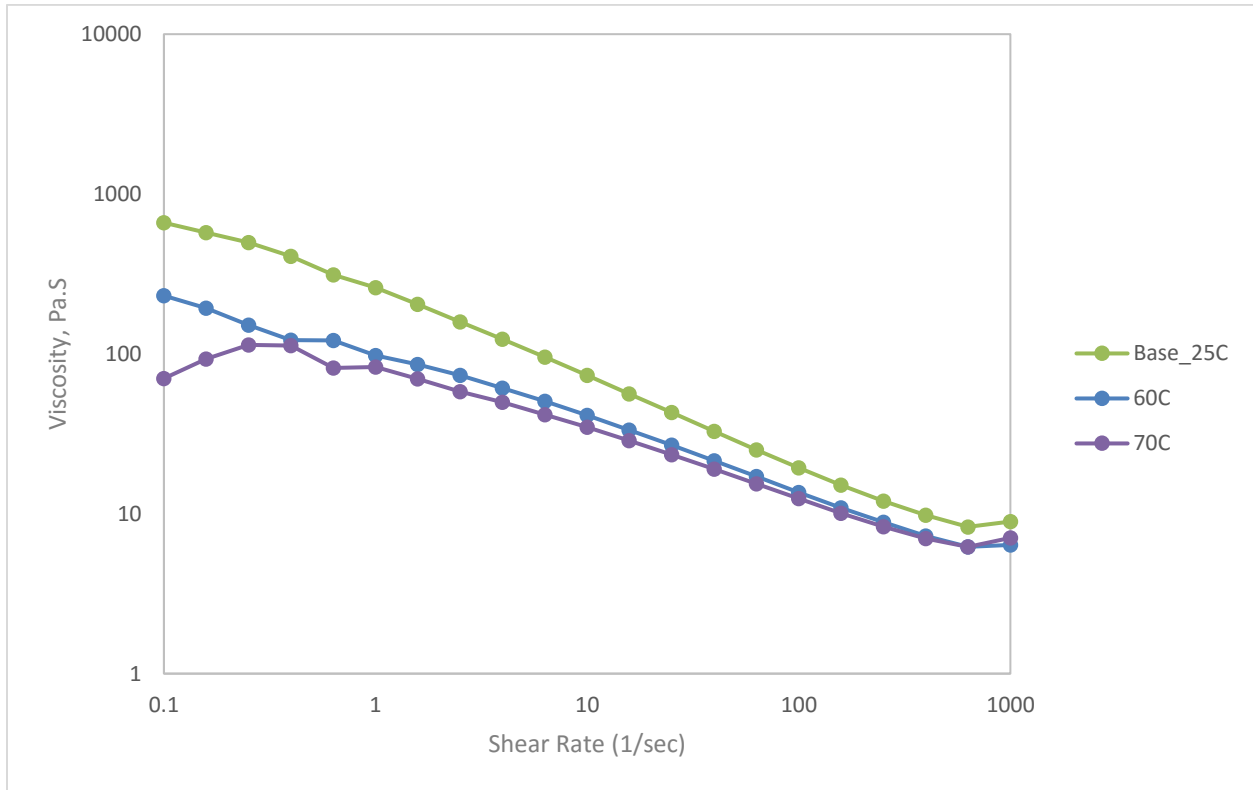


Figure 57: Sample 2 viscosity vs. shear rate at 25, 60 and 70°C

### **4.3 Core Flooding Results**

Core flooding simulates reservoir conditions well, and therefore is useful for investigating the EOR performances of polymer systems. In the present research, the main goal of the core tests was to determine the oil recovery percentage using green polymer formulations. To do so, two core flood experiments were conducted to investigate and compare the recoveries of the xanthan and modified xanthan gums.

In this section, the results of the core flood experiments are presented and discussed.

#### **4.3.1 Porosity and Permeability Calculations**

The porosity and permeability calculations are shown in the Appendix.

#### **4.3.2 EOR Potential of the Modified Xanthan Gum**

To assess the additional recovery resulting from introducing the modified Xantahn gum, core flood experiments were conducted to investigate and compare the recoveries of the normal and modified xanthan gum (NP).

The core flood experiments were conducted as follows. First, the cores were saturated with 3% NaCl brine and oil to establish the experimental saturation and then, flooded by 3 pore volumes (PV) of 3% NaCl until no oil was produced. Then, the cores were flushed with either xanthan or NP with 3 PV until no more oil was produced. After that, the cores were flooded by 1 PV of 3% NaCl brine to make sure all of the mobile oil was produced.

##### **4.3.2.1 EOR by Xanthan Gum**

The core flooding experiment gave a 44.88% recovery of IOIP by water flooding (i.e., secondary recovery). Thus, the residual oil saturation ( $S_{or}$ ) at the end of this stage was 55.12%. Xanthan flooding (i.e., tertiary recovery) increased the recovery rate by 13.93%

of the IOIP beyond the secondary recovery stage, which is equivalent to 25.27% of the residual oil saturation (ROS); that gave a 58.8% total recovery of IOIP. Figure 58 shows the recovery from water and xanthan flooding by percentage. The recovery obtained via xanthan gum was comparable with the recovery obtained via HPAM, usually around 12% to 17% (Jour et al., 2018).

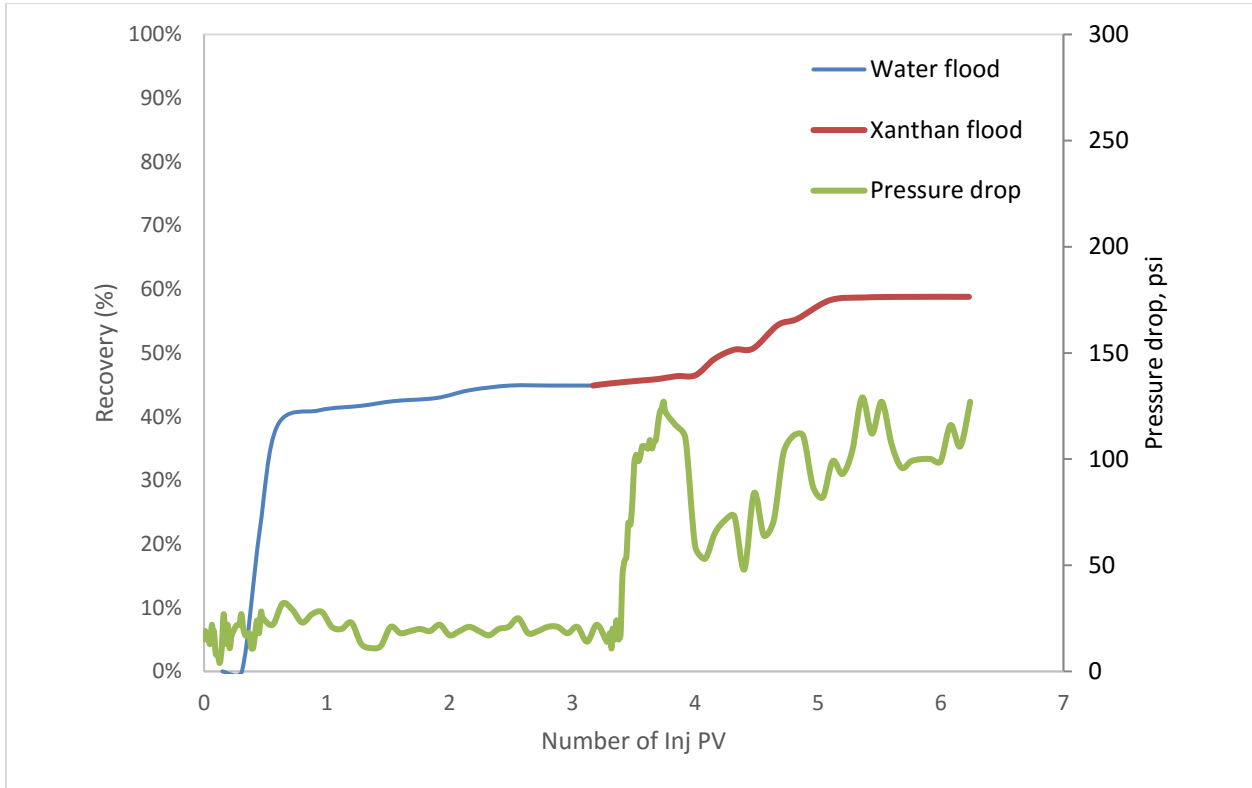


Figure 58: Xanthan recovery vs. No. of Inj PV.

Table 5 summarizes core #1 properties at initial stage (before the flood experiment).

Table 5: Core #1 properties

Core flooding	Xanthan
Polymer concentration (ppm)	1,500
Core length (inches)	6.04
Porosity	19.58
Permeability (md)	102.66
Swi %	39.88
Pore volume (cc)	34.00
Initial oil saturation %	60.22
Initial oil volume (cc)	20.5
Residual oil after water flooding (cc)	11.3

Table 6 summarizes results of the core flood experiment using Xanthan gum.

Table 6: Recovery Results using Xanthan gum

Recovery % of IOIP after water flooding	44.88
Recovery % of IOIP after chemical flooding	13.93
Recovery % of ROS by chemical flooding	25.27

#### 4.3.2.2 EOR by Modified Xanthan Gum

The recovery obtained via water flooding was 43.85% of the IOIP. The  $S_{or}$  was found to be 56.15%. Moreover, the NP obtained a recovery of 19.21% of the IOIP beyond the secondary recovery stage (i.e., tertiary recovery), which is equivalent 35% of the ROS, giving a total oil recovery of 63.1% of the IOIP. Figure 59 shows the recoveries in percentages.

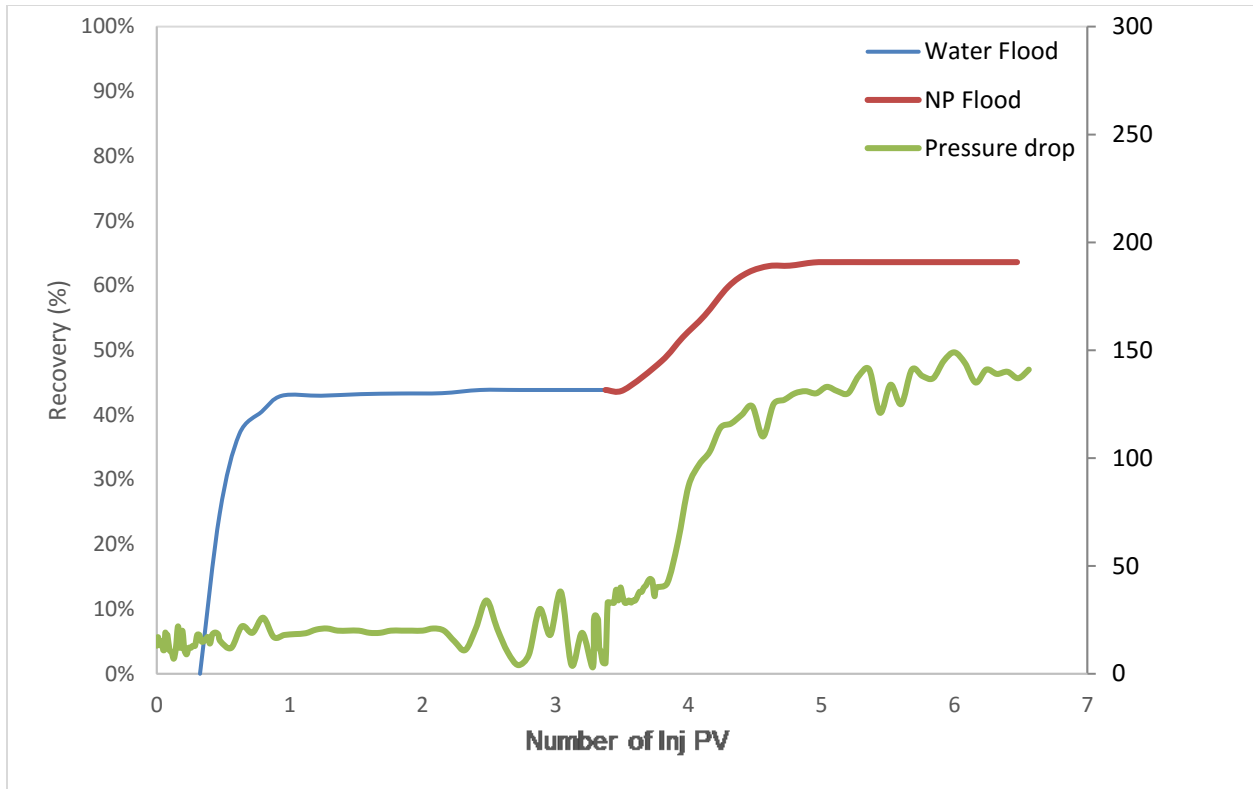


Figure 59: NP recovery vs. No. of Inj PV.

Table 7 summarizes core #2 properties at initial stage (before the flood experiment).

Table 7: Core #2 properties

Core flooding	NP
Polymer concentration (ppm)	1,500
Core length (inches)	5.94
Porosity	19.78
Permeability (md)	107.30
Swi %	40.61
Pore volume (cc)	33.83
Initial oil saturation %	59.49
Initial oil volume (cc)	20.25
Residual oil after water flooding (cc)	11.37

Table 8 summarizes results of the core flood experiment using NP.

Table 8: Recovery Results using NP

Recovery % of IOIP after water flooding	43.85
Recovery % of IOIP after chemical flooding	19.21
Recovery % of ROS by chemical flooding	35.18

### 4.3.2.3 Comparison of Xanthan and NP Recoveries

Form the core flood experiments, it was determined that the new polymer's recovery was 5.28% greater than that of the Xanthan gum as a percentage of OOIP as shown in Figure 60, and 9.91% as a percentage of ROS. This improvement can be attributed to the enhancement produced by the polymer solution's viscosity.

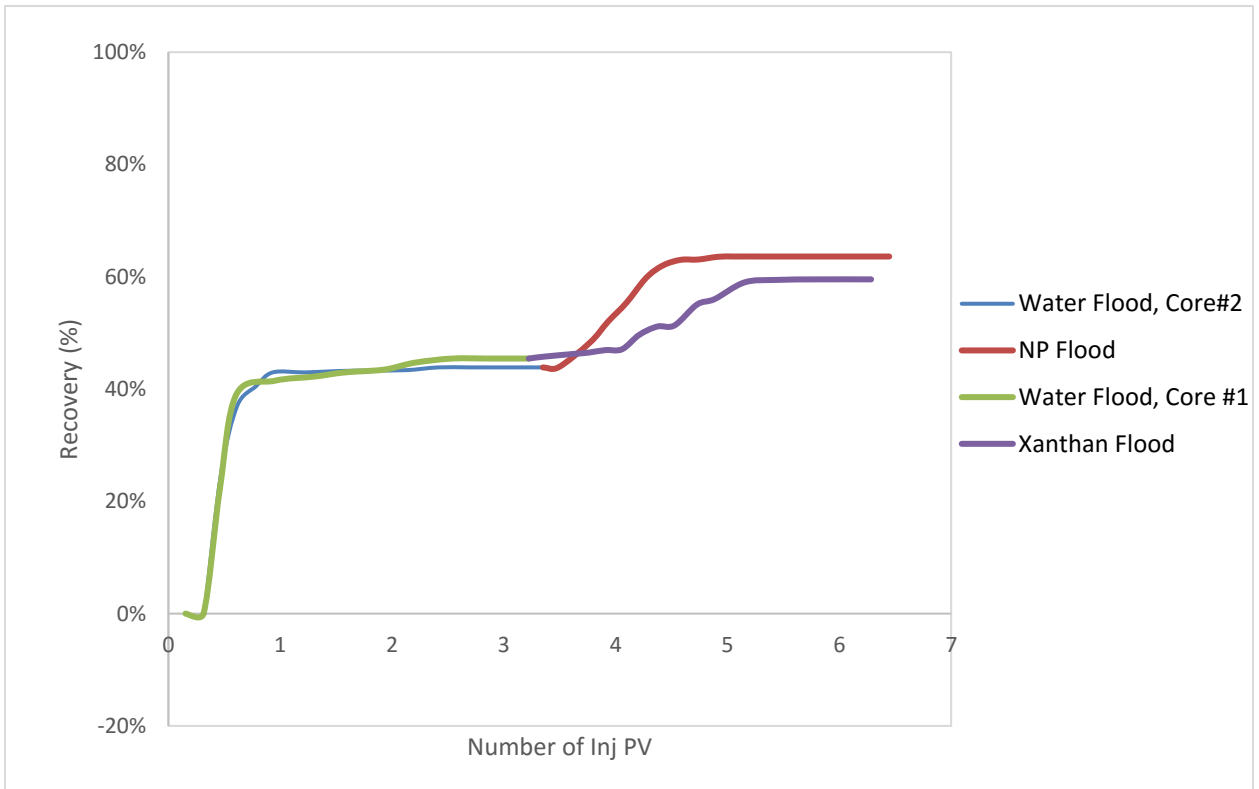


Figure 60: Recovery comparison of xanthan and NP vs. No. of Inj PV.

Table 9 summarizes and compares the results of the oil recovery using Xanthan gum and NP.

**Table 9: Oil recoveries results using Xanthan gum and NP**

Core flooding	Xanthan	NP	Incremental Recovery, %
Recovery % of IOIP after water flooding	44.88	43.85	
Recovery % of IOIP after chemical flooding	13.93	19.21	5.28
Recovery % of ROS by chemical flooding	25.27	35.18	9.91

#### **4.3.2.4 Pressure Drop Profile Observations**

Figure 61 compares the pressure drop changes resulting from the two core flood experiments conducted in this research, showing that the pressure drop during the initial period of seawater injection followed the same trend and stabilized at around 20 psi at the end of the brine injection period (after injection of about 3.36 PV). During the EOR period, the injection of the NP led to a considerable increase in pressure drop through the core sample, reaching 149 psi after injection of 6.08 PV. Conversely, the pressure drop increased to 124 psi during injection of the first PV of xanthan gum. This sudden increase was attributed to the increase in injection solution viscosity. Furthermore, from the pressure drop behaviors of Xanthan and modified Xanthan gum (NP), it can be recognized that in Xanthan gum case, the pressure drop was not stable and it was varying from 50 psi to 124 psi during the Xanthan flood. While in NP flood case, it had higher stability (varying from 114 psi to around 150 psi) and therefore, the NP has higher pressure drop stability (it does not fluctuate as

the pressure drop profile in Xanthan gum case) and consequently, NP is more elastic than base Xanthan gum. (see Figure 61).

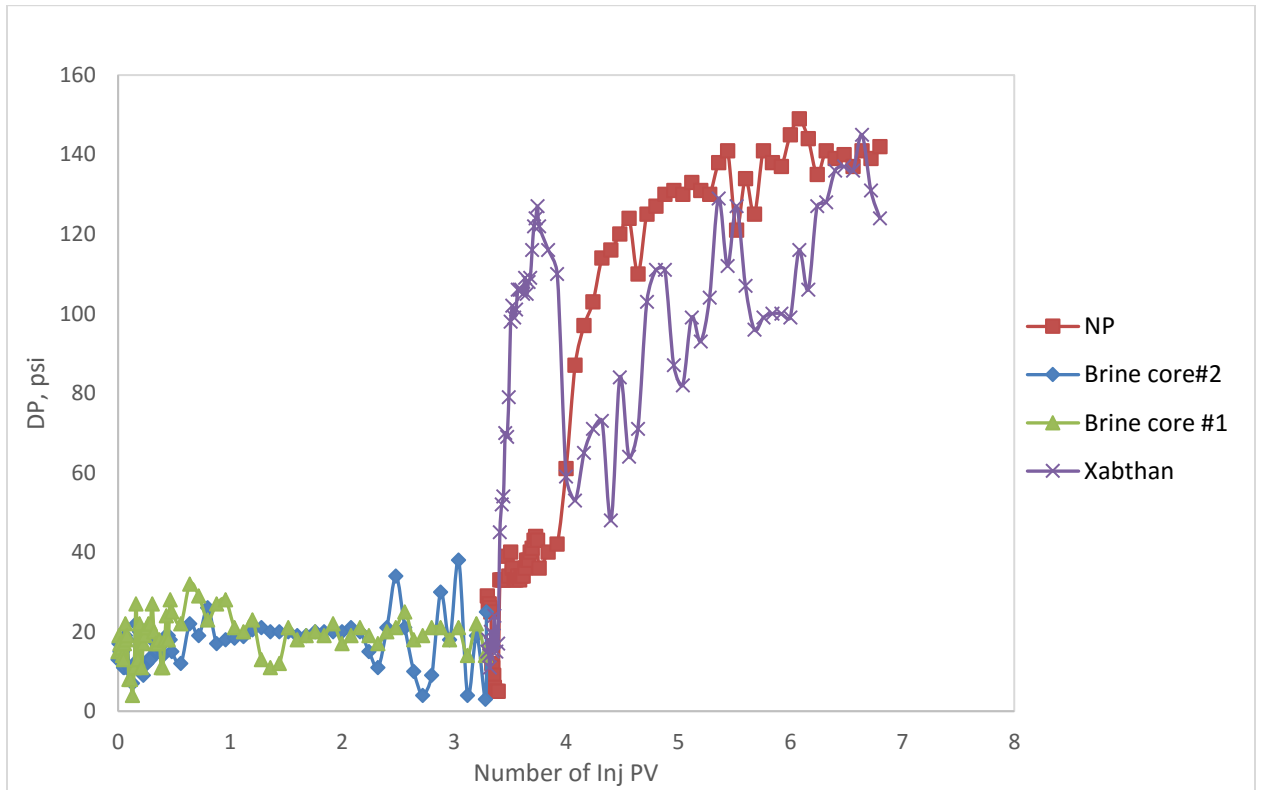


Figure 61: Pressure drop profile No. of Inj PV.

## CHAPTER 5

# CONCLUSIONS AND RECOMMENDATIONS

### 5.1 Conclusions

1. The FT-IR and NMR analyses showed that there was a successful chemical modification of the xanthan gum. The chemical structure of the xanthan gum was reformed and connected to the acrylic acid. The FT-IR spectrum of the xanthan gum showed absorption peaks at  $3,277\text{ cm}^{-1}$ . The FT-IR spectrum of the NP showed peaks identical to those of the xanthan gum. Moreover, a new peak appeared at  $1,645\text{ cm}^{-1}$ . The NMR analysis found a few additional new peaks at 5.80, 6.02, and 6.41 ppm for the NP, mirroring that which was found for the xanthan gum.
2. The chemically modified xanthan gum demonstrated increased rheological properties as compared to the xanthan gum. The viscosity at a  $0.1\text{ S}^{-1}$  shear rate and  $25^{\circ}\text{C}$  was 578 mPa.S for the xanthan and 2,200 mPa.S for the NP under the same experimental conditions. In addition, the stability of the xanthan gum developed with increases in temperature.
3. The development on the xanthan's viscosity was reflected in the oil recovered from the cores. The properties of the rocks were kept the same to allow for a reasonable comparison between the normal and modified xanthan gums. The results of the core flooding also confirmed that the modified xanthan gum offered a higher rate of oil recovery. The modified Xanthan gum recovered 5.28% additional oil compared to Xanthan due to the increased viscosity. For Core #1,

the recoveries were 44.88% and 13.91% of the IOIP for brine and xanthan flooding, respectively. For Core #2, the results were 43.85% and 19.21% recoveries of IOIP for brine and modified xanthan, respectively.

## **5.2 Recommendations**

1. The proposed modification for Xanthan gum should be tested on carbonate rock.
2. Further research should be conducted to confirm the reaction and also to identify other modified xanthan gums with increased concentrations of acrylic acid.
3. After many trials, the chemical reaction was found to be successful because it was very sensitive to temperature. Therefore, future work should take into consideration adjustments to the reaction temperature.
4. Synthesis of Xanthan gum using acryloyl chloride, and 3-ethoxy acryloyl chloride is recommended for investigation.

## References

- [1] Avery, M. R., Burkholder, L. A., & Gruenenfelder, M. A. (1986, January 1). Use of Crosslinked Xanthan Gels in Actual Profile Modification Field Projects. Society of Petroleum Engineers. doi:10.2118/14114-MS
- [2] Broseta, D., Medjahed, F., Lecourtier, J., & Robin, M. (1995, March 1). Polymer Adsorption/Retention in Porous Media: Effects of Core Wettability and Residual Oil. Society of Petroleum Engineers. doi:10.2118/24149-PA.
- [3] Bing Wei, Laura Romero-Zerón, Denis Rodrigue, Evaluation of Two New Self-assembly Polymeric Systems for Enhanced Heavy Oil Recovery, *Industrial & Engineering Chemistry Research*, 2014, 53, 43, 16600.
- [4] Corredor, L., Maini, B., & Husein, M. (2018, October 19). Improving Polymer Flooding by Addition of Surface Modified Nanoparticles. Society of Petroleum Engineers. doi:10.2118/192141-MS
- [5] Cannella, W. J., Huh, C., & Seright, R. S. (1988, January 1). Prediction of Xanthan Rheology in Porous Media. Society of Petroleum Engineers. doi:10.2118/18089-MS.
- [6] Eggert, R. W., Willhite, G. P., & Green, D. W. (1992, February 1). Experimental Measurement of the Persistence of Permeability Reduction in Porous Media Treated With Xanthan/Cr(III) Gel Systems. Society of Petroleum Engineers. doi:10.2118/19630-PA

- [7] Esraa Osama Moussa and Attia M Attia, 2016/10/20, 4, EP - 15, Optimum Polymer Concentration in EOR, 3, 10.17148/IARJSET.2016.31002
- [8] Green, D. and Willhite, G. (1997). Enhanced Oil Recovery. 1st ed. Richardson: Society of Petroleum Engineers.
- [9] Gao, C. J Petrol Explor Prod Technol (2016) 6: 749. <https://doi.org/10.1007/s13202-015-0213-7>
- [10] Gao, 2015/11/13, Application of a novel biopolymer to enhance oil recovery, 6, 10.1007/s13202-015-0213-7, Journal of Petroleum Exploration and Production Technology
- [11] G. Sworn, Xanthan gum, In Woodhead Publishing Series in Food Science, Technology and Nutrition, Handbook of Hydrocolloids (Second Edition), Woodhead Publishing, 2009, Pages 186-203, ISBN 9781845694142,
- [12] Gomaa, A. M., Mahmoud, M. A., & Nasr-El-Din, H. A. (2011, February 1). Effect of Shear Rate on the Propagation of Polymer-Based In-Situ-Gelled Acids Inside Carbonate Cores. Society of Petroleum Engineers. doi:10.2118/142927-PA
- [13] Hee Yeon Jang, Ke Zhang, Bo Hyun Chon, Hyoung Jin Choi, Enhanced oil recovery performance and viscosity characteristics of polysaccharide xanthan gum solution, Journal of Industrial and Engineering Chemistry, Volume 21, 2015, Pages 741-745, ISSN 1226-086X
- [14] Han, M., Fuseni, A., Zahrani, B., & Wang, J. (2014, March 31).

Laboratory Study on Polymers for Chemical Flooding in Carbonate Reservoirs. Society of Petroleum Engineers. doi:10.2118/169724-MS

- [15] Jordan R.M. Kennedy, Katherine E. Kent, Jennifer R. Brown, Rheology of dispersions of xanthan gum, locust bean gum and mixed biopolymer gel with silicon dioxide nanoparticles, *Materials Science and Engineering: C*, Volume 48, 2015, Pages 347-353, ISSN 0928-4931.
- [16] Joshi, S. J., Al-Wahaibi, Y. M., Al-Bahry, S., Elshafie, A., Al-Bemani, A. S., Al-Hashmi, A., ... Al-Mandhari, M. S. (2016, March 21). Production and Application of Schizophyllan in Microbial Enhanced Heavy Oil Recovery. Society of Petroleum Engineers. doi:10.2118/179775-MS
- [17] JOUR, Chao, Wang, Yuan, Zhe, Zhenhua, 2018/03/01, Experimental Study of Key Effect Factors and Simulation on Oil Displacement Efficiency for a Novel Modified Polymer BD-HMHEC, *Scientific Reports*, 3860, 8, 1, SN - 2045-2322, <https://doi.org/10.1038/s41598-018-22259-z>, 10.1038/s41598-018-22259-z
- [18] Kalpakci, B., Arf, T. G., Barker, J. W., Krupa, A. S., Morgan, J. C., & Neira, R. D. (1990, January 1). The Low-Tension Polymer Flood Approach to Cost-Effective Chemical EOR. Society of Petroleum Engineers. doi:10.2118/20220-MS.
- [19] Kulawardana, E. U., Koh, H., Kim, D. H., Liyanage, P. J., Upamali, K., Huh, C., ... Pope, G. A. (2012, January 1). Rheology and Transport of Improved EOR Polymers under Harsh Reservoir Conditions. Society of

Petroleum Engineers. doi:10.2118/154294-MS.

- [20] L Su, W.K Ji, W.Z Lan, X.Q Dong, Chemical modification of xanthan gum to increase dissolution rate, Carbohydrate Polymers, Volume 53, Issue 4, 2003, Pages 497-499, ISSN 0144-8617.
- [21] Leonhardt, B., Ernst, B., Reimann, S., Steigerwald, A., & Lehr, F. (2014, April 12). Field Testing The Polysaccharide Schizophyllan: Results of The First Year. Society of Petroleum Engineers. doi:10.2118/169032-MS.
- [22] Martin, F. D., Kovarik, F. S., Chang, P.-W., Goldman, I. M., & Philips, J. C. (1988, January 1). Gels for CO<sub>2</sub> Profile Modification. Society of Petroleum Engineers. doi:10.2118/17330-MS
- [23] Maldal, T., Gilje, E., Kristensen, R., Karstad, T., Nordbotten, A., Schilling, B. E. R., & Vikane, O. (1998, April 1). Planning And Development Of Polymer Assisted Surfactant Flooding For The Gullfaks Field, Norway. Society of Petroleum Engineers. doi:10.2118/35378-PA
- [24] Nannan, Z. (2018, September 14). Oil Reservoir Indigenous Biopolymers Enhance Oil Recovery. Retrieved from [http://english.cas.cn/newsroom/research\\_news/201809/t20180914\\_197382.shtml](http://english.cas.cn/newsroom/research_news/201809/t20180914_197382.shtml)
- [25] Necla Mine Eren, Paulo H.S. Santos, Osvaldo Campanella, Mechanically modified xanthan gum: Rheology and polydispersity aspects, Carbohydrate Polymers, Volume 134, 2015, Pages 475-484, ISSN 0144-8617.

- [26] Patrizio Raffa, Antonius A. Broekhuis, Francesco Picchioni, Polymeric surfactants for enhanced oil recovery: A review, In Journal of Petroleum Science and Engineering, Volume 145, 2016, Pages 723-733, ISSN 0920-4105, <https://doi.org/10.1016/j.petrol.2016.07.007>.
- [27] Primary recovery. (n.d.). Retrieved from [https://www.glossary.oilfield.slb.com/en/Terms/p/primary\\_recovery.aspx](https://www.glossary.oilfield.slb.com/en/Terms/p/primary_recovery.aspx)
- [28] Quadri, S. M. R., Shoaib, M., AlSumaiti, A. M., & Alhassan, S. M. (2015, December 6). Screening of Polymers for EOR in High Temperature, High Salinity and Carbonate Reservoir Conditions. International Petroleum Technology Conference. doi:10.2523/IPTC-18436-MS.
- [29] Reddy, B. R., Patil, R., & Patil, S. (2012, March 1). Chemical Modification of Biopolymers To Design Cement Slurries With Temperature-Activated Viscosification--A Laboratory Study. Society of Petroleum Engineers. doi:10.2118/141005-PA.
- [30] Reddy, B. R. (2011, January 1). Viscosification-on-Demand: Chemical Modification of Biopolymers to Control Their Activation by Triggers in Aqueous Solutions. Society of Petroleum Engineers. doi:10.2118/141007-MS.
- [31] Rellegadla, Prajapat, Agrawal, 2017/05/13, Polymers for enhanced oil recovery: fundamental and selection criteria, 101, 10.1007/s00253-017-8307-4, Applied Microbiology and Biotechnology

- [32] Sun, S., Luo, Y., Cao, S. et al. 2013. Construction and evaluation of an exopolysaccharide-producing engineered bacterial strain by protoplast fusion for microbial enhanced oil recovery. *Bioresource Technol* 144: 44-49.
- [33] T. Yanaki, T. Norisuye, Triple helix and random coil of scleroglucan in dilute solution, *Polymer Journal*, 15 (1983), pp. 187-396.
- [34] Wei, B. , Romero-Zerón, L. and Rodrigue, D. (2015), Improved viscoelasticity of xanthan gum through self-association with surfactant:  $\beta$ -cyclodextrin inclusion complexes for applications in enhanced oil recovery. *Polym Eng Sci*, 55: 523-532.
- [35] Wei, B. (2015), Flow characteristics of three enhanced oil recovery polymers in porous media. *J. Appl. Polym. Sci.*, 132, 41598, doi: [10.1002/app.41598](https://doi.org/10.1002/app.41598)
- [36] Wang, X., Xin, H., Zhu, Y. et al. *Colloid Polym Sci* (2016) 294: 1333. <https://doi.org/10.1007/s00396-016-3898-3>
- [37] Xiong, Loss, Shields, Taylor, Hochreiter, Andrew L, Manish, Polyacrylamide degradation and its implications in environmental systems, *npj Clean Water*, 17, Volume 1 ,Issue 1, 2018, SN - 2059-7037, 10.1038/s41545-018-0016-8
- [38] Yifeng Zhang, Huiling Kong, Yapeng Fang, Katsuyoshi Nishinari, Glyn O. Phillips, Schizophyllan: A review on its structure, properties, bioactivities and recent developments, In *Bioactive Carbohydrates and*

Dietary Fibre, Volume 1, Issue 1, 2013, Pages 53-71, ISSN 2212-6198,  
<https://doi.org/10.1016/j.bcdf.2013.01.002>.

- [39] Yangang Bi, Wusong Li, Congcong Liu, Zejun Xu, Xinru Jia. (2017)  
Dendrimer-Based Demulsifiers for Polymer Flooding Oil-in-Water  
Emulsions. *Energy & Fuels* 31:5, pages 5395-5401.

## Appendix: Porosity and Permeability Calculations

Core #1:

Dry sample weight = 362.75 g

Saturated sample weight = 397.47 g

Brine weight in sample = Saturated sample weight - Dry sample weight

$$= 397.47 - 362.75 = 34.72 \text{ g}$$

Volume of brine inside the core (pore volume) = Brine weight / Brine density

$$= 34.94 / 1.02 = 34.04 \text{ cm}^3$$

Volume of the sample = Area of base x Length

$$= \pi \times d^2 / 4 \times L$$

$$= \pi \times 3.8^2 / 4 \times 15.35 = 174 \text{ cm}^3$$

Porosity = Pore volume / sample volume

$$= 34.04 \text{ cm}^3 / 173.89 \text{ cm}^3 = 19.58 \text{ cm}^3$$

Measuring the permeability of the sample using distilled water was accomplished and found to be 102.7md at 23<sup>0</sup>C by plotting the flow rate vs pressure drop (see Table 10 and Figure 62):

Table 10: Flow rate and pressure data of core #1

q	q	P <sub>in</sub>	P <sub>out</sub>	DP	DP
cc/min	cc/s	Psi	Psi	psi	Atm
0.5	0.0083	1026.9	1025.4	1.5	0.10204
1.00	0.0167	1026.6	1023.9	2.7	.18367
2.00	0.0333	1042.0	1036.5	5.5	.37415
4.00	0.0667	1071.0	1059.0	12	0.81632

The slope was obtained by plotting q vs. dp (see Figure 62).

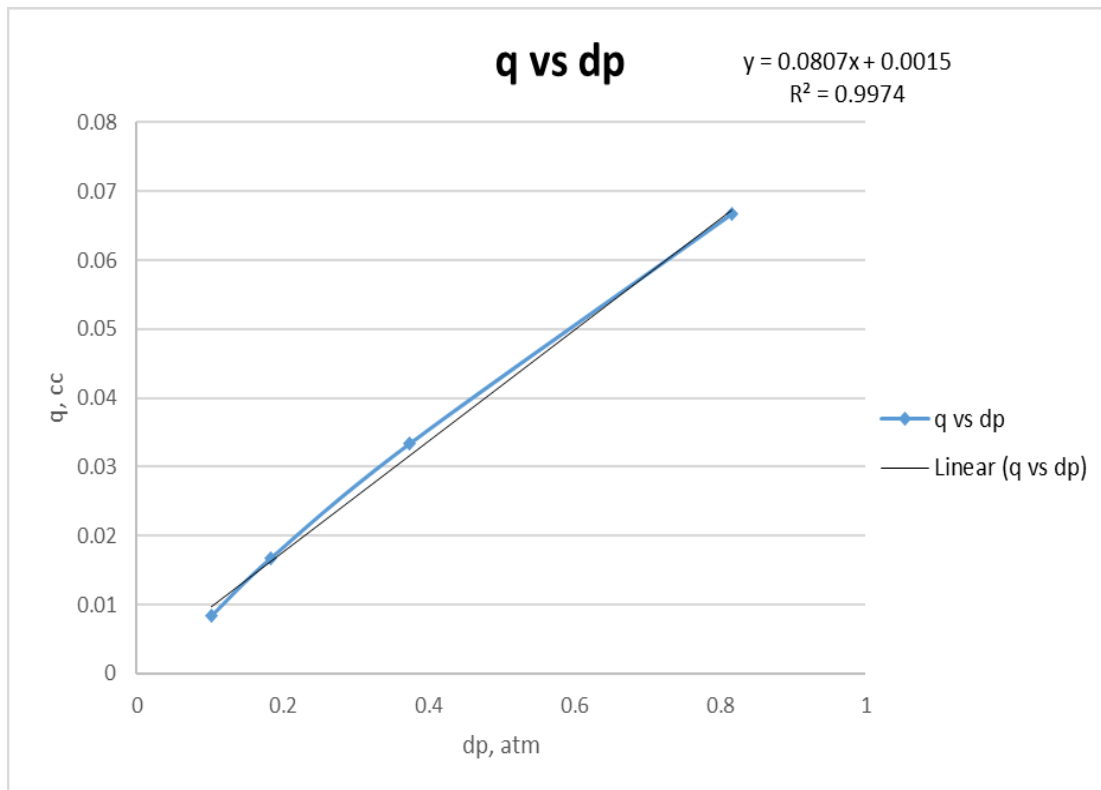


Figure 62: The q vs. dp values for Core #1.

$$m = 0.0807 = \frac{AK}{\mu L}$$

$$q = \frac{AK}{\mu L} DP$$

meaning:

$$K = \frac{\mu L m}{A} \times 1000$$

$$K = \frac{4 \times 0.94 \times 0.0807 \times 15.34}{3.14 \times 3.8^2} \times 1000 = 102.7 \text{ md}$$

The same procedure was repeated for Core #2 (see Table 11 and Figure 63).

Core #2:

Dry sample weight = 361.04 g

Saturated sample weight = 395.53 g

Brine weight in sample = Saturated sample weight - Dry sample weight

$$= 395.53 - 361.04 = 34.49 \text{ g}$$

Volume of brine inside the core (pore volume) = Brine weight / Brine

density

$$= 34.49 / 1.02 = 33.81 \text{ cm}^3$$

Volume of sample = Area of base x Length

$$= \pi \times d^2 / 4 \times L$$

$$= \pi \times 3.8^2 / 4 \times 15.08 = 170.94 \text{ cm}^3$$

Porosity = Pore volume / sample volume

$$= 33.81 \text{ cm}^3 / 170.94 \text{ cm}^3 = 19.78 \text{ cm}^3$$

Measuring the permeability of the sample using distilled water was accomplished by the core flooding machine and found to be 107.3md at 23°C, as follows:

Table 11: Flow rate and pressure data of core #2

q	q	P <sub>in</sub>	P <sub>out</sub>	DP	DP
cc/min	cc/s	Psi	Psi	psi	Atm
0.5	0.0083	994.1	993.1	1.0	0.06803
1.00	0.0167	1103.7	1101.0	2.7	.18367
2.00	0.0333	1178.6	1173.2	5.4	.36735
4.00	0.0667	1144.4	1133.3	11.1	0.75510

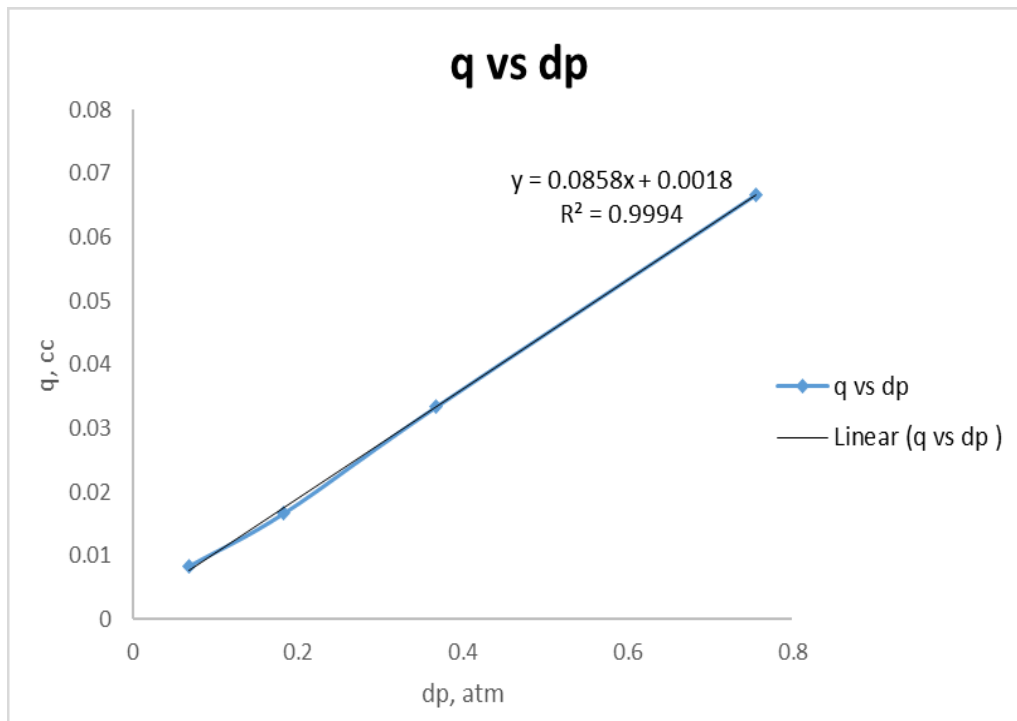


Figure 63: The q vs. dp values for Core #2.

$$m = 0.0807 = \frac{AK}{\mu L}$$

$$q = \frac{AK}{\mu L} DP$$

meaning:

$$K = \frac{\mu L m}{A} \times 1000$$

$$K = \frac{4 \times 0.94 \times 0.0858 \times 15.08}{3.14 \times 3.8^2} \times 1000 = 107.3 \text{ md}$$

Even though the cores were originally one 12-inch core that was cut into two cores, the permeability and porosity were measured and determined to be very close to one another.

The differences could be due to a malfunction of the pressure gauge or human error.

## Vitae

Name : Mohammad Said Mohammad

Nationality : Egyptian

Date of Birth :3/8/1992

Email : [mohammadsaeed1412@gmail.com](mailto:mohammadsaeed1412@gmail.com)

Address : Dhahran, Saudi Arabia

Academic Background :M.Sc. in Petroleum Engineering (March 2019)

King Fahd University of Petroleum and Minerals  
Dhahran, Saudi Arabia

B.Sc in Petroleum Engineering (May 2015)

King Fahd University of Petroleum and Minerals  
Dhahran, Saudi Arabia